Electronic Supporting Information

for

Wavelength dependent photochemistry of BODIPY-phenols and their applications in in fluorescent labeling of proteins

Katarina Zlatić,[a] Matej Cindrić,[a] Ivana Antol,*[a] Lidija Uzelac,[b] Branka Mihaljević,[c] Marijeta Kralj,*[b] Nikola Basarić[a]*

[a] Department of Organic Chemistry and Biochemistry, Ruđer Bošković Institute, Bijenička cesta 54, 10 000 Zagreb, Croatia. IA E-mail: ivana.antol@irb.hr; NB E-mail: nbasaric@irb.hr
[b] Department of Molecular Medicine, Ruđer Bošković Institute, Bijenička cesta 54, 10 000 Zagreb, Croatia. MK E-mail: marijeta.kralj@irb.hr
[c] Department of Material Chemistry, Ruđer Bošković Institute, Bijenička cesta 54, 10 000 Zagreb

Contents:

1. Experimental procedures

5-Phenyldipyrromethane[1]

Benzaldehyde (4 mL, 0.04 mol) and pyrrole (60 g, 0.9 mol) were stirred in a flask under N_2 atmosphere. To the mixture trifluoroacetic acid (TFA, 0.3 mL, 4.0 mmol) was added and the mixture was stirred at rt for 1 h. To the mixture an aqueous solution of NaOH (50 mL, 0.1 M) was added, and the mixture was extracted with CH_2Cl_2 (3×50 mL). The extracts were dried over anhydrous $MgSO_4$, filtered and the solvent was removed on a rotary evaporator. Excess of the pyrrole from the mixture was removed by a vacuum distillation and the residue was chromatographed on a column of silica gel using CH_2Cl_2 as eluent to afford the pure product (7.7 g, 87%).

^{1}H NMR ($CDCl_3$, 300 MHz) / ppm: 7.91 (br s, 2H), 7.35-7.29 (m, 3H), 7.25-7.20 (m, 2H), 6.70-6.68 (m, 2H), 6.16 (dd, J = 2.7 Hz, 5.7 Hz, 2H), 5.93-5.90 (m, 2H), 5.46 (s, 1H); ^{13}C NMR ($CDCl_3$, 75 MHz, APT) / ppm: 142.1 (s), 132.5 (s, 2C), 128.7 (d, 2C), 128.4 (d, 2C), 127.0 (d), 117.2 (d, 2C), 108.5 (d, 2C), 107.2 (d, 2C).

1-Chloro-5-phenyldipyrromethane[2] and 1,8-dichloro-5-phenyldipyrromethane[3]

5-Phenyldipyrromethane (3.4 g, 0.01 mol) was dissolved in anhydrous THF (50 mL) under N_2 inert atmosphere and the solution was cooled to -78 °C. A solution of *N*-chlorosuccinimide (NClS, 2.9 g, 0.04 mol) in THF (50 mL) was added to the cooled solution by a dropping funnel. The reaction mixture was stirred at -78 °C for 4 h and then it was placed in a refrigerator at 5 °C over night. The next day, a column of silica gel with CH_2Cl_2-hexane (1:1) as eluent was charged with the cold reaction mixture. The chromatography gave fractions enriched in products, which were rechromatographed on silica gel using CH_2Cl_2-hexane (1:1) as eluent to afford monochloro derivative (796 mg, 41%) and a mixture of mono- and dichloro derivative (758 mg, 1:1, yield of dichloro derivative 17%).

1-Chloro-5-phenyldipyrromethane

^{1}H NMR ($CDCl_3$, 300 MHz) / ppm: 7.82 (br s, 1H), 7.77 (br s, 1H), 7.35-7.18 (m, 5H), 6.69 (dd, J = 2.6 Hz, 4.0 Hz, 1H), 6.16 (dd, J = 2.7 Hz, 5.6 Hz, 1H), 5.96-5.92 (m, 2H), 5.81-5.79 (m, 1H), 5.37 (s, 1H).

1,8-Dichloro-5-phenyldipyrromethane

^{1}H NMR ($CDCl_3$, 300 MHz) / ppm: 7.80 (br s, 2H), 7.35-7.29 (m, 3H), 7.21-7.19 (m, 2H), 5.97-5.95 (m, 2H), 5.83-5.82 (m, 2H), 5.31 (s, 1H).

4,4-Difluoro-3-chloro-8-phenyl-4-bora-3a,4a-diaza-s-indacene (6)[4] and 4,4-difluoro-3,5-dichloro-8-phenyl-4-bora-3a,4a-diaza-s-indacene (9)[5]

A mixture of mono- and dichlorinated dipyrroomethane (796 mg, NMR ratio 1:1) was dissolved in toluene (20 mL). To the solution 2,3-dichloro-5,6-dicyano-1,4-benzoquinone (DDQ, 1.0 g, 4 mmol) was added and the reaction mixture was heated at the temperature of reflux for 1 h. The reaction mixture was filtered through a filter paper, and the solid was washed with toluene. The mixture was concentrated on a rotary evaporator to the volume of ≈ 20 mL. To the residue, under N_2 inert atmosphere, trimethylamine (TEA, 3.1 mL, 22 mmol) was added followed by the addition of BF_3OEt_2 (2.7 mL, 22 mmol). The reaction mixture was stirred and heated at 70 °C overnight. To the cooled mixture, aqueous NaOH (20 mL, 0.1 M) was added and an extraction with EtOAc was carried out (2×20 mL). Th extracts were dried over anhydrous $MgSO_4$, filtered and the solvent was removed on a rotary evaporator. The residue was chromatographed on a column of silica gel using CH_2Cl_2 as eluent to afford pure **6** (197 mg, 28%) and **9** (78 mg 11%).

In another procedure starting from pure dichlorinated dipyrromethane (1.1 g, 4.0 mmol), the reaction after chromatographic separation gave pure product **9** (582 mg, 49%).

4,4-Difluoro-3-chloro-8-phenyl-4-bora-3a,4a-diaza-s-indacene (6)

^{1}H NMR ($CDCl_3$, 300 MHz) / ppm: 7.94 (br s, 1H), 7.60 – 7.52 (m, 5H), 6.90 (m, 2H), 6.57 (d, J = 3.2 Hz, 1H), 6.43 (d, J = 4.2 Hz, 1H); ^{13}C NMR ($CDCl_3$, 75 MHz, APT) / ppm: 144.5 (d), 131.9 (d), 131.5 (d), 130.8 (d, 2C), 130.5 (d, 2C), 128.5 (d), 118.9 (d), 118.4 (d), signals of quaternary C atoms were not observed.

4,4-Difluoro-3,5-dichloro-8-phenyl-4-bora-3a,4a-diaza-s-indacene (9)

^{1}H NMR ($CDCl_3$, 300 MHz) / ppm: 7.54-7.48 (m, 5H), 6.84 (d, J = 4.2 Hz, 2H), 6.44 (d, J = 4.2 Hz, 2H); ^{13}C NMR ($CDCl_3$, 75 MHz, APT) / ppm: 145.0 (s), 144.0 (s), 133.8 (s, 2C), 132.4 (s, 2C), 131.7 (d, 2C), 130.9 (d), 130.4 (d, 2C), 128.6 (d, 2C), 118.9 (d, 2C).

Chlorination of BODIPY by $CuCl_2$

4,4-Difluoro-8-phenyl-4-bora-3a,4a-diaza-s-indacen (20 mg, 0.08 mmol), and $CuCl_2 \times H_2O$ (38 mg, 0.22 mmol) were dissolved in CH_3CN (20 mL). The reaction mixture was heated at the temperature of reflux for 6 h. To the cooled mixture, H_2O (20 mL) was added and the mixture was extracted with CH_2Cl_2 (3×20 mL). The extracts were dried over anhydrous $MgSO_4$, filtered and the solvent was removed on a rotary evaporator. The residue was chromatographed on a column of silica gel using CH_2Cl_2 as eluent to afford pure **6** (5 mg, 22%) and **9** (10 mg 40%).

HPLC analysis and separations

For the analysis of samples (including those after irradiation experiments) Shimadzu or Agilent 1260 Infinity II HPLC instruments equipped with a diode array detector and a Phenomenex Luna 3u C18 100A column were used. The mobile phase was a mixture of CH_3OH-H_2O, containing 0.1 % TFA. The following method was used:

Table S1. Method for the analysis of samples by HPLC on a Phenomenex Luna 3u C18 100A column

Solvent **B** / %	100	100	0	0
t / min	0	10	20	40

A = MeOH
B = H_2O - MeOH = (1:1) + 0.1% TFA,
flow = 0.8 mL/min
Injected volume = 10 µL

Semipreparative HPLC was conducted on a Varian Pro Star HPLC instrument with UV-vis detector and a Phenomenex Jupiter 5u C18 300A column. The mobile phase was a mixture of CH_3OH-H_2O, containing 0.1 % TFA. The following methods were used:

Table S2. Method for the separation of **1×TFA-5×TFA**on a Phenomenex Jupiter 5u C18 300A column.

Solvent **B** / %	100	100	0	0
t / min	0	20	40	60

A = CH_3OH
B = CH_3OH-H_2O = (1:1) + 0.1% TFA,
flow = 3.5 mL/min
Injected volume = 200 µL
Detection wavelength 530 nm.

2. UV-Vis and fluorescence spectra

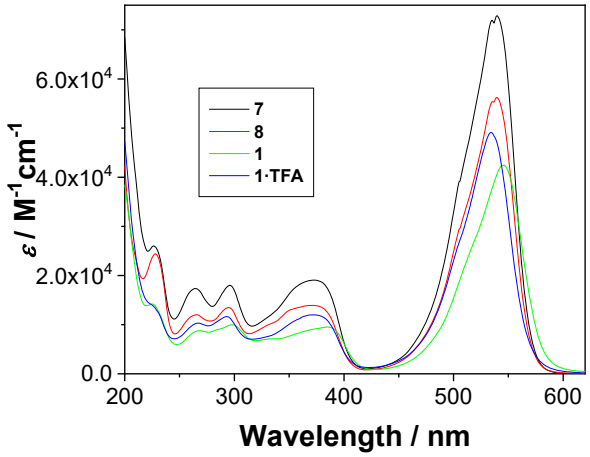

Fig S1. Absorption spectra in CH_3CN.

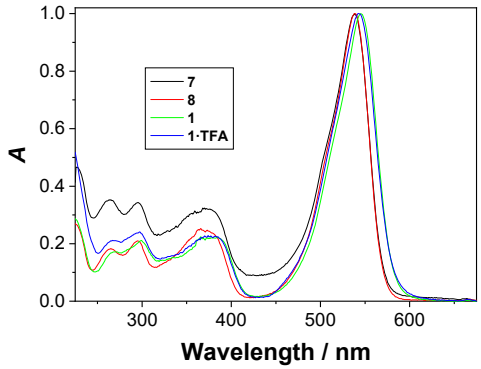

Fig S2. Normalized absorption spectra in CH_3CN.

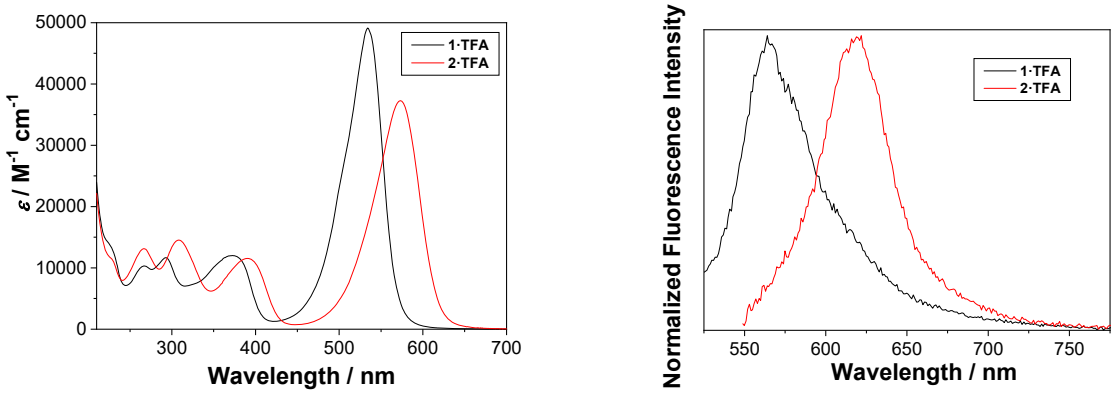

Fig S3. Left: Absorption spectra of **1·TFA** and **2·TFA** in CH_3CN; and Right: Normalized fluorescence spectra in CH_3CN (λ_{exc} = 500 nm).

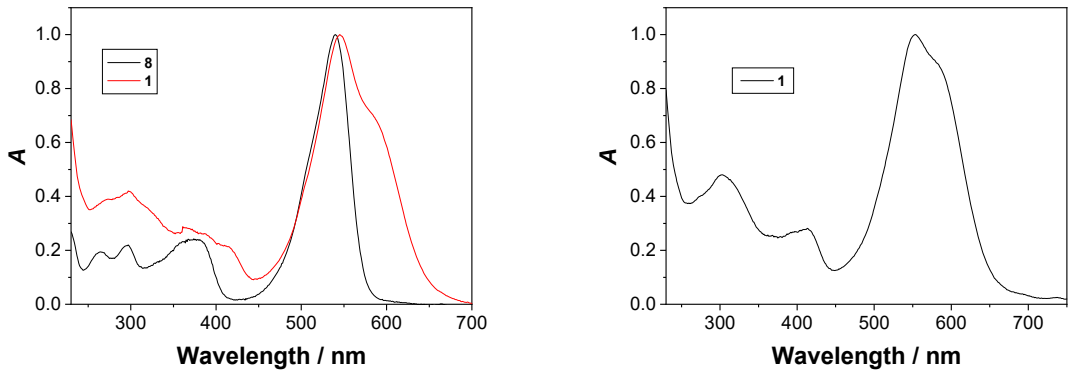

Fig S4. Normalized absorption spectra in CH_3CN-H_2O (1:1 v/v) in the presence of phosphate buffer (50 mM) at pH 7 (left) and pH 9 (right).

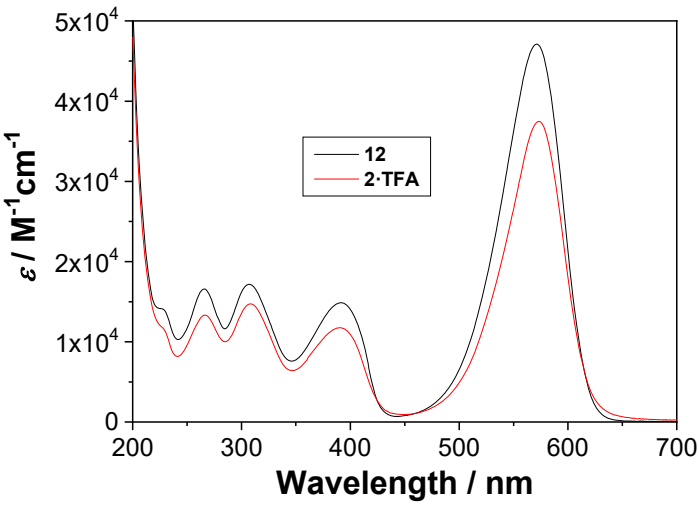

Fig S5. Absorption spectra in CH_3CN.

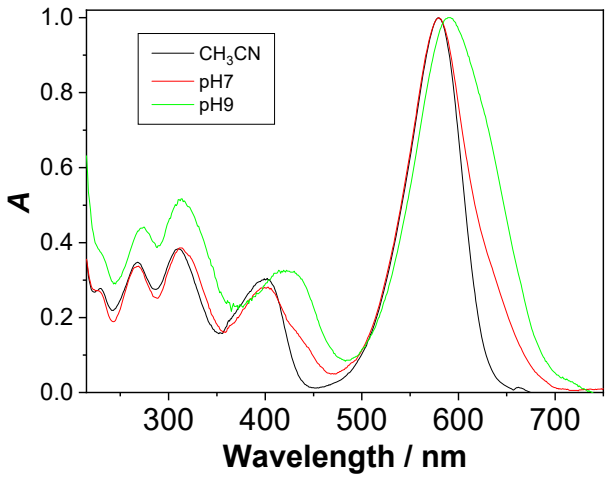

Fig S6. Normalized absorption spectra of **2·TFA** in CH_3CN or **2** in CH_3CN-H_2O (1:1 v/v) in the presence of phosphate buffer (50 mM) at pH 7 and pH 9.

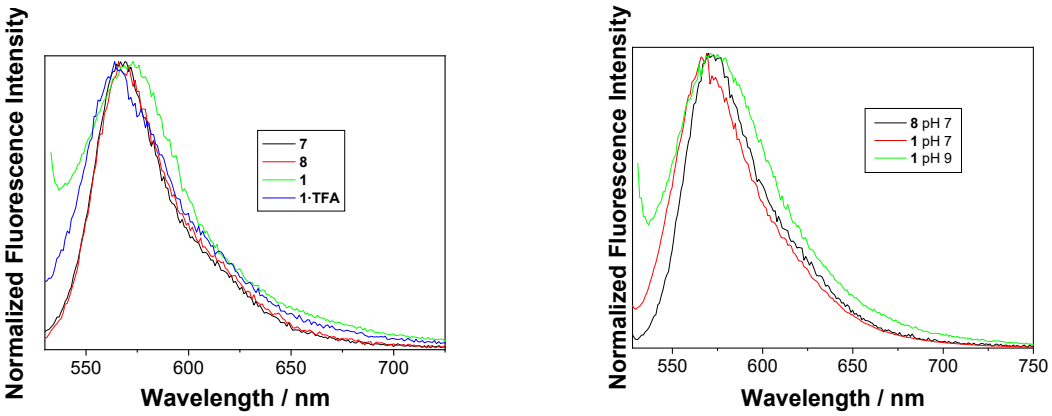

Fig S7. Left: Normalized fluorescence spectra in CH_3CN (λ_{ex} = 500 nm); and Right: Normalized fluorescence spectra in H_3CN-H_2O (1:1 v/v) in the presence of phosphate buffer (50 mM) at pH 7 and pH 9.

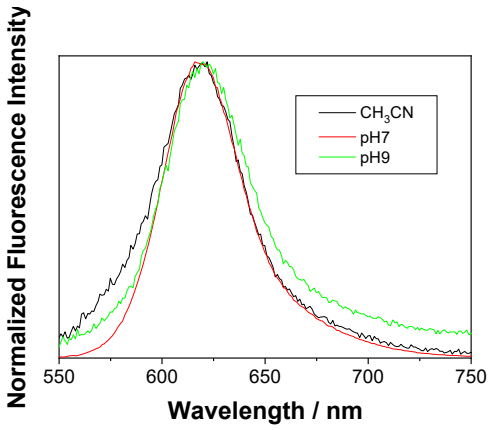

Fig S8. Normalized fluorescence spectra (λ_{ex} = 500 nm) of **2·TFA** in CH_3CN and **2** in CH_3CN-H_2O (1:1 v/v) in the presence of phosphate buffer (50 mM) at pH 7 and pH 9.

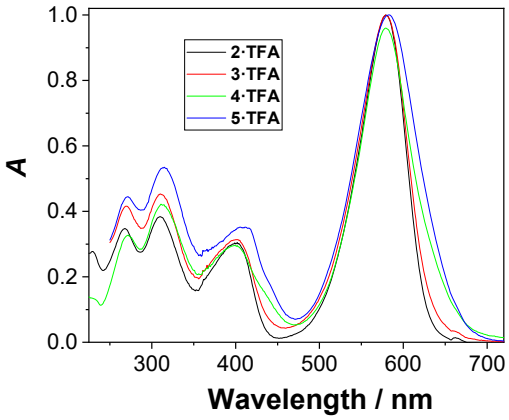

Fig S9. Normalized absorption spectra in CH_3CN.

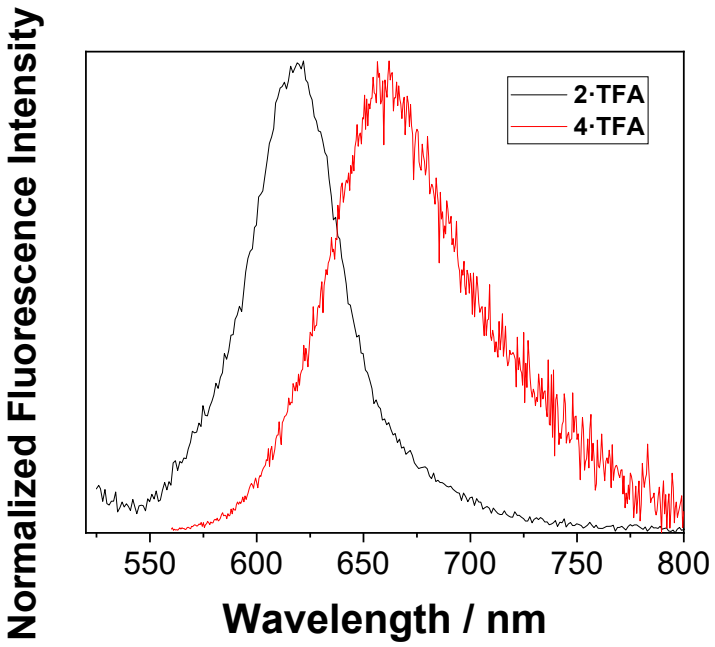

Fig S10. Normalized emission spectra in CH_3CN of **2·TFA** (λ_{ex} = 500 nm) and **4·TFA** (λ_{ex} = 550 nm).

The following equation was used for the determination of fluorescence quantum yields:

$$\Phi = \Phi_R \frac{I}{I_R} \frac{A_R}{A} \left(\frac{n_D}{n_D^R}\right)^2 \qquad \text{(S1)}$$

wherein

Φ - quantum yield of fluorescence

Φ_R - quantum yield of fluorescence of reference compound, Fluorescence quantum yields were measured using rhodamine B in CH_3OH as a reference (Φ_f = 0.66)[6]

I - intensity of fluorescence (integral of the corrected emission spectrum)

I_R - intensity of fluorescence (integral of the corrected emission spectrum) for the reference compound

A - absorbance of the solution at the excitation wavelength

A_R - absorbance of the solution of the reference compound at the excitation wavelength

n_D - refractive index of the solvent

n_D^R - refractive index of the solvent used to dissolve the reference compound (CH_3OH)

3. Computations

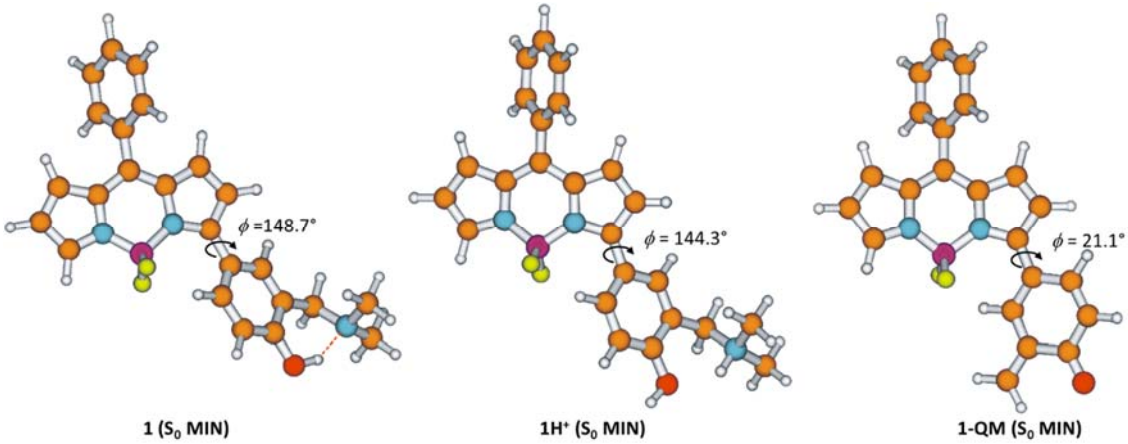

Fig S11. Optimized geometries of **1**, **1H**$^+$ and **1-QM** in the ground state at the PBE0/6-311G(2d,p) level of theory.

Table S3. TD-DFT calculated vertical exitation energies (E_{exc}), oscilator strenght (f) and leading configurations for **1** at the PBE0/6-311+G(2d,p)//PBE0/6-311G(2d,p) level of theory.

State	E_{exc}/eV	f	Leading configuration		Weight
1	2.612	0.7196	Singlet-A	109a ->110a	0.70569
2	3.418	0.1033	Singlet-A	108a ->110a	0.63867
3	3.702	0.0719	Singlet-A	105a ->110a	0.51243
4	3.761	0.0065	Singlet-A	107a ->110a	0.59635
5	3.963	0.0239	Singlet-A	104a ->110a	0.54398
6	3.973	0.1208	Singlet-A	103a ->110a	0.50744
7	4.006	0.0103	Singlet-A	106a ->110a	0.49492
8	4.143	0.0075	Singlet-A	102a ->110a	0.69733
9	4.307	0.0221	Singlet-A	109a ->111a	0.68734
10	4.367	0.0362	Singlet-A	109a ->112a	0.68886
11	4.581	0.0567	Singlet-A	109a ->113a	0.59477
12	4.819	0.1899	Singlet-A	109a ->114a	0.58861
13	5.054	0.0155	Singlet-A	109a ->115a	0.66702
14	5.202	0.0172	Singlet-A	109a ->116a	0.58748
15	5.227	0.1101	Singlet-A	101a ->110a	0.56799
16	5.398	0.0031	Singlet-A	108a ->112a	0.40738
17	5.473	0.0082	Singlet-A	108a ->111a	0.47098
18	5.477	0.0009	Singlet-A	109a ->117a	0.52943
19	5.534	0.0217	Singlet-A	108a ->113a	0.47662
20	5.541	0.0007	Singlet-A	99a ->110a	0.61868
21	5.639	0.0046	Singlet-A	109a ->118a	0.63565
22	5.651	0.0038	Singlet-A	108a ->112a	0.40861
23	5.707	0.0128	Singlet-A	109a ->119a	0.62591
24	5.759	0.0084	Singlet-A	108a ->114a	0.45304
25	5.791	0.0024	Singlet-A	100a ->110a	0.63157
26	5.837	0.0527	Singlet-A	109a ->120a	0.47234
27	5.865	0.0029	Singlet-A	109a ->121a	0.49118
28	5.874	0.0124	Singlet-A	105a ->111a	0.50264

29	5.898	0.0083	Singlet-A	107a ->113a	0.41455
30	5.912	0.0022	Singlet-A	105a ->112a	0.38681
31	5.941	0.0654	Singlet-A	105a ->112a	0.3979
32	5.962	0.0101	Singlet-A	109a ->122a	0.58958
33	5.978	0.0095	Singlet-A	107a ->114a	0.37457
34	6.034	0.0131	Singlet-A	109a ->124a	0.64019
35	6.099	0.024	Singlet-A	107a ->111a	0.40798
36	6.11	0.0022	Singlet-A	104a ->111a	0.42961
37	6.123	0.0039	Singlet-A	109a ->125a	0.47044
38	6.139	0.0221	Singlet-A	107a->112a	0.51649
39	6.151	0.0009	Singlet-A	108a ->115a	0.4928
40	6.174	0.0199	Singlet-A	103a ->111a	0.41323

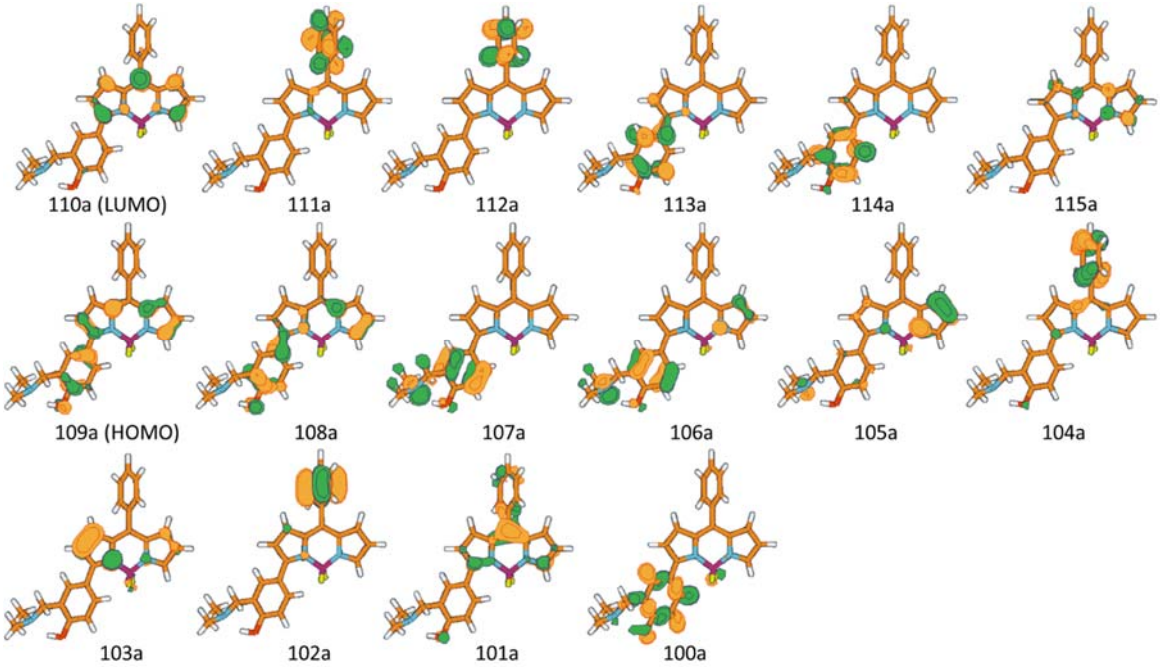

Fig S12. Selected Kohn-Sham orbitals of **1** at the PBE0/6-311+G(2d,p)//PBE0/6-311G(2d,p) level of theory.

Table S4. TD-DFT calculated vertical exitation energies (E_{exc}), oscilator strenght (f) and leading configurations for **1H**$^+$ at the PBE0/6-311+G(2d,p)//PBE0/6-311G(2d,p) level of theory.

State	E_{exc}/eV	f	Leading configuration		Weight
1	2.864	0.5981	Singlet-A	109a ->110a	0.69699
2	3.497	0.2225	Singlet-A	108a ->110a	0.68574
3	3.554	0.034	Singlet-A	107a ->110a	0.66643
4	3.674	0.0435	Singlet-A	106a ->110a	0.67394
5	3.747	0.0133	Singlet-A	109a ->111a	0.66987
6	3.891	0.0152	Singlet-A	105a ->110a	0.68818
7	4.094	0.0553	Singlet-A	109a ->112a	0.60979
8	4.358	0.001	Singlet-A	109a ->113a	0.53379
9	4.557	0.2456	Singlet-A	104a ->110a	0.54436
10	4.854	0.0008	Singlet-A	103a ->110a	0.52322
11	4.875	0.0022	Singlet-A	109a ->114a	0.69123

12	5.002	0.0127	Singlet-A	109a ->116a	0.54362
13	5.016	0.0107	Singlet-A	108a ->111a	0.54931
14	5.069	0.0001	Singlet-A	107a ->111a	0.49159
15	5.101	0.0101	Singlet-A	109a ->117a	0.63586
16	5.233	0.0219	Singlet-A	108a ->112a	0.60198
17	5.242	0.0004	Singlet-A	109a ->115a	0.47329
18	5.287	0.0132	Singlet-A	107a ->111a	0.41112
19	5.298	0.0251	Singlet-A	102a ->110a	0.46023
20	5.332	0.0098	Singlet-A	105a ->111a	0.4704
21	5.376	0.0236	Singlet-A	107a ->112a	0.41695
22	5.384	0.007	Singlet-A	109a ->118a	0.58727
23	5.44	0.0228	Singlet-A	104a ->111a	0.54491
24	5.487	0.0054	Singlet-A	108a ->117a	0.38283
25	5.49	0.0189	Singlet-A	109a ->119a	0.63364
26	5.53	0.0014	Singlet-A	108a ->113a	0.59356
27	5.584	0.0041	Singlet-A	107a ->112a	0.42028
28	5.62	0.0078	Singlet-A	105a ->112a	0.44582
29	5.624	0.0026	Singlet-A	101a ->110a	0.6143
30	5.725	0.0023	Singlet-A	107a ->113a	0.54591
31	5.768	0.0097	Singlet-A	104a ->112a	0.42612
32	5.777	0.0065	Singlet-A	109a ->120a	0.53721
33	5.868	0.0012	Singlet-A	106a ->113a	0.56182
34	5.913	0.0068	Singlet-A	109a ->121a	0.49484
35	5.936	0.0006	Singlet-A	99a ->110a	0.66625
36	5.971	0.0028	Singlet-A	105a ->113a	0.59357
37	5.975	0.0124	Singlet-A	100a ->110a	0.61227
38	6.01	0.0601	Singlet-A	108a ->114a	0.49494
39	6.024	0.1166	Singlet-A	109a ->122a	0.32787
40	6.072	0.0278	Singlet-A	104a ->113a	0.4323

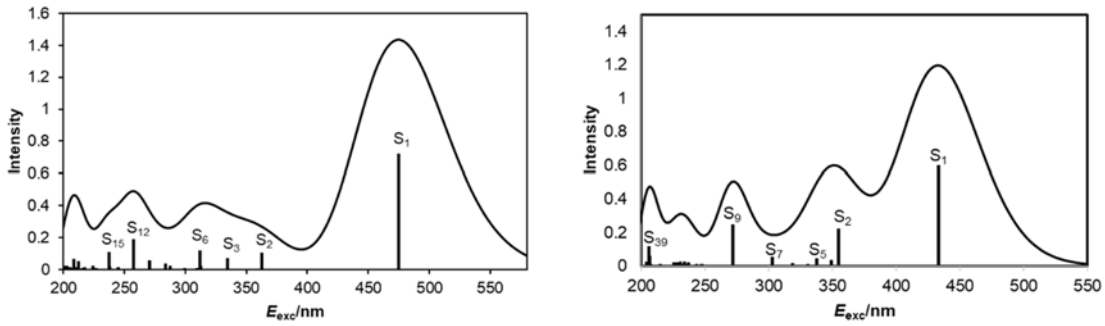

Fig S13. Simulated absorption spectra of **1** (left) and **1H**$^+$ (right) calculated at TD DFT level of theory using PBE0 functional and Pople type 6-311+G(2d,p) basis set.

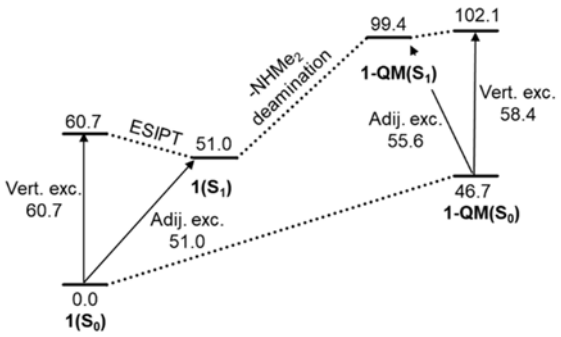

Fig S14. Energy diagram for the excited sate deamination reaction for **1**. Stationary points for the ground and the S_1 state with respect to the ground state minimum **1** were computed at the PBE0/6-311G(2d,p) level of theory. Relative energies are given in kcal mol^{-1}.

Table S5: Total electronic energies for ground state (S_0) and the first excited state (S_1), zero point vibrational energies (ZVPE) and number of imaginary frequencies calculated at PBE0/6-311G(2d,p) level of theory.

Structure	Opt. state	E_{tot} (S_0)/a.u.	E_{tot} (S_1)/a.u.	ZPVE/a.u.	N_{Imag}	E_{exc}/kcal mol^{-1}
1	S_0	-1390.79818	-1390.701475	0.42226	0	60.7 (Vertical)
1	S_1	-1390.75521	-1390.71692	0.42077	0	51.0 (Adiabatic)
1-QM	S_0	-1255.69471	-1255.60169	0.32383	0	58.4 (Vertical)
1-QM	S_1	-1255.68996	-1255.60600	0.31997	0	55.7(Adiabatic)
$NHMe_2$	S_0	-135.033831		0.09255	0	
1H$^+$	S_0	-1391.18455	-1391.07841	0.43670	0	66.6(Vertical)
1H$^+$	S_1	-1391.18084	-1391.08210	0.43339	0	64.3(Adiabatic)

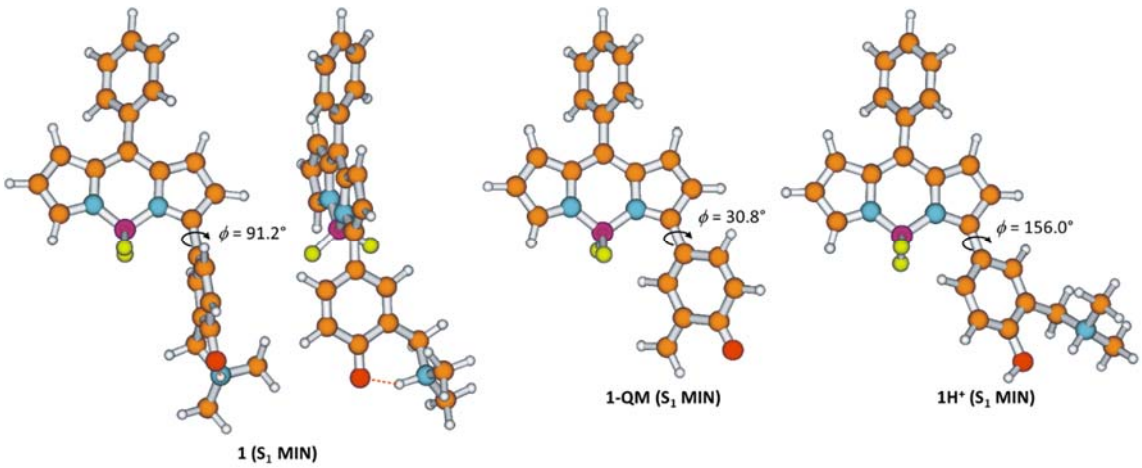

Fig S15. Optimized geometries of minima on the S_1 potential energy surface at the PBE0/6-311G(2d,p) level of theory.

Table S6: Cartesian geometries (Å) for stationary points in the ground (S_0) and the first excited singlet state (S_1) calculated at the PBE0/6-311G(2d,p) level of theory

	1 (S_0 minimum)				**1** (S_1 minimum)		
B	0.876916	1.873047	0.122185	B	0.347092	1.279395	0.326011
N	0.696634	0.318417	0.172445	N	0.678219	-0.219215	0.410563
C	1.767295	-0.566215	0.149777	C	1.902299	-0.797206	0.163340
C	3.086797	-0.151453	0.001785	C	3.060896	0.021816	-0.039615
C	3.378624	1.203659	-0.195149	C	2.910227	1.423910	-0.005641
N	2.361958	2.130625	-0.244432	N	1.670914	2.012030	0.165505
C	-0.442452	-0.403036	0.197127	C	-0.249429	-1.213127	0.502455
C	1.254810	-1.884068	0.162616	C	1.720586	-2.177078	0.101170
C	4.176378	-1.146221	0.015918	C	4.364695	-0.588623	-0.275567
C	4.599580	1.878925	-0.390256	C	3.863854	2.459824	-0.049820
C	2.903960	3.331033	-0.464534	C	1.834250	3.354929	0.220815
C	4.294255	3.218124	-0.569095	C	3.176015	3.667102	0.087676
C	-0.109579	-1.783272	0.186514	C	0.348943	-2.433279	0.316040
F	0.058783	2.434289	-0.826814	F	-0.508066	1.507459	-0.770928
F	0.639999	2.415954	1.377060	F	-0.332947	1.689961	1.475936
C	-1.802518	0.110350	0.234400	C	-1.670651	-0.883768	0.747878
H	-0.823973	-2.590744	0.226711	H	-0.136111	-3.397856	0.348804
H	1.851893	-2.782501	0.138839	H	2.486135	-2.909290	-0.097905
H	2.280152	4.210543	-0.528524	H	0.983544	4.002884	0.364153
H	4.981879	4.029711	-0.750727	H	3.599516	4.660248	0.103205
H	5.576541	1.420857	-0.391897	H	4.930441	2.324203	-0.131885
C	5.058184	-1.249433	-1.060863	C	5.231877	-0.101219	-1.265446
C	6.077423	-2.187926	-1.046330	C	6.470076	-0.679271	-1.485548
C	6.238314	-3.027155	0.046906	C	6.887594	-1.764122	-0.725939
C	5.370346	-2.927744	1.124565	C	6.044480	-2.261141	0.259122
C	4.342820	-1.997880	1.108803	C	4.805497	-1.685890	0.480525
H	4.924106	-0.601583	-1.919836	H	4.904923	0.727652	-1.882613
H	6.747279	-2.266125	-1.895693	H	7.111750	-0.285142	-2.267289
H	7.039697	-3.757760	0.059046	H	7.858118	-2.216221	-0.899200
H	5.495536	-3.574774	1.985904	H	6.361035	-3.099678	0.871405
H	3.671690	-1.909955	1.955994	H	4.169710	-2.064479	1.272343
C	-2.820902	-0.661684	-0.337223	C	-2.519647	-0.617117	-0.345079
C	-4.144050	-0.264551	-0.327236	C	-3.823182	-0.256595	-0.164056
C	-4.484310	0.936795	0.319851	C	-4.376236	-0.205386	1.172385
C	-3.483012	1.711975	0.900820	C	-3.500604	-0.480689	2.270124
C	-2.164599	1.314441	0.850905	C	-2.185900	-0.786004	2.050217
H	-2.564021	-1.585173	-0.847683	H	-2.083455	-0.635396	-1.336255
C	-5.198010	-1.043368	-1.064780	C	-4.662397	0.229383	-1.302230
O	-5.755334	1.354163	0.391486	O	-5.602971	0.061304	1.357778
H	-3.768564	2.631567	1.398323	H	-3.927204	-0.429809	3.264300
H	-1.408026	1.927015	1.321955	H	-1.515268	-0.962579	2.880704
H	-6.314580	0.578512	0.126183	H	-6.183690	-0.036579	-0.047721
N	-6.461252	-1.120484	-0.329483	N	-6.087032	-0.188948	-1.118558
H	-5.417336	-0.539497	-2.013957	H	-4.659958	1.323130	-1.321720

H	-4.818698	-2.047660	-1.317043	H	-4.300065	-0.128108	-2.268237
C	-7.538287	-1.594841	-1.177485	C	-7.026474	0.657648	-1.870809
C	-6.337765	-1.935331	0.867961	C	-6.278684	-1.624378	-1.398544
H	-7.267473	-1.891929	1.438505	H	-7.283592	-1.916613	-1.096823
H	-6.123947	-2.989074	0.626115	H	-6.142390	-1.808013	-2.465236
H	-5.529447	-1.554418	1.493996	H	-5.546021	-2.195991	-0.830805
H	-8.475180	-1.593338	-0.616959	H	-8.044508	0.319677	-1.681069
H	-7.651717	-0.933007	-2.038502	H	-6.918763	1.690006	-1.540787
H	-7.357950	-2.618040	-1.545469	H	-6.809947	0.588371	-2.938012
	1H$^+$ (S_0 minimum)				**1H**$^+$(S_1 minimum)		
B	0.851011	1.835111	0.138185	B	0.888174	1.858646	0.165368
N	0.706888	0.280428	0.199810	N	0.716198	0.313619	0.128283
C	1.779875	-0.588716	0.162421	C	1.773505	-0.571063	0.040771
C	3.104714	-0.142568	-0.005385	C	3.145875	-0.156385	0.003603
C	3.357306	1.207393	-0.212740	C	3.405150	1.212731	-0.136297
N	2.319578	2.120464	-0.257095	N	2.354811	2.133226	-0.189551
C	-0.423037	-0.458387	0.233170	C	-0.442197	-0.399059	0.025035
C	1.291121	-1.906134	0.176748	C	1.260952	-1.881053	-0.118056
C	4.208951	-1.115446	0.003337	C	4.208449	-1.154042	0.028404
C	4.567510	1.913321	-0.418605	C	4.615362	1.933657	-0.270900
C	2.838554	3.323838	-0.484301	C	2.873145	3.348266	-0.366005
C	4.235974	3.237960	-0.601023	C	4.278079	3.265142	-0.428515
C	-0.085128	-1.822739	0.219036	C	-0.105130	-1.773685	-0.137804
F	-0.010273	2.364515	-0.792900	F	0.052297	2.461278	-0.751833
F	0.618084	2.377724	1.394702	F	0.623257	2.339811	1.444654
C	-1.783973	0.075829	0.273087	C	-1.779631	0.120306	0.104509
H	-0.785112	-2.643209	0.266555	H	-0.810371	-2.587183	-0.215193
H	1.897261	-2.797662	0.139734	H	1.856501	-2.772856	-0.227051
H	2.202622	4.195498	-0.543816	H	2.236226	4.219794	-0.411672
H	4.904146	4.063804	-0.789239	H	4.950218	4.100390	-0.555322
H	5.553752	1.476040	-0.420906	H	5.605298	1.508020	-0.242574
C	5.105013	-1.180182	-1.065702	C	5.274773	-1.103825	-0.880595
C	6.143329	-2.096723	-1.053583	C	6.283643	-2.049628	-0.840435
C	6.309786	-2.947550	0.029775	C	6.258207	-3.062801	0.108514
C	5.426896	-2.886633	1.098716	C	5.207207	-3.127918	1.014451
C	4.376620	-1.983833	1.084240	C	4.190465	-2.191389	0.972269
H	4.964654	-0.526729	-1.919358	H	5.282844	-0.338181	-1.647882
H	6.824061	-2.148302	-1.895837	H	7.090821	-2.002617	-1.563052
H	7.128011	-3.658808	0.041204	H	7.051890	-3.800520	0.140088
H	5.559530	-3.542429	1.951863	H	5.185902	-3.909186	1.766242
H	3.696525	-1.924493	1.926716	H	3.388812	-2.232262	1.701859
C	-2.799109	-0.617656	-0.387027	C	-2.837636	-0.629945	-0.445957
C	-4.111141	-0.166557	-0.381801	C	-4.144024	-0.182597	-0.415360
C	-4.419588	0.999747	0.318120	C	-4.429827	1.040782	0.202599
C	-3.435014	1.692546	0.997549	C	-3.416532	1.786849	0.781212
C	-2.128997	1.237902	0.969323	C	-2.112507	1.341896	0.729319
H	-2.548969	-1.507136	-0.956697	H	-2.619009	-1.560468	-0.958636
C	-5.181508	-0.853223	-1.162352	C	-5.246428	-0.933229	-1.084115

O	-5.735249	1.388810	0.299327	O	-5.746088	1.420117	0.214769
H	-3.682447	2.594516	1.549549	H	-3.645625	2.725128	1.278453
H	-1.365023	1.790933	1.500607	H	-1.339934	1.930356	1.205261
H	-6.600802	-0.343787	0.182264	H	-6.601286	-0.335546	0.292999
N	-6.358509	-1.225298	-0.290960	N	-6.371258	-1.247419	-0.124774
H	-5.591776	-0.202390	-1.938650	H	-5.703833	-0.344233	-1.883130
H	-4.821572	-1.771499	-1.628791	H	-4.901540	-1.881369	-1.499324
C	-7.521959	-1.660187	-1.099432	C	-7.570570	-1.752721	-0.834637
C	-6.000892	-2.225696	0.744270	C	-5.946142	-2.162994	0.962363
H	-6.849646	-2.364388	1.412189	H	-6.755495	-2.256209	1.684859
H	-5.760374	-3.166853	0.250179	H	-5.722220	-3.137346	0.528579
H	-5.137626	-1.864275	1.299759	H	-5.057714	-1.753334	1.439270
H	-8.357738	-1.879288	-0.436581	H	-8.368045	-1.925114	-0.113309
H	-7.793694	-0.862716	-1.789199	H	-7.887292	-1.013878	-1.569164
H	-7.248024	-2.555717	-1.656526	H	-7.315941	-2.687294	-1.333687
H	-5.838618	2.225719	0.763865	H	-5.835730	2.290188	0.618061

1-QM(S_0 minimum)				**1-QM**(S_1 minimum)			
B	0.455350	1.457514	-0.027068	B	0.469383	1.423100	0.001840
N	0.256863	-0.095763	0.006720	N	0.253993	-0.121644	0.014255
C	-0.990562	-0.695931	0.091758	C	-0.989519	-0.710675	0.053829
C	-2.181532	0.026694	0.000499	C	-2.191873	0.028482	-0.015886
C	-2.147742	1.407502	-0.202486	C	-2.131344	1.413321	-0.186616
N	-0.943214	2.069883	-0.290808	N	-0.911548	2.060723	-0.248665
C	1.189936	-1.070358	0.048265	C	1.194984	-1.116716	0.029256
C	-0.808421	-2.089982	0.216092	C	-0.825463	-2.117377	0.137445
C	-3.482393	-0.663473	0.085959	C	-3.494197	-0.646889	0.065717
C	-3.179351	2.336703	-0.457569	C	-3.146412	2.372949	-0.416757
C	-1.191497	3.347785	-0.576972	C	-1.135528	3.352993	-0.494029
C	-2.572823	3.557374	-0.687284	C	-2.515680	3.587838	-0.603205
C	0.541744	-2.323814	0.162357	C	0.518227	-2.365671	0.092741
F	0.900161	1.897095	1.212103	F	0.936569	1.848940	1.240513
F	1.319470	1.829852	-1.026230	F	1.341237	1.791629	-0.998970
C	2.635814	-0.900707	0.004886	C	2.618946	-0.965772	0.013816
H	1.041126	-3.276662	0.244912	H	0.996486	-3.330008	0.159513
H	-1.598576	-2.814517	0.336526	H	-1.624444	-2.835126	0.230408
H	-0.379985	4.050553	-0.697348	H	-0.311849	4.045480	-0.589787
H	-3.051372	4.495042	-0.923926	H	-2.975907	4.541499	-0.812175
H	-4.233417	2.107700	-0.487841	H	-4.203443	2.163392	-0.466976
C	-4.414049	-0.277469	1.050907	C	-4.445687	-0.221025	0.997646
C	-5.639799	-0.917435	1.137663	C	-5.679790	-0.843752	1.081309
C	-5.957159	-1.939819	0.255143	C	-5.991178	-1.895044	0.230775
C	-5.041153	-2.322990	-0.713892	C	-5.058518	-2.320802	-0.704926
C	-3.809437	-1.693444	-0.796853	C	-3.819914	-1.706455	-0.785991
H	-4.160376	0.514607	1.746600	H	-4.196856	0.588430	1.674998
H	-6.349209	-0.617310	1.900963	H	-6.400079	-0.509950	1.820229
H	-6.918867	-2.436553	0.321065	H	-6.958545	-2.380710	0.295572
H	-5.288128	-3.113168	-1.414338	H	-5.299965	-3.131851	-1.383322

H	-3.101149	-1.979047	-1.566424	H	-3.105149	-2.024406	-1.536797
C	3.294902	0.165116	0.521185	C	3.294951	0.199269	0.394733
C	4.732380	0.251429	0.482338	C	4.704390	0.314408	0.337688
C	5.532234	-0.856287	-0.137616	C	5.518180	-0.861002	-0.065936
C	4.751072	-1.968715	-0.669590	C	4.766740	-2.043406	-0.444667
C	3.410883	-1.980659	-0.591848	C	3.410313	-2.088752	-0.392455
H	2.753257	0.971345	0.999201	H	2.737166	1.031978	0.801252
C	5.387066	1.306364	0.992497	C	5.346705	1.475866	0.647708
O	6.747711	-0.826967	-0.192688	O	6.741677	-0.831199	-0.075636
H	5.305907	-2.775405	-1.134413	H	5.345857	-2.895129	-0.783262
H	2.863989	-2.816108	-1.017542	H	2.904517	-2.995895	-0.702048
H	6.469907	1.334957	0.943622	H	6.428776	1.509560	0.597485
H	4.855562	2.134064	1.448899	H	4.795727	2.367421	0.924623

4. Irradiation experiments

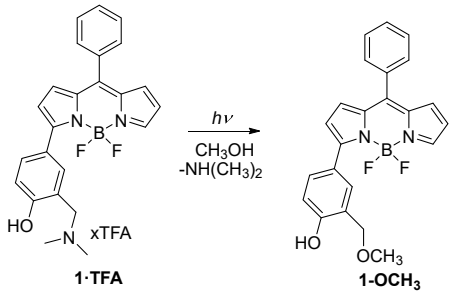

Scheme S1. Photochemical reaction of **1·TFA**.

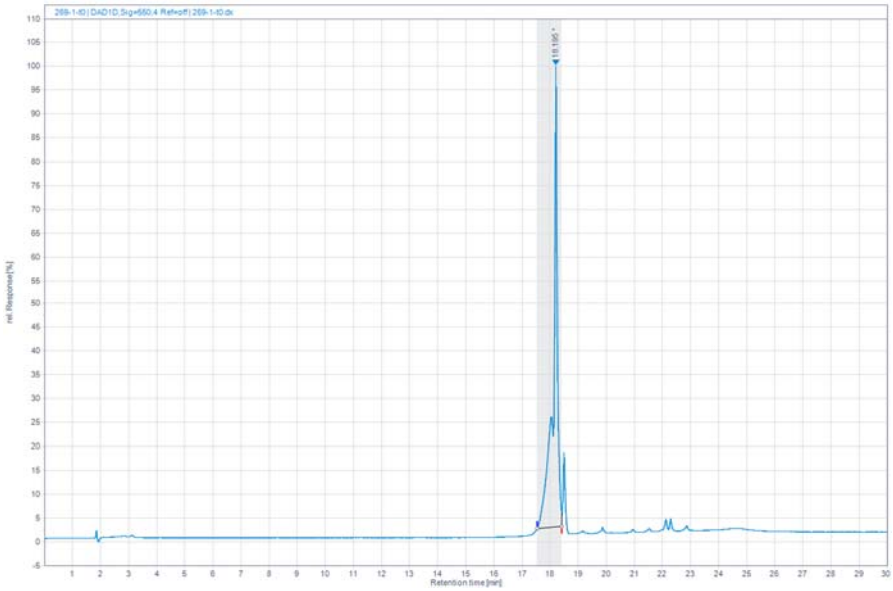

Fig S16. HPLC chromatogram of **1·TFA** before the irradiation**.**

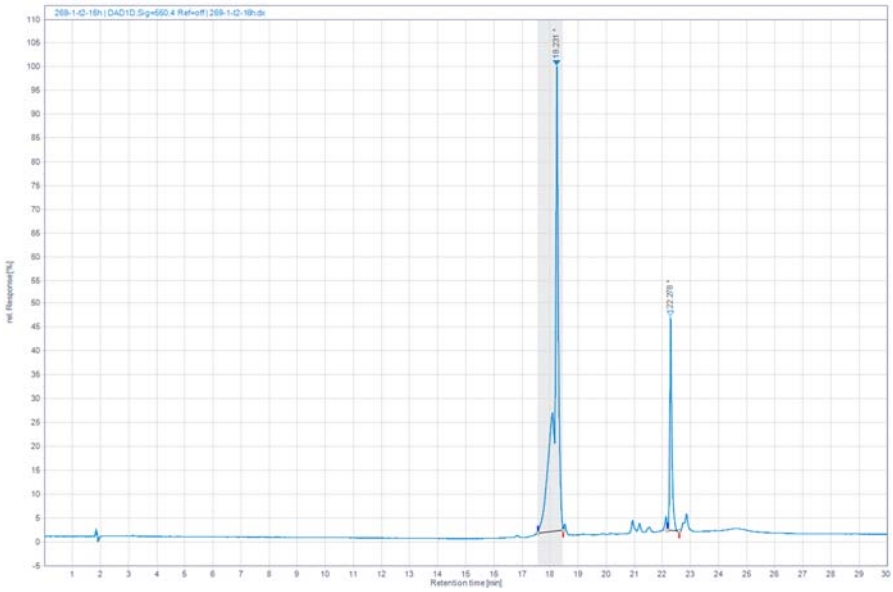

Fig S17. HPLC chromatogram of **1·TFA** after 16 h irradiation in CH_3OH at 350 nm (8 lamps × 8W).

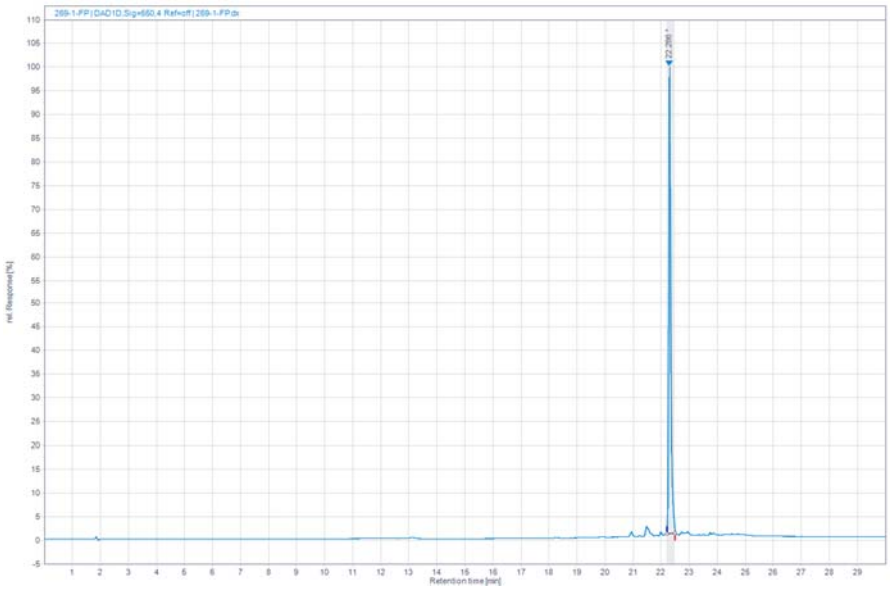

Fig S18. HPLC chromatogram of **1-OCH$_3$** after preparative HPLC separation from the photolysis mixture.

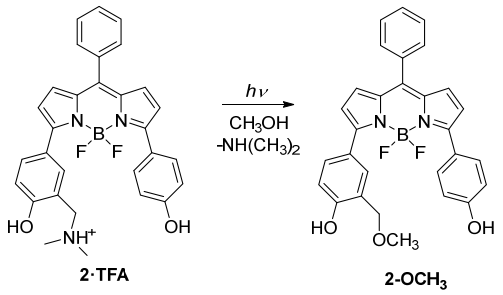

Scheme S2. Photochemical reaction of **2·TFA**.

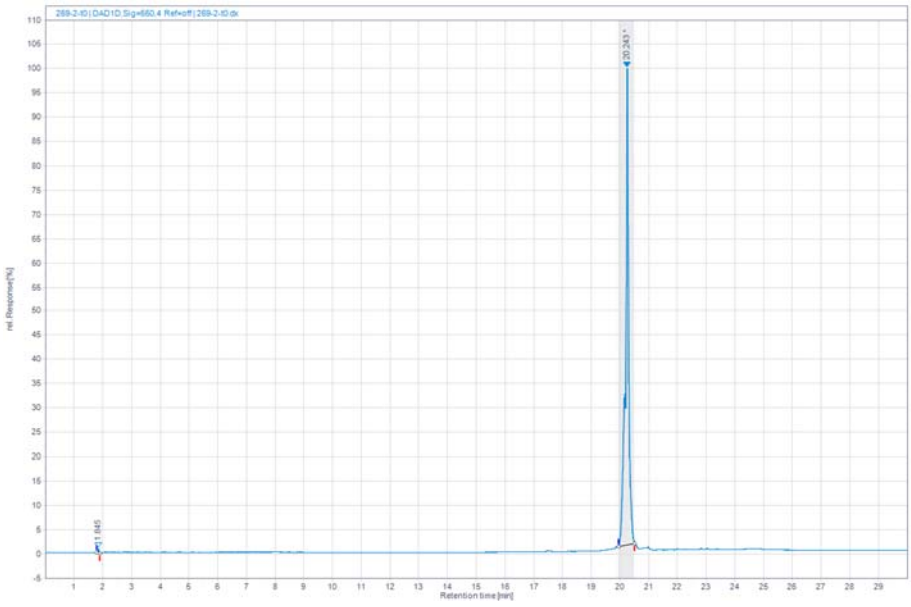

Fig S19. HPLC chromatogram of **2·TFA** before the irradiation**.**

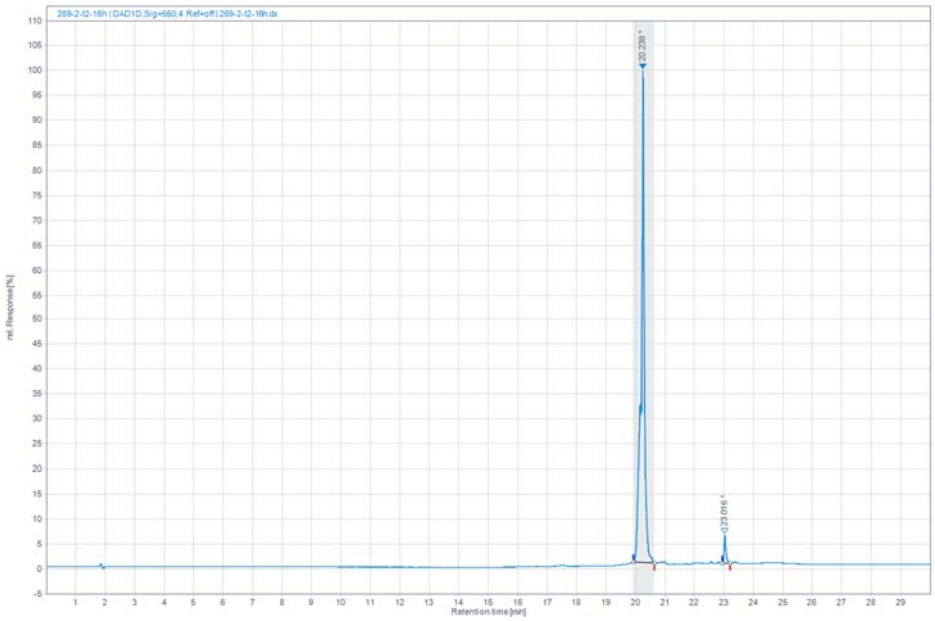

Fig S20. HPLC chromatogram of **2·TFA** after 16 h irradiation in CH_3OH at 350 nm (8 lamps × 8W).

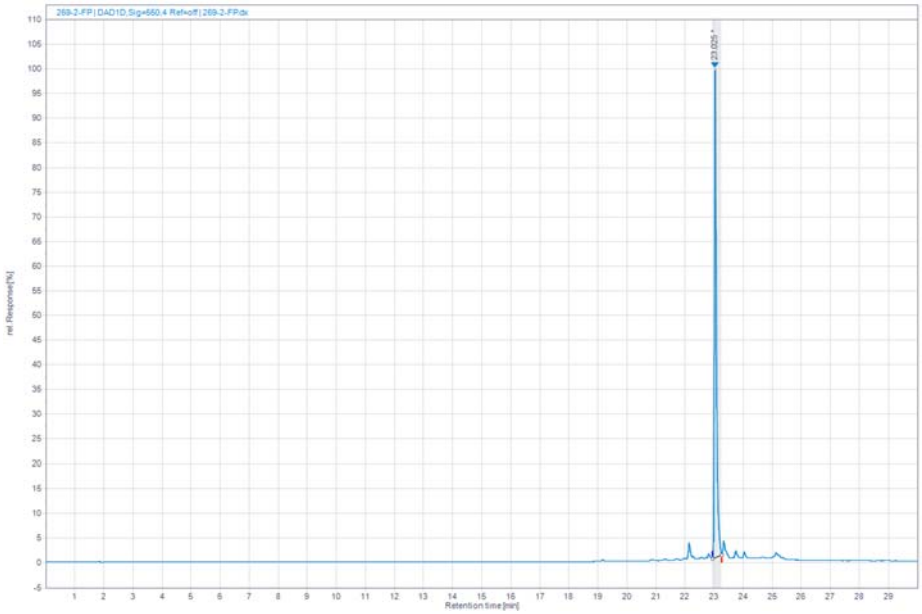

Fig S21. HPLC chromatogram of **2-OCH$_3$** after preparative HPLC separation from the photolysis mixture.

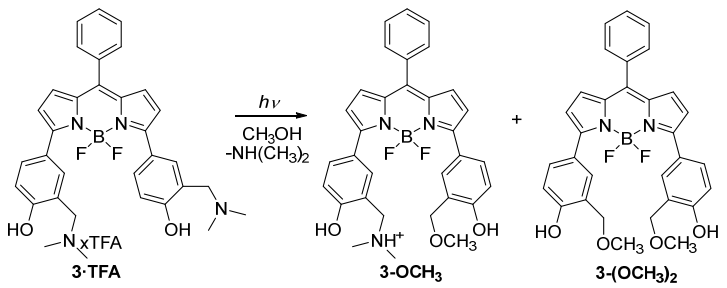

Scheme S3. Photochemical reaction of **3·TFA**.

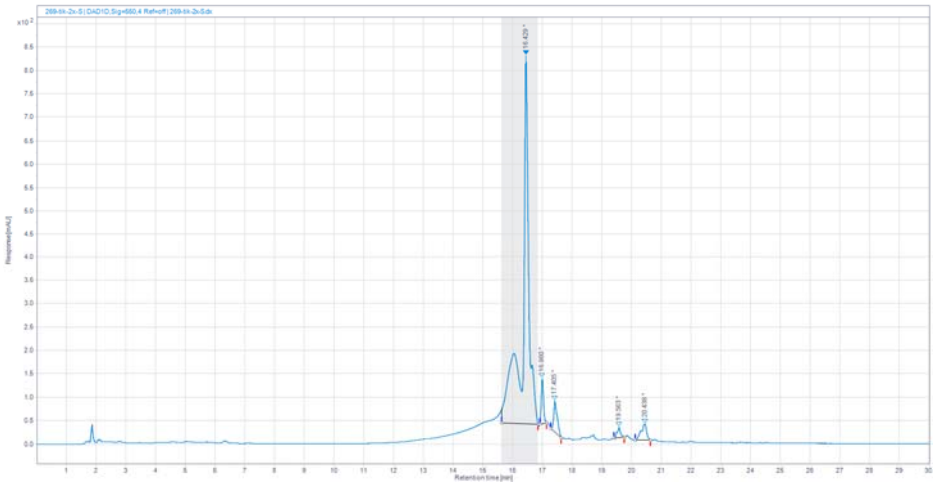

Fig S22. HPLC chromatogram of **3·TFA** before the irradiation**.**

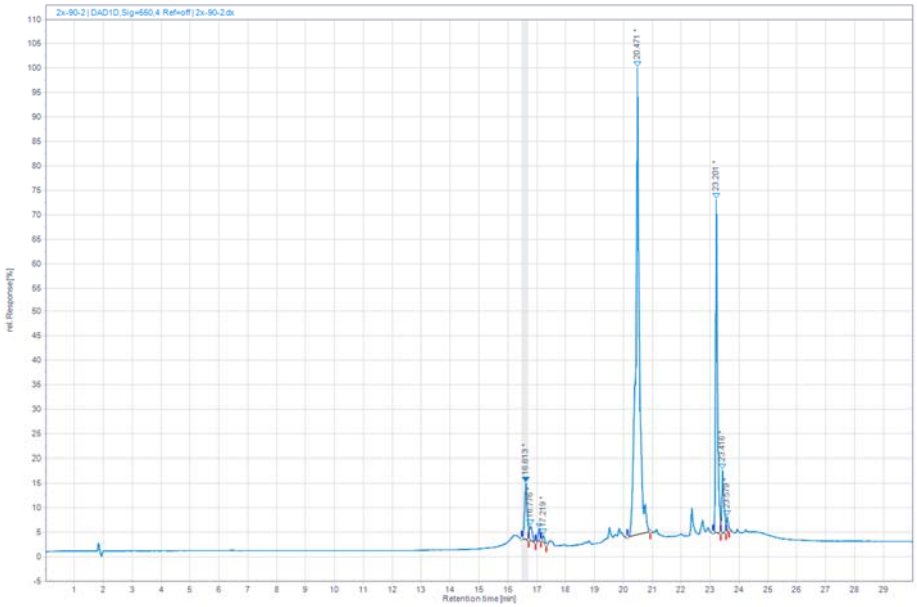

Fig S23. HPLC chromatogram of **3·TFA** after 16 h irradiation in CH_3OH at 350 nm (8 lamps × 8W).

Characterization of products by HPLC-MS after the irradiation of 3·TFA

Table S7. Calculated molecular weights of **3·TFA** and anticipated photoproducts **3-OCH$_3$** and **3-(OCH$_3$)$_2$**

Compound	3·TFA	3-OCH$_3$	3-(OCH$_3$)$_2$
M_r	567.5	553.4	540.4

HPLC-MS analysis after the irradiation of 3·TFA in CH$_3$OH at 350 nm

9.25-10.12 min: (ESI-) 565.2, (ESI+) 567.4, (ESI+) 568.4;

10.42-11.24 min: (ESI-) 565.2, (ESI+) 567.4, (ESI+) 568.4;

13.29-13.96 min: (ESI-) 552.1 (ESI+) 554.4

HPLC-MS analysis after the irradiation of 3·TFA in CH$_3$OH-H$_2$O at pH 7 at 350 nm

9.59-9.97 min: (ESI-) 565.2, (ESI+) 567.4, (ESI+) 568.4,

13.32-13.74 min: (ESI-) 552.1 (ESI+) 554.4,

16.43-16.94 min: (ESI-) 539.1

HPLC-MS analysis after the irradiation of 3·TFA in CH$_3$OH-H$_2$O at pH 9 at 350 nm

9.46-9.87 min: (ESI-) 565.2, (ESI+) 567.4, (ESI+) 568.4,

13.20-13.67 min: (ESI-) 552.1 (ESI+) 554.4,

14.34-14.78 min: (ESI-) 552.1 (ESI+) 554.4,

16.43-16.92 min: (ESI-) 539.1

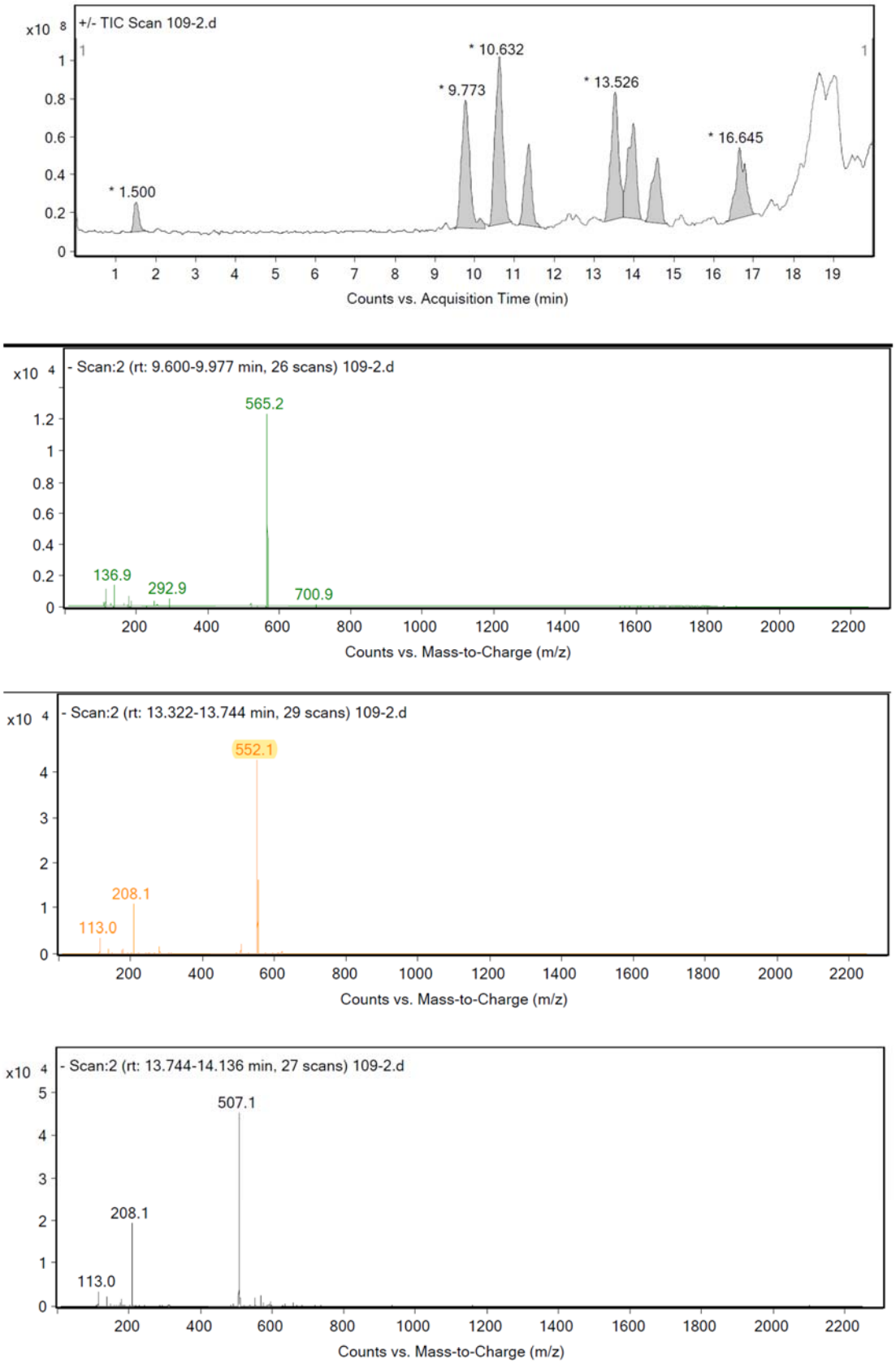

Fig S24. HPLC-MS chromatogram and the corresponding ESI-MS of **3·TFA** after 16 h irradiation at 350 nm (8 lamps × 8W) in CH_3OH-H_2O (pH 7).

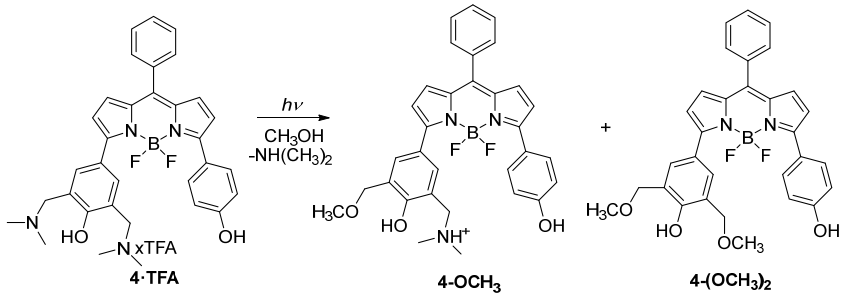

Scheme S4. Photochemical reaction of **4·TFA**.

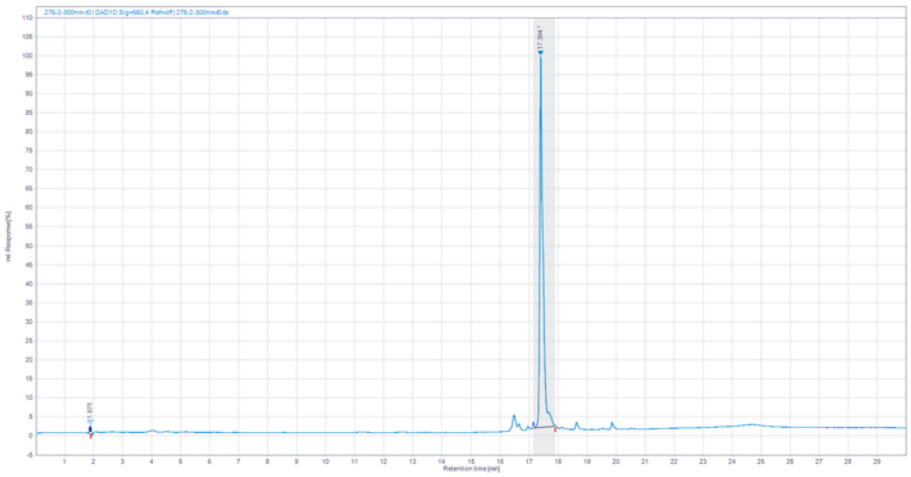

Fig S25. HPLC chromatogram of **4·TFA** before the irradiation.

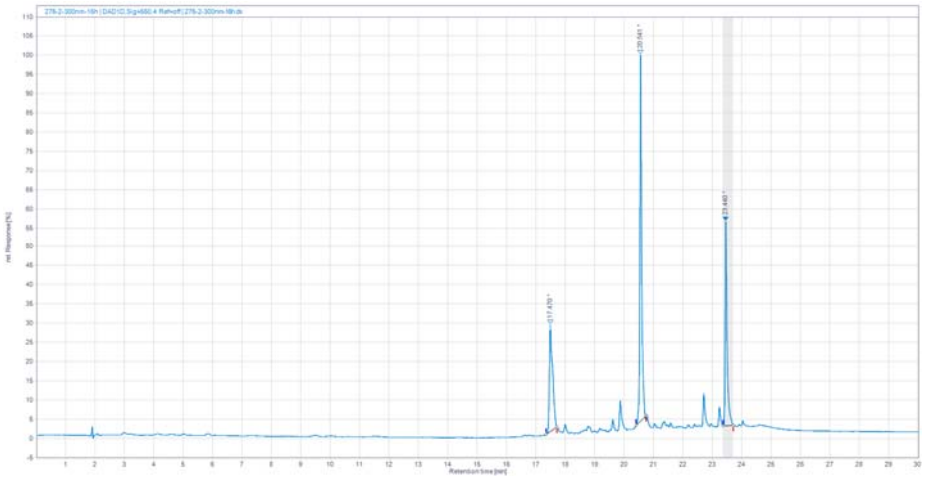

Fig S26. HPLC chromatogram of **4·TFA** after 16 h irradiation at 350 nm (8 lamps × 8W) in CH_3OH-H_2O (1:1, v/v) in the presence of phosphate buffer (pH 7.0, 50 mM).

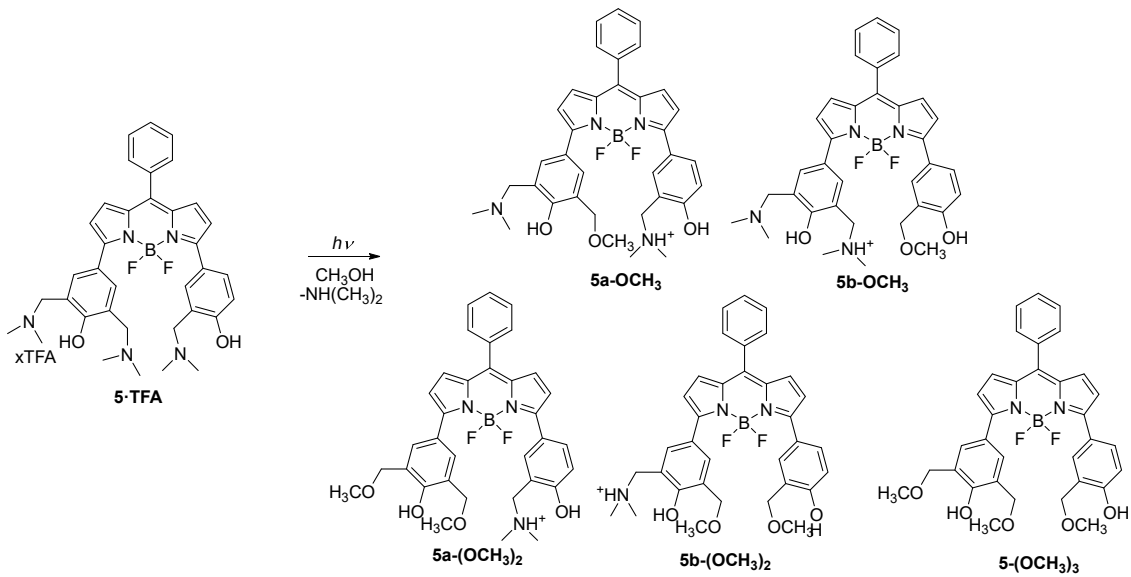

Scheme S5. Photochemical reaction of **5·TFA**.

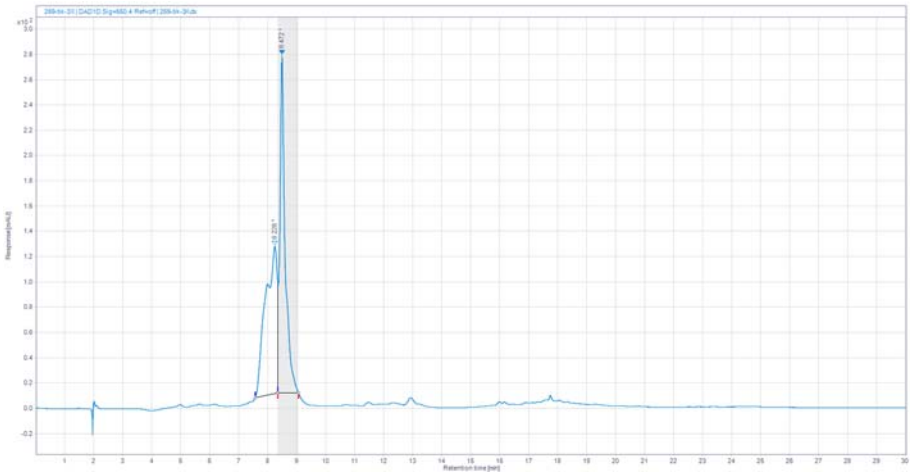

Fig S27. HPLC chromatogram of **5·TFA** before the irradiation.

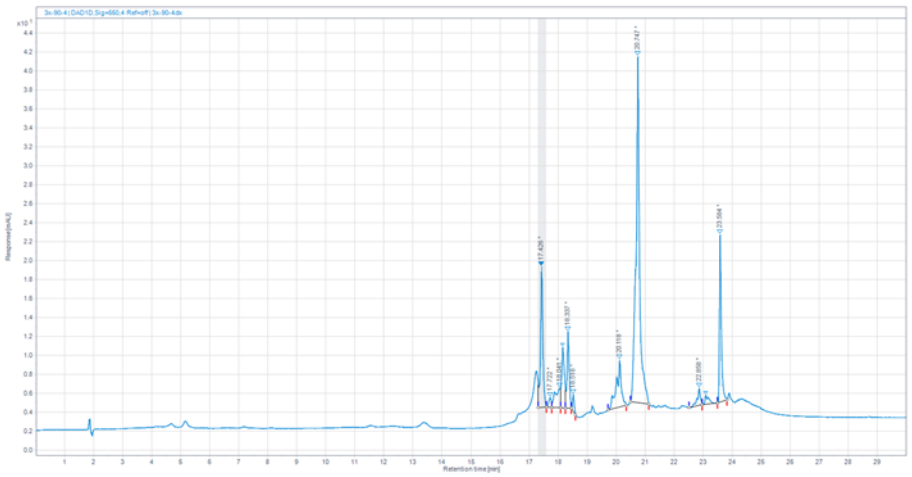

Fig S28. HPLC chromatogram of **5·TFA** after 16 h irradiation in CH_3OH at 350 nm (8 lamps × 8W).

Table S8. Calculated molecular weights of **5·TFA** and anticipated photoproducts **5-OCH$_3$**, **5-(OCH$_3$)$_2$** and **5-(OCH$_3$)$_3$**

Compound	**5·TFA**	**5-OCH$_3$**	**5-(OCH$_3$)$_2$**	**5-(OCH$_3$)$_3$**
M$_r$	624.6	610.5	584.4	597.5

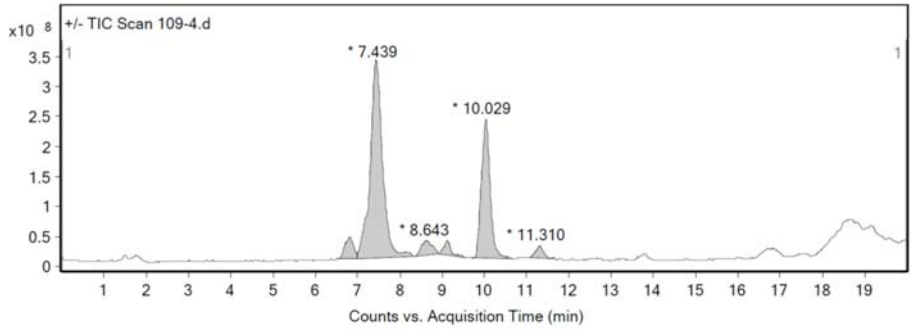

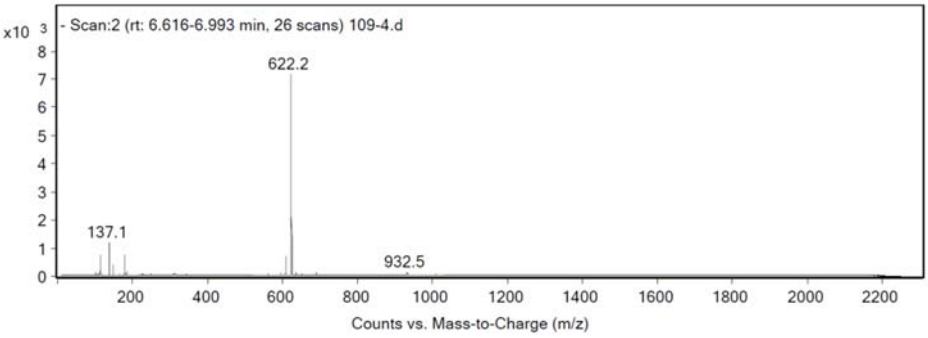

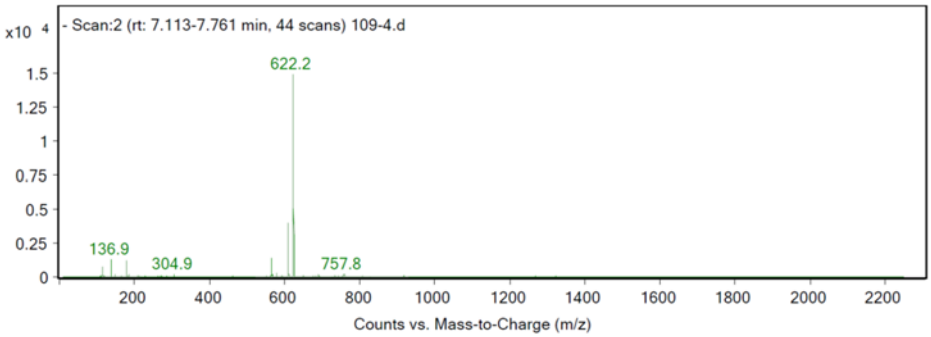

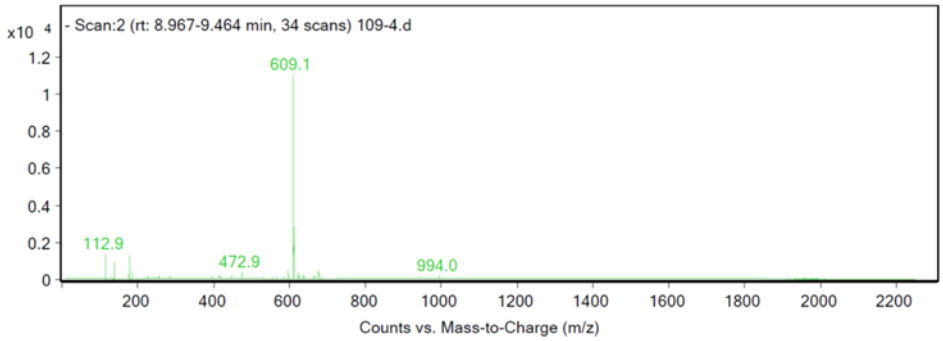

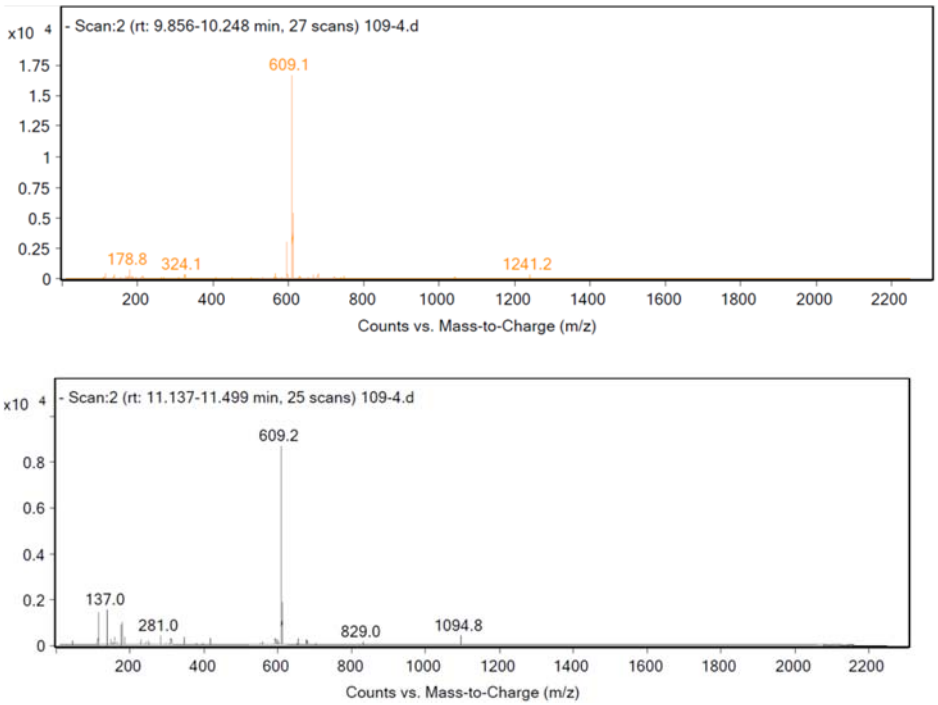

Fig S29. HPLC-MS chromatogram and the corresponding ESI-MS of **5·TFA** after 16 h irradiation at 350 nm (8 lamps × 8W) in CH_3OH.

HPLC-MS analysis after the irradiation of 5·TFA in CH_3OH at 350 nm

6.62-6.99 min: (ESI-) 622.2, (ESI+) 624.4, (ESI+) 625.4,

7.11-7.75 min: (ESI-) 622.2, (ESI+) 624.4, (ESI+) 625.4,

8.97-9.46 min: (ESI-) 609.1 (ESI+) 611.5,

9.85-10.24 min: (ESI-) 609.1 (ESI+) 611.5,

11.13-11.49 min: (ESI-) 609.1 (ESI+) 611.5

HPLC-MS analysis after the irradiation of 5·TFA in CH_3OH-H_2O at pH 7 at 350 nm

9.31-9.86 min: (ESI-) 609.2 (ESI+) 611.4,

9.86-10.25 min: (ESI-) 609.2 (ESI+) 611.4,

13.59-13.93 min: (ESI-) 596.2 (ESI+) 598.4

HPLC-MS analysis after the irradiation of 5·TFA in CH_3OH-H_2O at pH 7 at 350 nm

9.83-10.23 min: (ESI-) 609.2 (ESI+) 611.4,

13.53-13.91 min: (ESI-) 596.1 (ESI+) 598.4

Quantum yields for the photomethanolysis were calculated by use of Eqs. S2-S4. The measurement was performed in triplicate and the average value was reported.

The number of the absorbed photons for the ferrioxalate actinometer was calculated from:

$$n(\text{absorbed photons}) = \frac{\Delta A_{510} \times V_{irr}}{\varepsilon_{510} \times \ell \times \Phi_{lit.}} \times \frac{V_{\text{phen}}}{V_{irr}} \qquad \text{(S2)}$$

where:

ΔA_{510} absorbance difference at 510 nm for the irradiated and non-irradiated sample

V_{irr} volume of the solution which was irradiated

V_{phen} added volume of the phenanthroline solution

ε_{510} molar absorption coefficient for $[Fe(phen)_3]^{2+}$, that is 11100 M^{-1} cm^{-1}

l length of the optical path (1 cm in all experiments)

$\Phi_{\text{lit.}}$ quantum yield for the actinometer, $\Phi_{300} = 1.25$

The quantum yield of the photomethanolysis (for 300 nm irradiation) was calculated according to:

$$\Phi = \frac{A_{300} \cdot V_{\text{irr}} \cdot x(\text{photoproduct})}{\varepsilon_{300} \cdot \ell \cdot n(\text{total photons}) \cdot (1 - T_{355})} \qquad \text{(S3)}$$

For the absorbances in the range 0.4-0.8 the number of absorbed photons was calculated according to:

$$n(\text{absorbed photons}) = n(\text{total photons}) \times (1 - T) \qquad \text{(S4)}$$

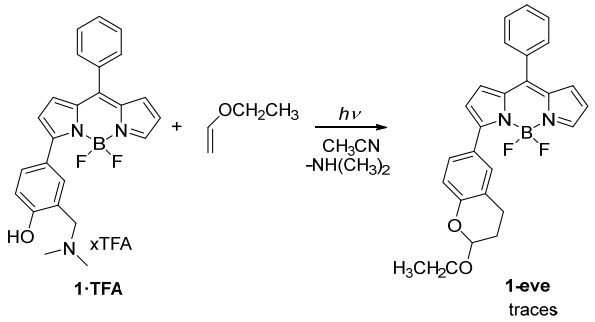

Scheme S6. Photolysis of **1·TFA** in the presence of EVE.

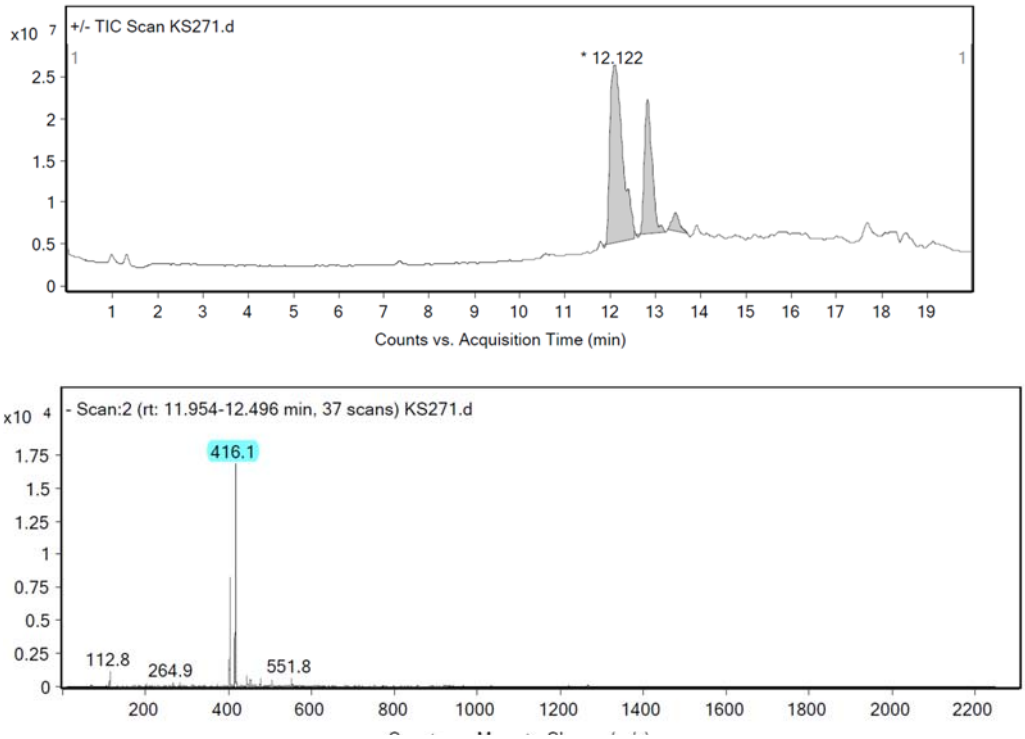

112.8		1170.31
401		2106.98
402.1	1	8306.45
403	1	2966.15
415		4329.22
416.1	1	16869.81
417	1	5217.42
418	1	906.23
444.1	1	797.37
551.8		605.08

Fig S30. HPLC-MS chromatogram and the corresponding ESI-MS of **1·TFA** after 10 h irradiation at 350 nm (8 lamps × 8W) in CH_3CN in the presence of EVE.

5. Laser Flash Photolysis

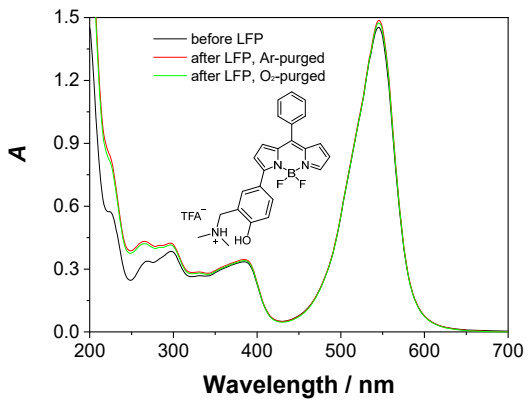

Fig S31. Absorption spectra of **1·TFA** in CH_3CN, before and after the LFP experiment.

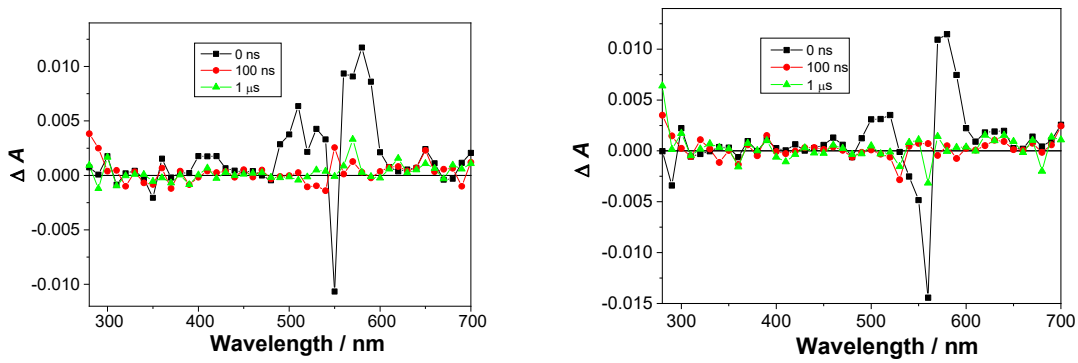

Fig S32. Transient absorption spectra of **1·TFA** in Ar-purged (left) and O_2-purged (right) CH_3CN solution (c = 2.7×10^{-5} M, A_{355} = 0.29). Laser energy was 21 mJ/pulse.

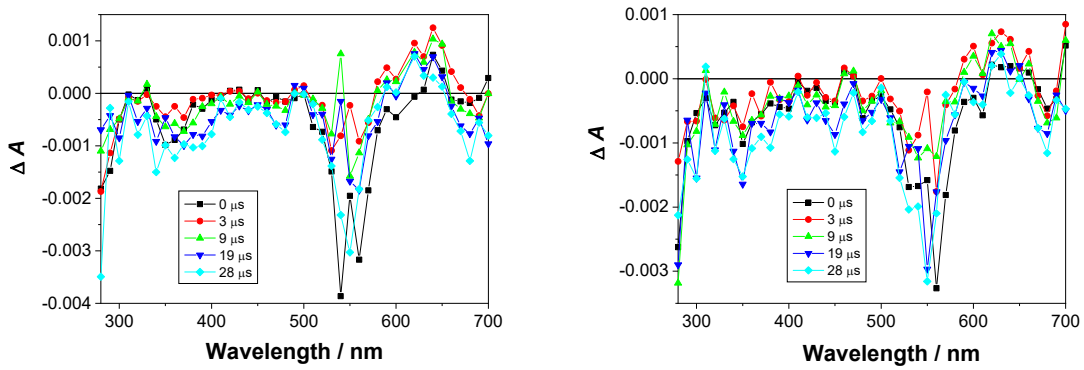

Fig S33. Transient absorption spectra of **1·TFA** in Ar-purged (left) and O_2-purged (right) CH_3CN solution (c = 2.7×10^{-5} M, A_{355} = 0.29). Laser energy was 21 mJ/pulse.

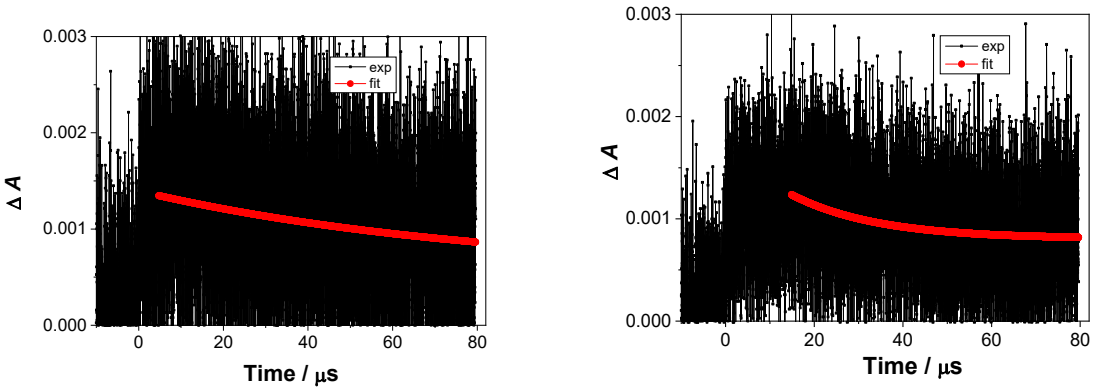

Fig S34. Decay of transient absorption of **1·TFA** in Ar-purged (left) and O_2-purged (right) CH_3CN solution ($c = 2.7\times10^{-5}$ M, $A_{355} = 0.29$) at 640 nm. The fitting revealed lifetimes of τ = 50 ± 30 μs in Ar-purged solution, and τ = 27 ± 7 μs in O_2-purged solution.

There may be something short-lived, $\tau \approx 10$ ns, but it may be an artefact.

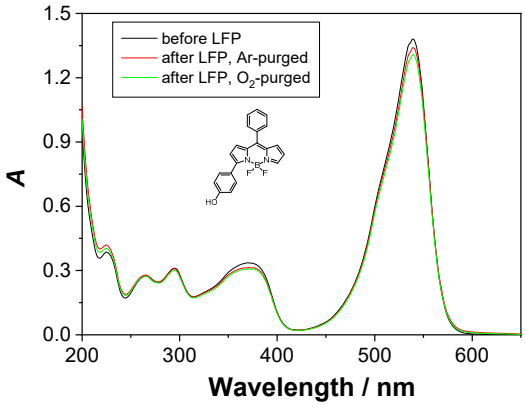

Fig S35. Absorption spectra of **8** in CH_3CN, before and after the LFP experiment.

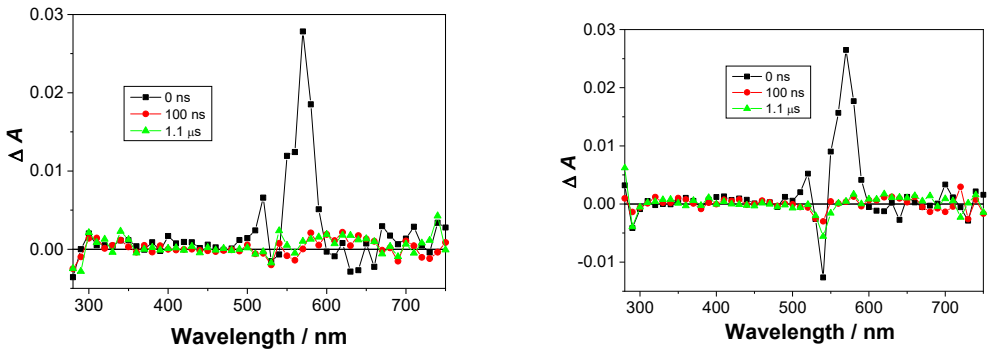

Fig S36. Transient absorption spectra of **8** in Ar-purged (left) and O_2-purged (right) CH_3CN solution ($c = 2.2\times10^{-5}$ M, $A_{355} = 0.29$). Laser energy was 21 mJ/pulse.

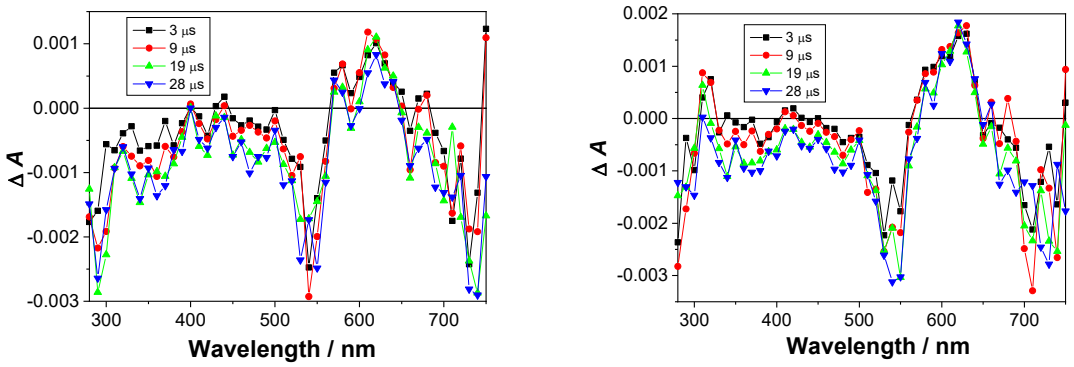

Fig S37. Transient absorption spectra of **8** in Ar-purged (left) and O_2-purged (right) CH_3CN solution ($c = 2.2\times10^{-5}$ M, $A_{355} = 0.29$). Laser energy was 21 mJ/pulse.

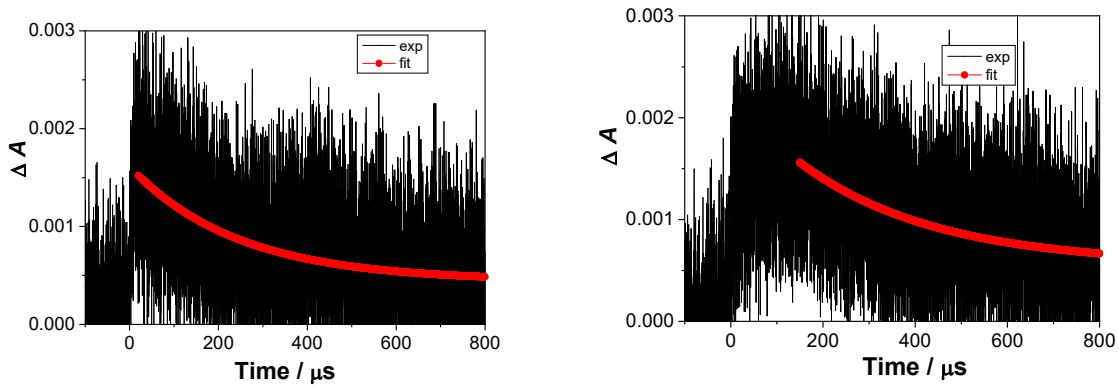

Fig S38. Decay of transient absorbance of **8** in Ar-purged (left) and O_2-purged (right) CH_3CN solution ($c = 2.2\times10^{-5}$ M, $A_{355} = 0.32$) at 640 nm. Laser energy was 22 mJ/pulse. The decay was fit to an exponential function with the lifetimes of $\tau = 240 \pm 20$ μs in Ar-purged solution, and $\tau = 290 \pm 40$ μs in O_2-purged solution.

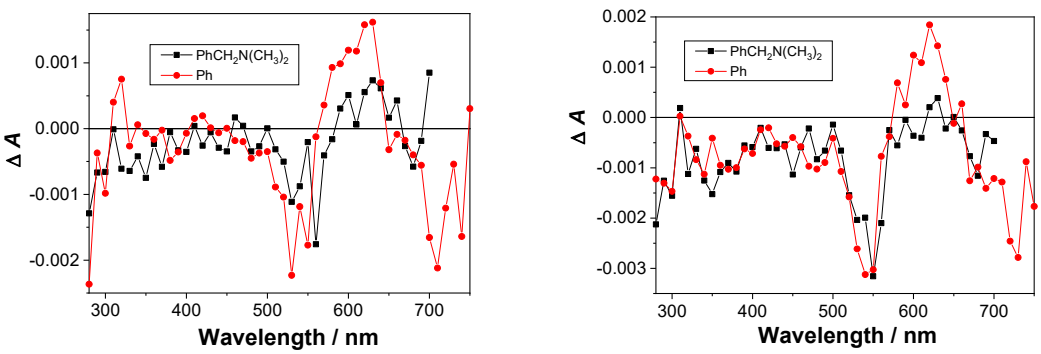

Fig S39. Transient absorption spectra measured in O_2-purged CH_3CN for the phenolic compound **8** and the photoreactive compound **1·TFA**, measured 3 μs (left) or 28 μs after the laser pulse (right). The solutions were optically matched at the excitation wavelength.

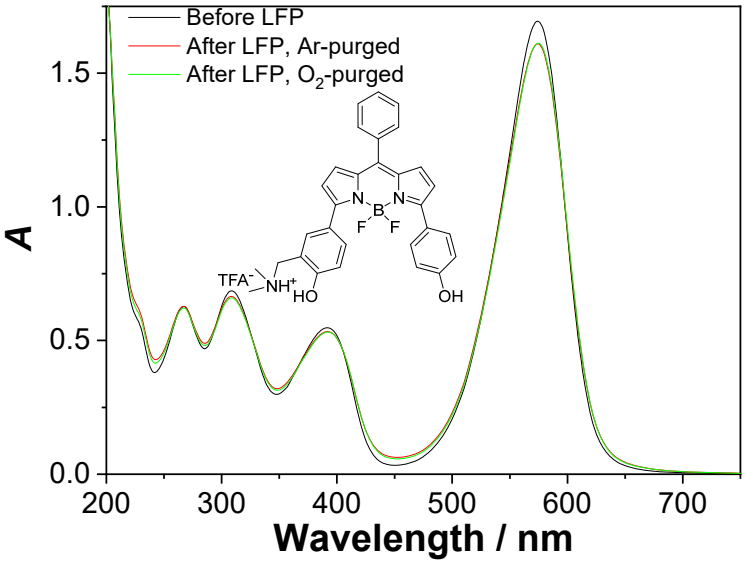

Fig S40. Absorption spectra of **2·TFA** in CH_3CN, before and after the LFP experiment.

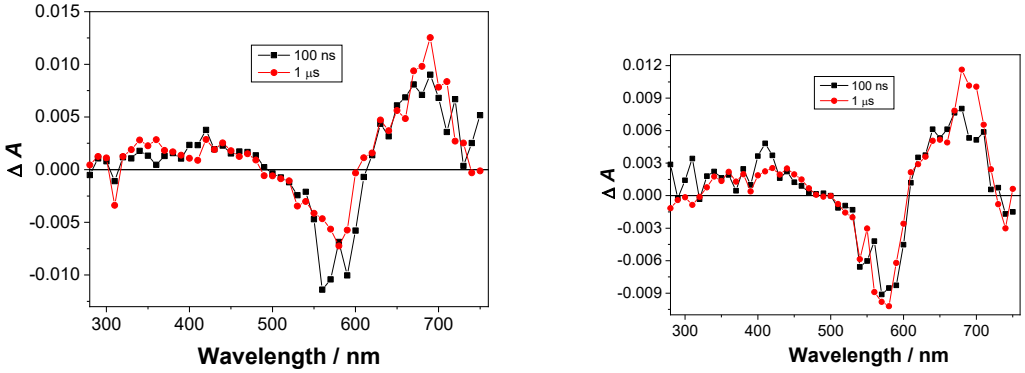

Fig S41. Transient absorption spectra of **2·TFA** in Ar-purged (left) and O_2-purged (right) CH_3CN solution ($c = 4.7\times10^{-5}$ M, $A_{355} = 0.32$). Laser energy was 22 mJ/pulse.

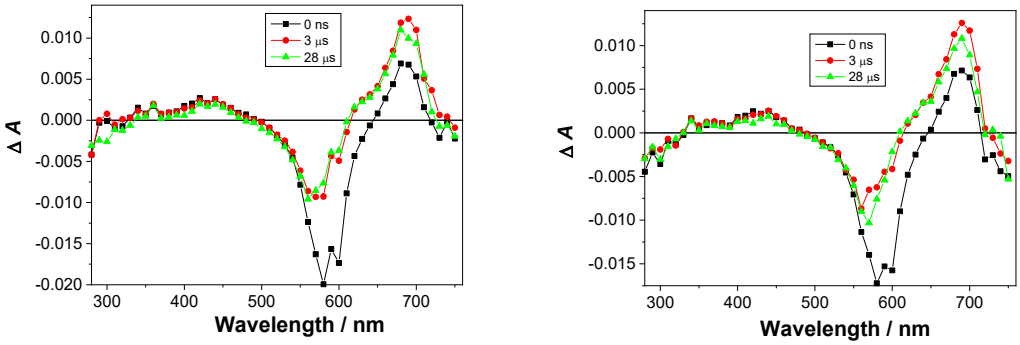

Fig S42. Transient absorption spectra of **2·TFA** in Ar-purged (left) and O_2-purged (right) CH_3CN solution ($c = 4.7\times10^{-5}$ M, $A_{355} = 0.32$). Laser energy was 22 mJ/pulse.

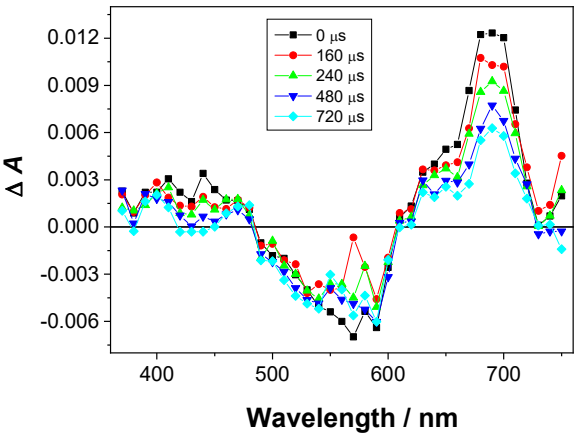

Fig S43. Transient absorption spectra of **2·TFA** in O_2-purged CH_3CN solution ($c = 4.7\times10^{-5}$ M, $A_{355} = 0.32$). Laser energy was 22 mJ/pulse.

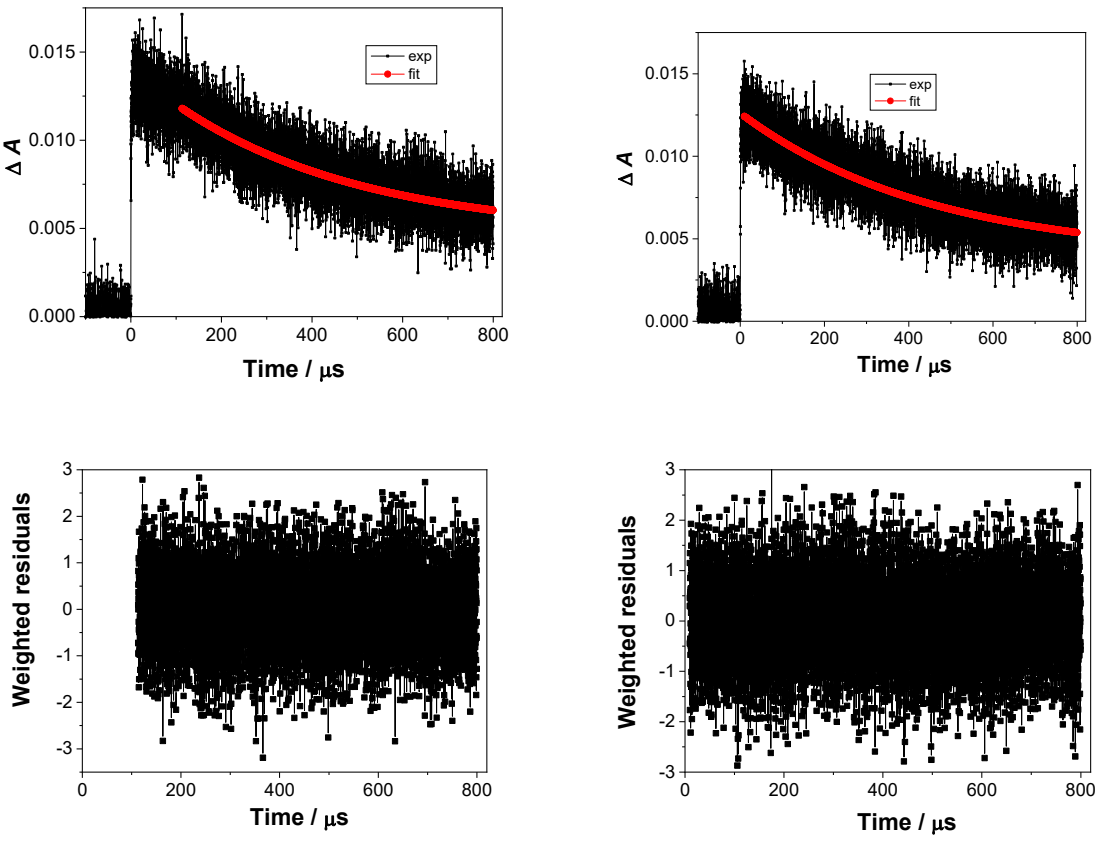

Fig S44. Decay of transient absorbance at 680 nm in Ar-purged (left) and O_2-purged (right) CH_3CN solution of **2·TFA** ($c = 4.7\times10^{-5}$ M, $A_{355} = 0.32$). Laser energy was 22 mJ/pulse. Bottom panels are weighted residuals between calculated and experimental values.

One transient was detected with the maximum of absorption at 680 nm, tentatively assigned to quinone methide or phenoxyl radical-cation since it is not quenched by O_2. The estimated lifetime in Ar-purged solution was $\tau = 430 \pm 20$ μs, and in O_2-purged solution $\tau = 430 \pm 40$ μs.

The transient at 350-500 nm could be QM or phenoxyl radical-cation; but it may be something that has a shorter lifetime of τ≈ 280 ± 10 μs. It is also not quenched by O_2.

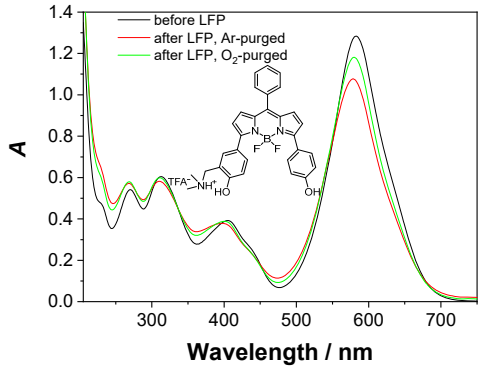

Fig S45. Absorption spectra of **2** in CH_3CN-H_2O (1:1 v/v), in the presence of sodium phosphate buffer (50 mM, pH 7.0) before and after the LFP experiment.

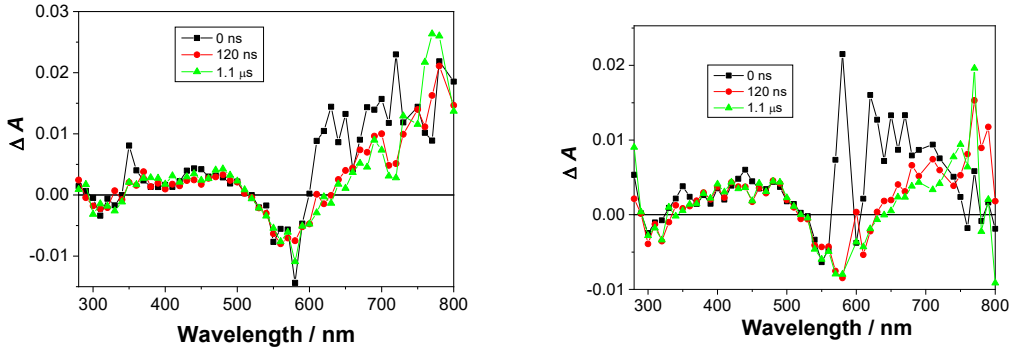

Fig S46. Transient absorption spectra of **2** in Ar-purged (left) and O_2-purged (right) CH_3CN-H_2O (1:1 v/v), in the presence of sodium phosphate buffer (50 mM, pH 7.0) (c = 4.7×10^{-5} M, A_{355} 0.32). Laser energy was 22 mJ/pulse.

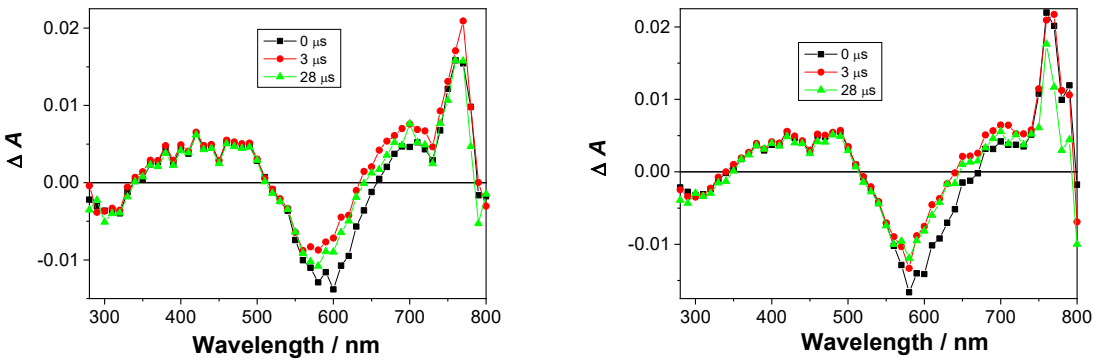

Fig S47. Transient absorption spectra of **2** in Ar-purged (left) and O_2-purged (right) CH_3CN-H_2O (1:1 v/v), in the presence of sodium phosphate buffer (50 mM, pH 7.0) (c = 4.7×10^{-5} M, A_{355} = 0.32). Laser energy was 22 mJ/pulse.

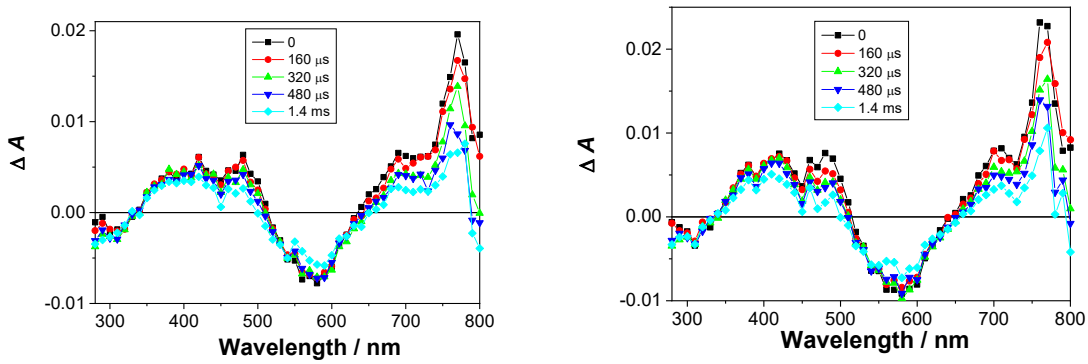

Fig S48. Transient absorption spectra of **2** in Ar-purged (left) and O_2-purged (right) CH_3CN-H_2O (1:1 v/v), in the presence of sodium phosphate buffer (50 mM, pH 7.0) ($c = 4.7\times10^{-5}$ M, $A_{355} = 0.32$). Laser energy was 22 mJ/pulse.

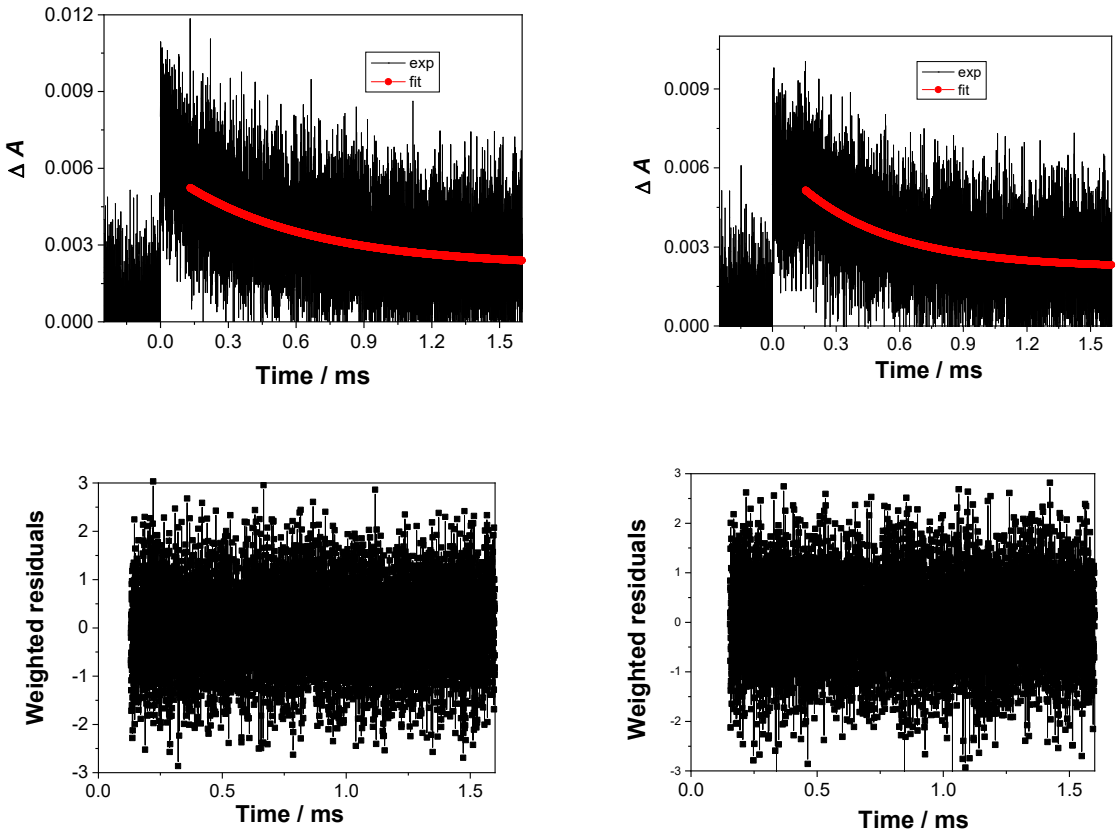

Fig S49. Decay of transient absorbance of **2** in Ar-purged (left) and O_2-purged (right) CH_3CN solution ($c = 4.7\times10^{-5}$ M, $A_{355} = 0.32$) at 680 nm. Laser energy was 22 mJ/pulse. Bottom panels are weighted residuals between calculated and experimental values.

One transient was detected with the maximum of absorption at 770 nm and a shoulder at 680 nm, tentatively assigned to quinone methide or phenoxyl radical-cation since it is not quenched by O_2. The estimated lifetime in Ar-purged solution was $\tau = 520 \pm 50$ µs, and in O_2-purged solution $\tau = 500 \pm 100$ µs.

The transient at 350-500 nm could be QM; it seems that it has the same decay kinetics.

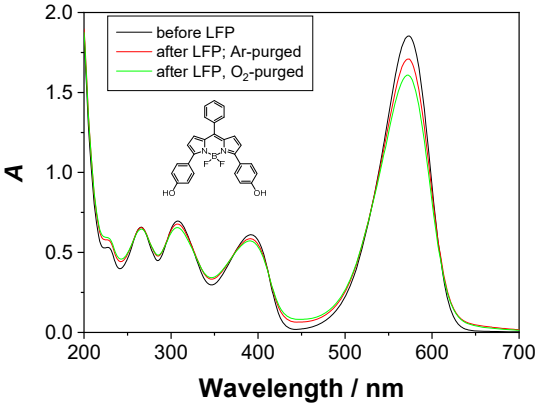

Fig S50. Absorption spectra of **12** in CH_3CN, before and after the LFP experiment.

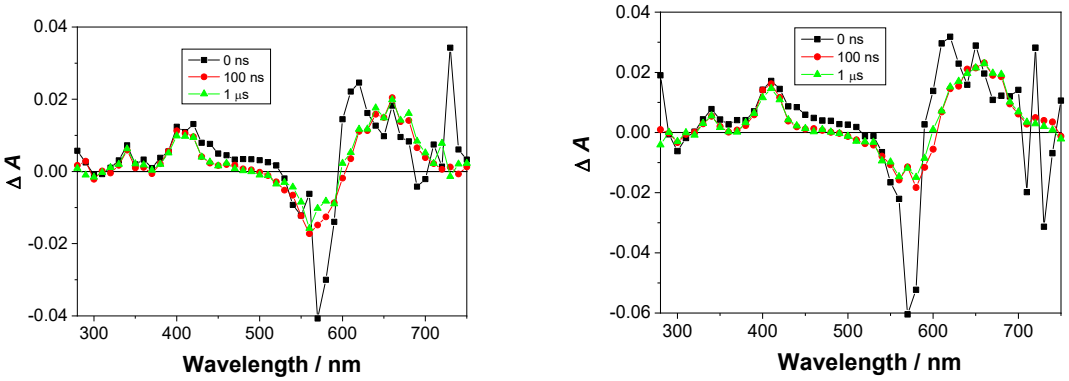

Fig S51. Transient absorption spectra of **12** in Ar-purged (left) and O_2-purged (right) CH_3CN solution (c = 3.6×10^{-5} M, A_{355} = 0.30). Laser energy was 23 mJ/pulse.

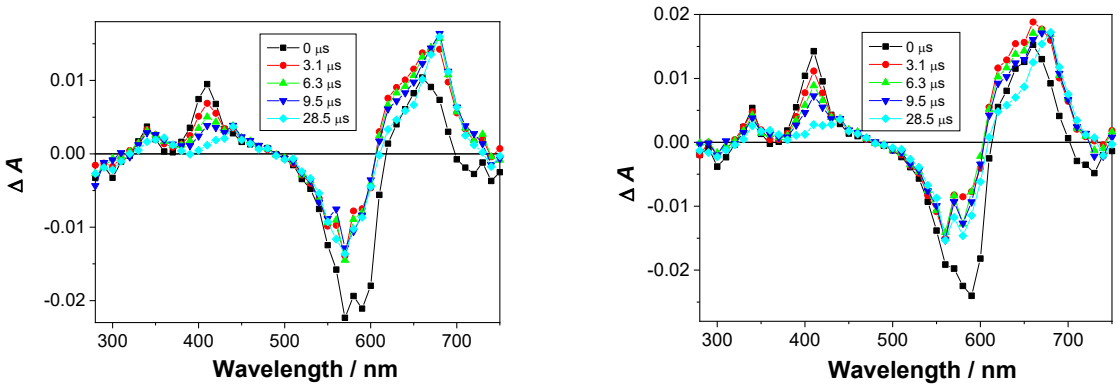

Fig S52. Transient absorption spectra of **12** in Ar-purged (left) and O_2-purged (right) CH_3CN solution (c = 3.6×10^{-5} M, A_{355} = 0.30). Laser energy was 23 mJ/pulse.

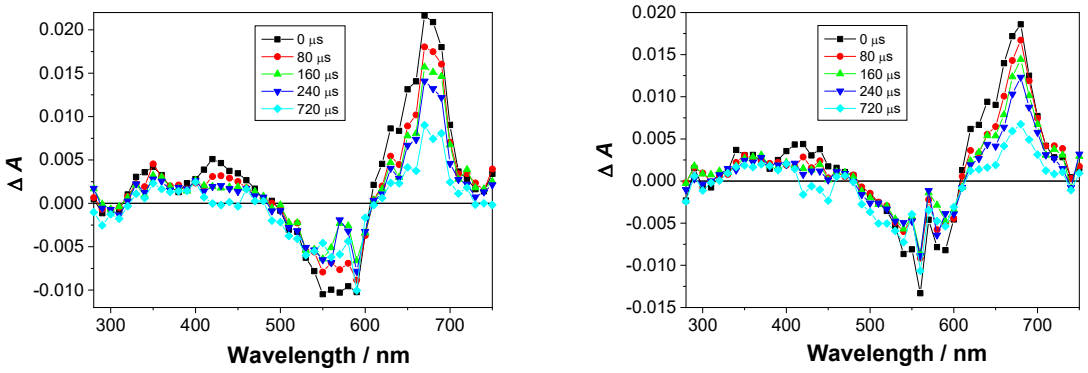

Fig S53. Transient absorption spectra of **12** in Ar-purged (left) and O_2-purged (right) CH_3CN solution (c = 3.6×10^{-5} M, A_{355} = 0.30). Laser energy was 23 mJ/pulse.

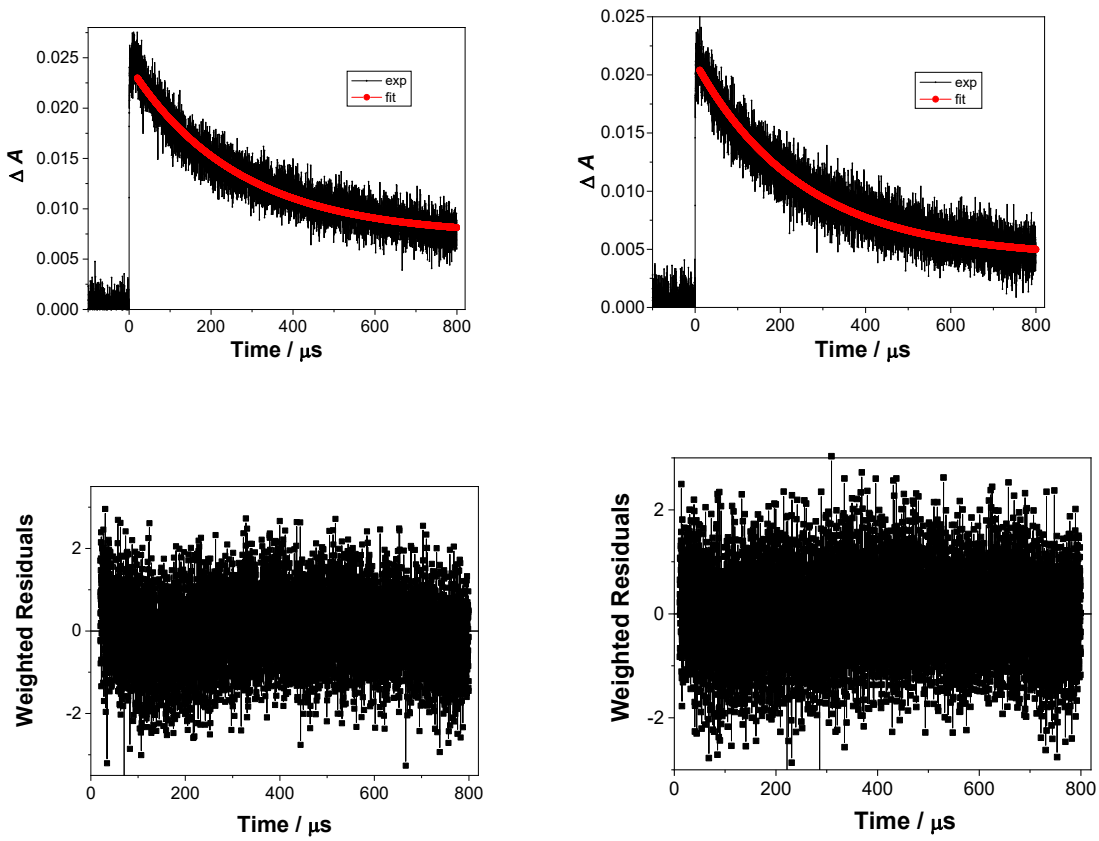

Fig S54. Decay of transient absorbance of **12** in Ar-purged (left) and O_2-purged (right) CH_3CN solution (c = 3.6×10^{-5} M, A_{355} = 0.32) at 680 nm. Laser energy was 23 mJ/pulse. Bottom panels are weighted residuals between calculated and experimental values.

One transient was detected with the maximum of absorption at 680 nm, tentatively assigned to phenoxyl radical since it was not quenched by O_2. The estimated lifetime in Ar-purged solution was $\tau \approx 520 \pm 20$ µs, and in O_2-purged solution $\tau = 570 \pm 20$ µs.

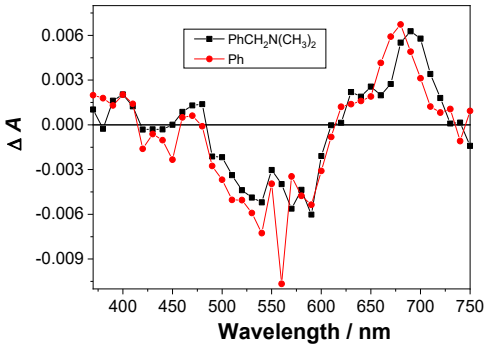

Fig S55. Transient absorption spectra measured in O_2-purged CH_3CN for **12** and **2·TFA**, measured 720 μs after the laser pulse. The solutions were optically matched at the excitation wavelength.

6. Antiproliferative Activity

MTT tests

The experiments were carried out on human carcinoma cell lines HCT-116 (colon), H460 (lung), and MCF-7. The cells were cultured as monolayers and maintained in Dulbecco's modified Eagle medium (DMEM) supplemented with 10% fetal bovine serum (FBS), 2 mM L-glutamine, 100 U/mL penicillin and 100 μg/mL streptomycin in a humidified atmosphere with 5% CO_2 at 37 °C.

The cells were inoculated in parallel on two 96-well microtiter plates on day 0, at 3×10^4 cells/mL (H460, HCT-116), 4.5×10^4 cells/mL (MCF-7). Test agents were added in ten-fold dilutions (10^{-8} to 10^{-4} M) on the next day and incubated for further 72 h. Working dilutions were freshly prepared on the day of testing. One of the plates was left in the dark, while the other was irradiated in a Luzchem reactor (6 cool white lamps 15 min) at 4, 24, and 48 hours after the addition of the tested compounds. After 72 h of incubation the cell growth rate was evaluated by performing the MTT assay which detects dehydrogenase activity in viable cells. The absorbance, which is directly proportional to the number of living, metabolically active cells, was measured on a microplate reader at 570 nm. The percentage of growth (PG) of the cell lines was calculated according as previously described.[7] Each test was performed in quadruplicate in at least two individual experiments.

Table S9. Growth inhibition, IC_{50} (μM), of **1·TFA-5·TFA** [a]

	MCF-7		H460		HCT 116	
	Dark	VIS[b]	Dark	VIS[b]	Dark	VIS[b]
1·TFA	3±1	3±2	22±9	14±3	14±1	9±4
2·TFA	2±0.3	0.2±0.1	2±0.3	1±0.1	1±0.2	0.4±0.2
3·TFA	0.2±0.04	0.2±0.02	1±0.1	1±0.4	1±0.3	1±1
4·TFA	1±0.3	0.3±0.2	2±0.1	1±0.3	2±0.4	1±0.3
5·TFA	1±0.1	0.1±0.04	2±0.1	1±0.3	2±0.01	1±0.01

[a] The cells were treated with TFA salts; [b] The cells were irradiated with 6 cool white lamps (3×15 min).

The irradiation of MCF-7 and HCT-116 cells treated with **2·TFA**, resulted in an order of magnitude enhanced activity. On the other hand, no enhancement of the activity was observed in cells treated with **3·TFA** and only modest with **1·TFA**. Although the exact mechanism for the enhancement activity is not known, it is very likely that it is connected to production of singlet oxygen[8] or some phenoxyl radicals, which were detected by LFP, and which can engage in the reaction with intracellular molecules. Although we have demonstrated that proteins can be alkylated in the photoinduced reaction, which involves the formation of QMs, the enhanced activity cannot be related to the production of QMs, since the photodeamination is not feasible from S_1. Unfortunately, we did not observe any enhancement of the antiproliferative effect on the cells treated and irradiated at 300 nm, the wavelength that can induce formation of QMs. In the protein alkylation experiment, there was only BSA and the dye in the buffer, whereas intracellular media is more complex and the dye distribution inside the cell is anticipated to direct the photoinduced effect.

^{1}H NMR ($CDCl_3$, 300 MHz) of 5-Phenyldipyrromethane

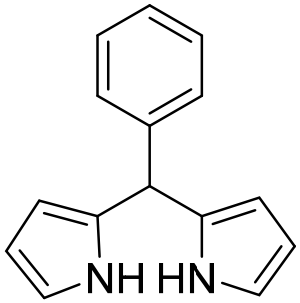

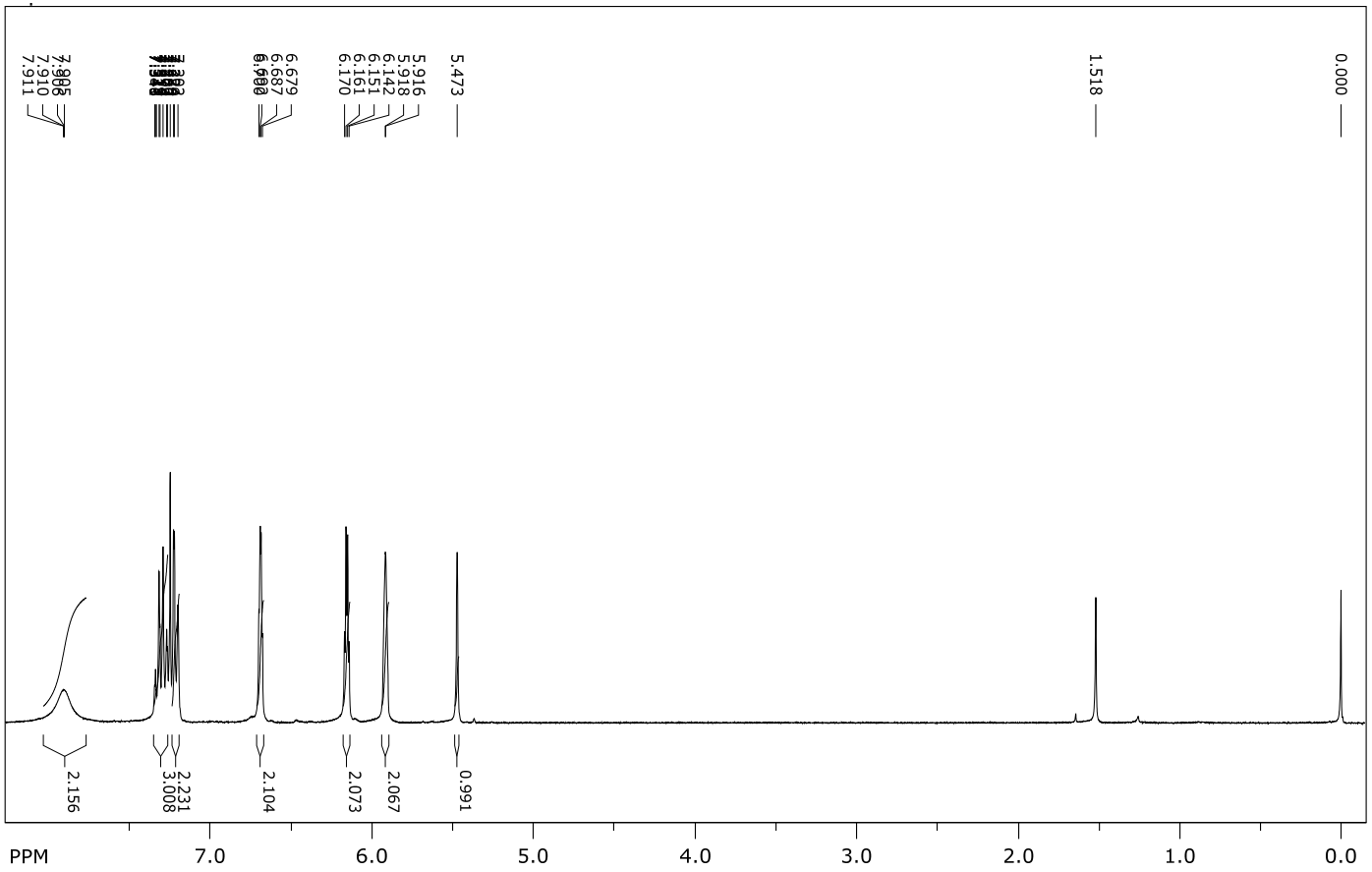

^{13}C NMR ($CDCl_3$, 75 MHz) of 5-Phenyldipyrromethane

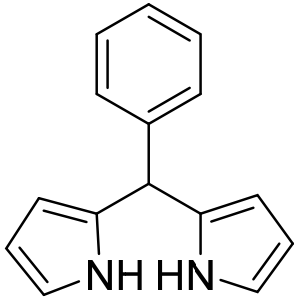

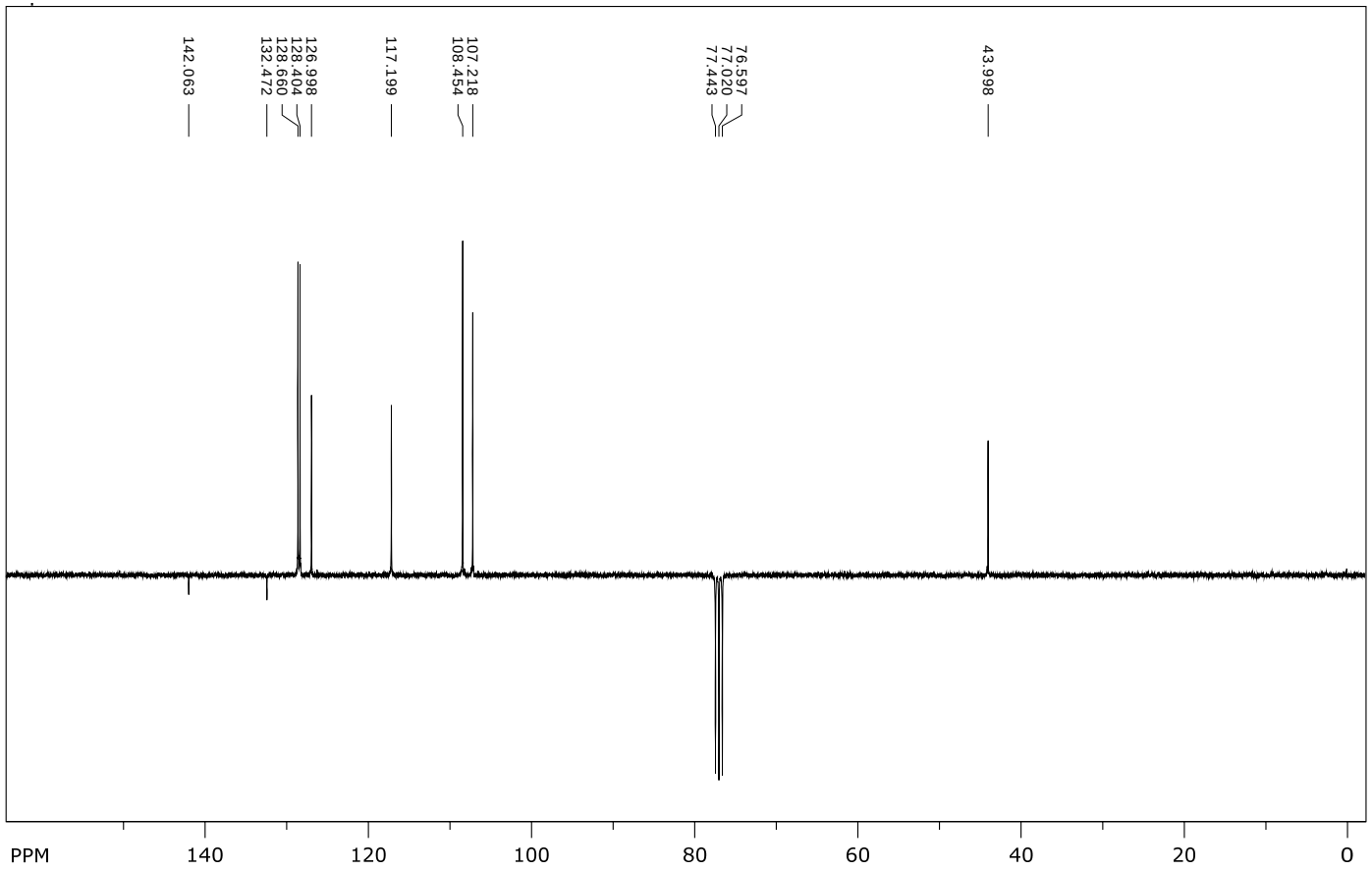

^{1}H NMR ($CDCl_3$, 300 MHz) of 1-Chloro-5-phenyldipyrromethane

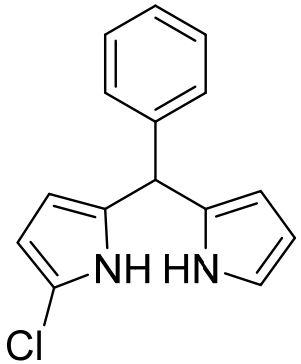

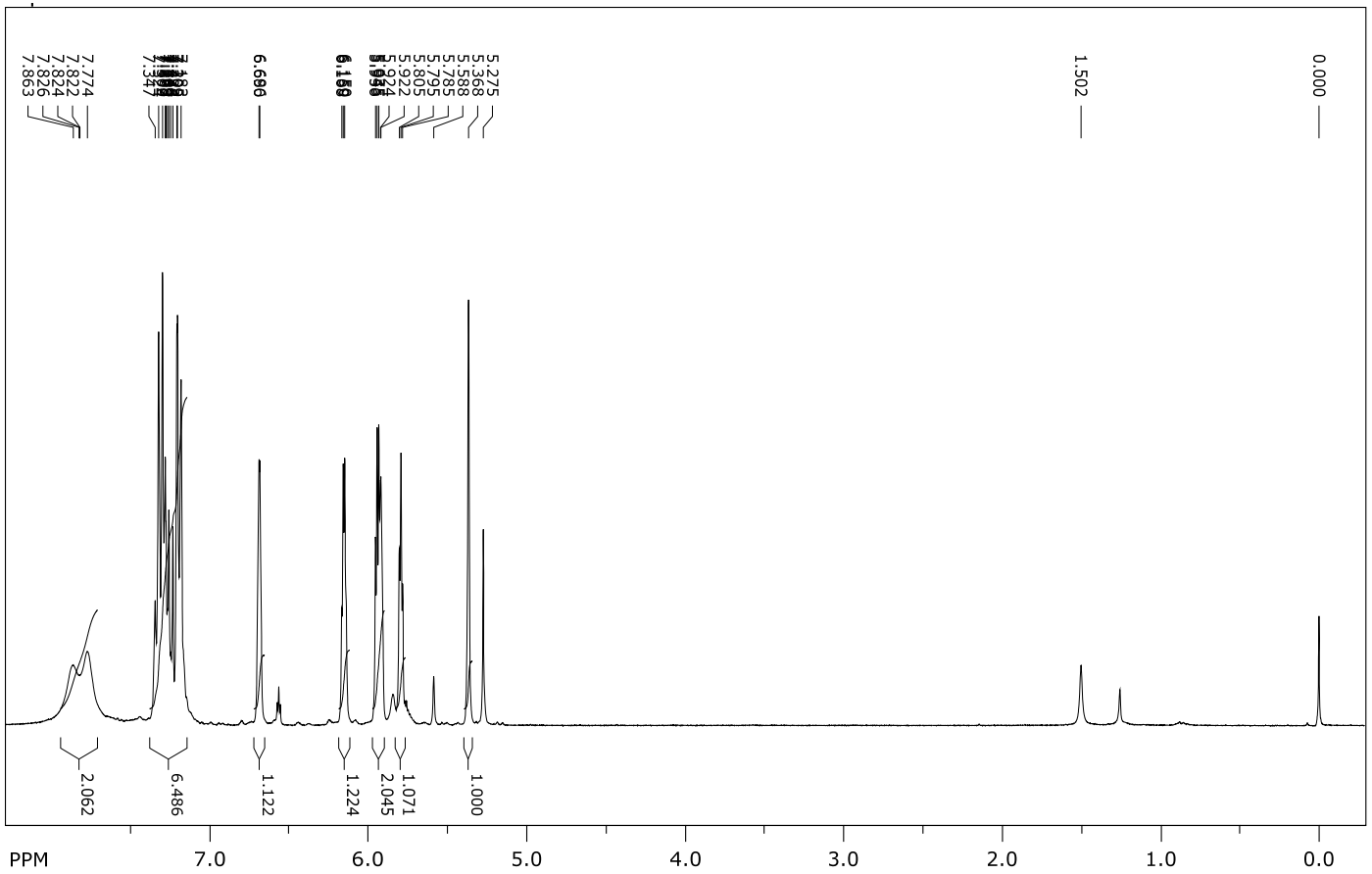

^{1}H NMR ($CDCl_3$, 300 MHz) of 1,8-dichloro-5-phenyldipyrromethane

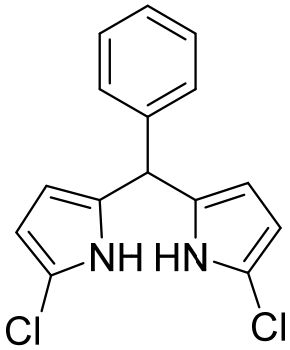

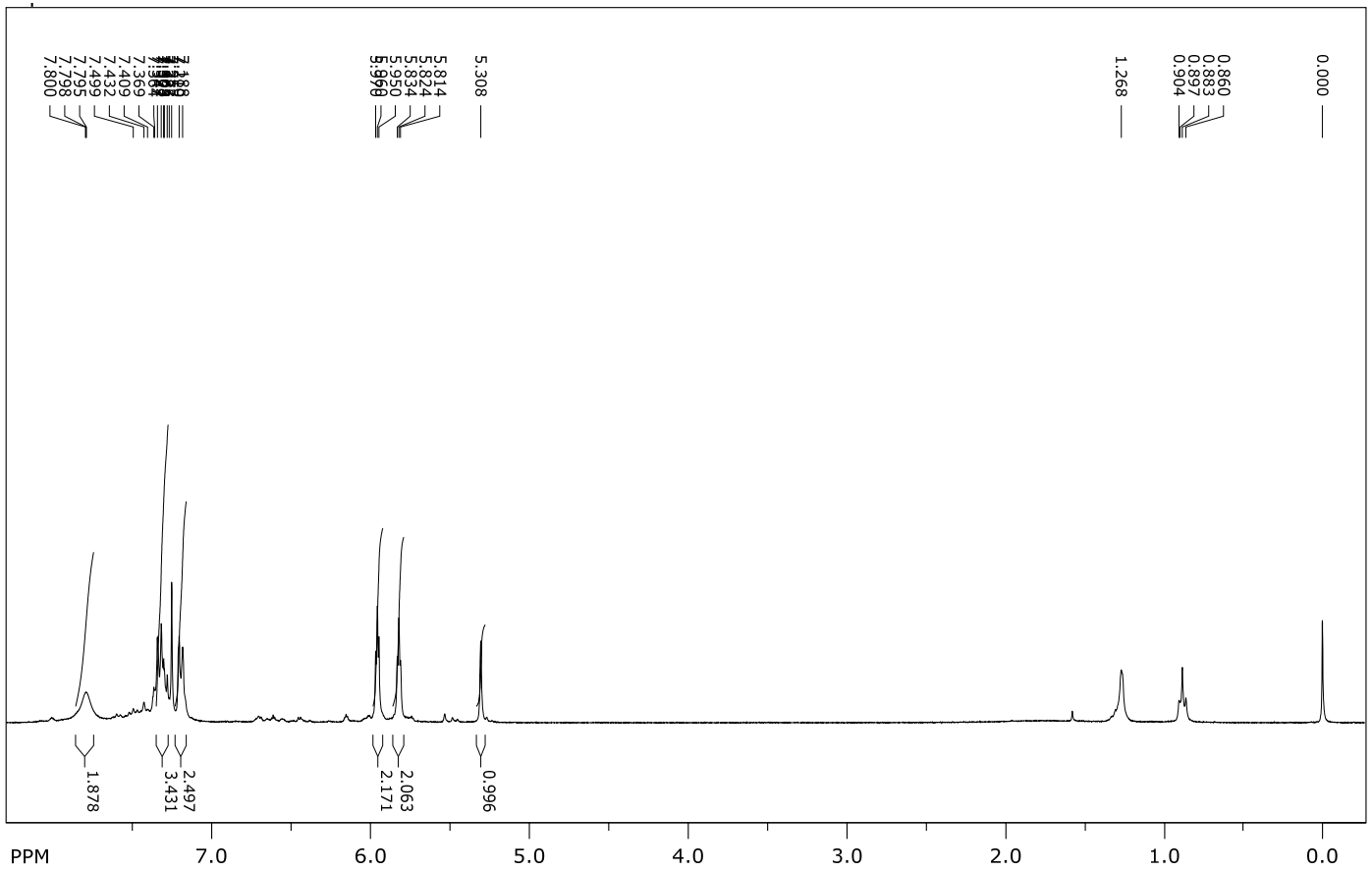

^{1}H NMR ($CDCl_3$, 300 MHz) of 6

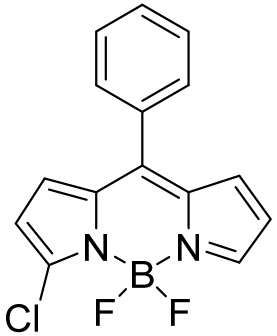

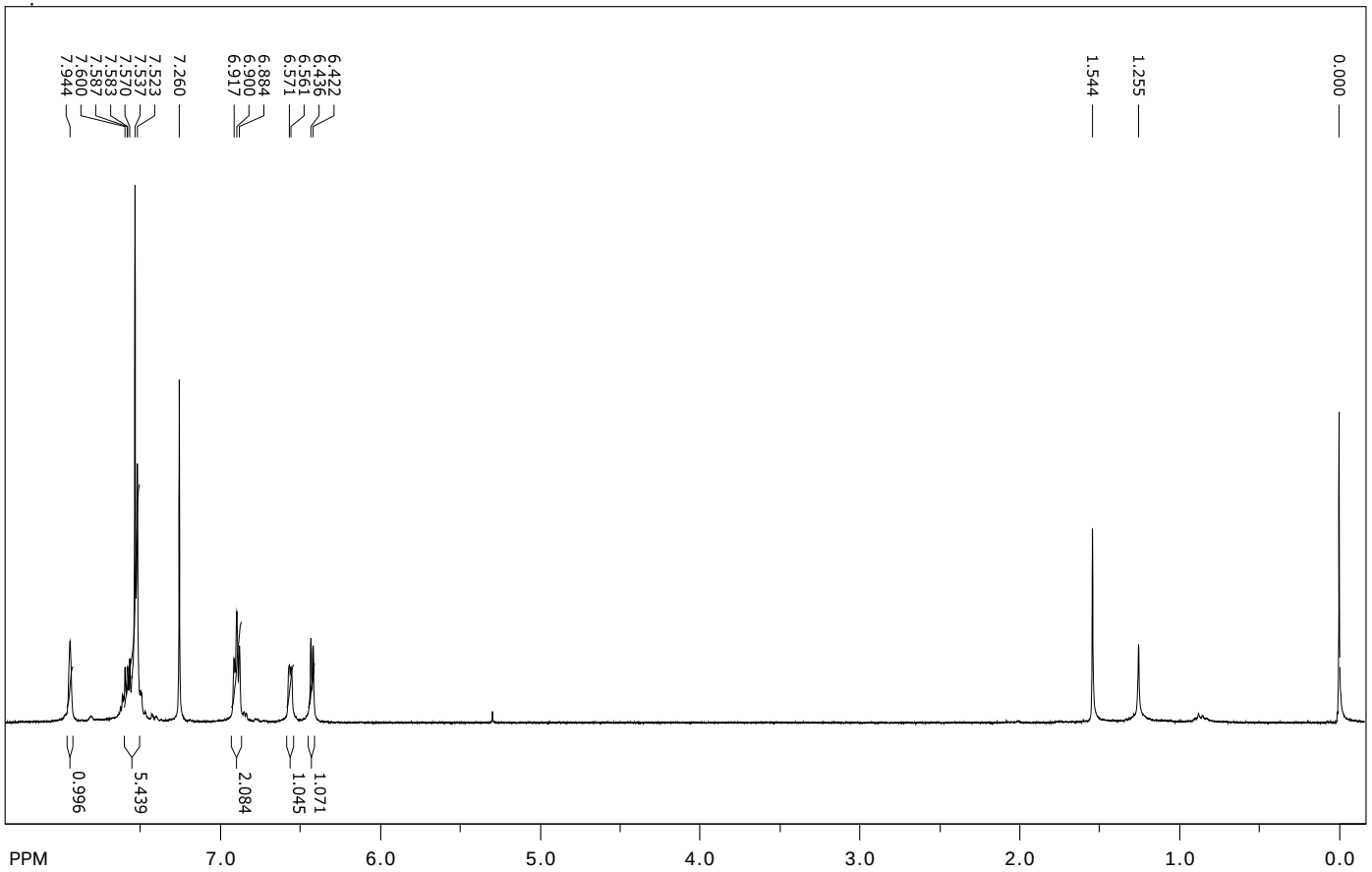

^{13}C NMR ($CDCl_3$, 75 MHz) of 6

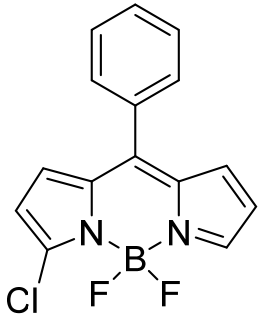

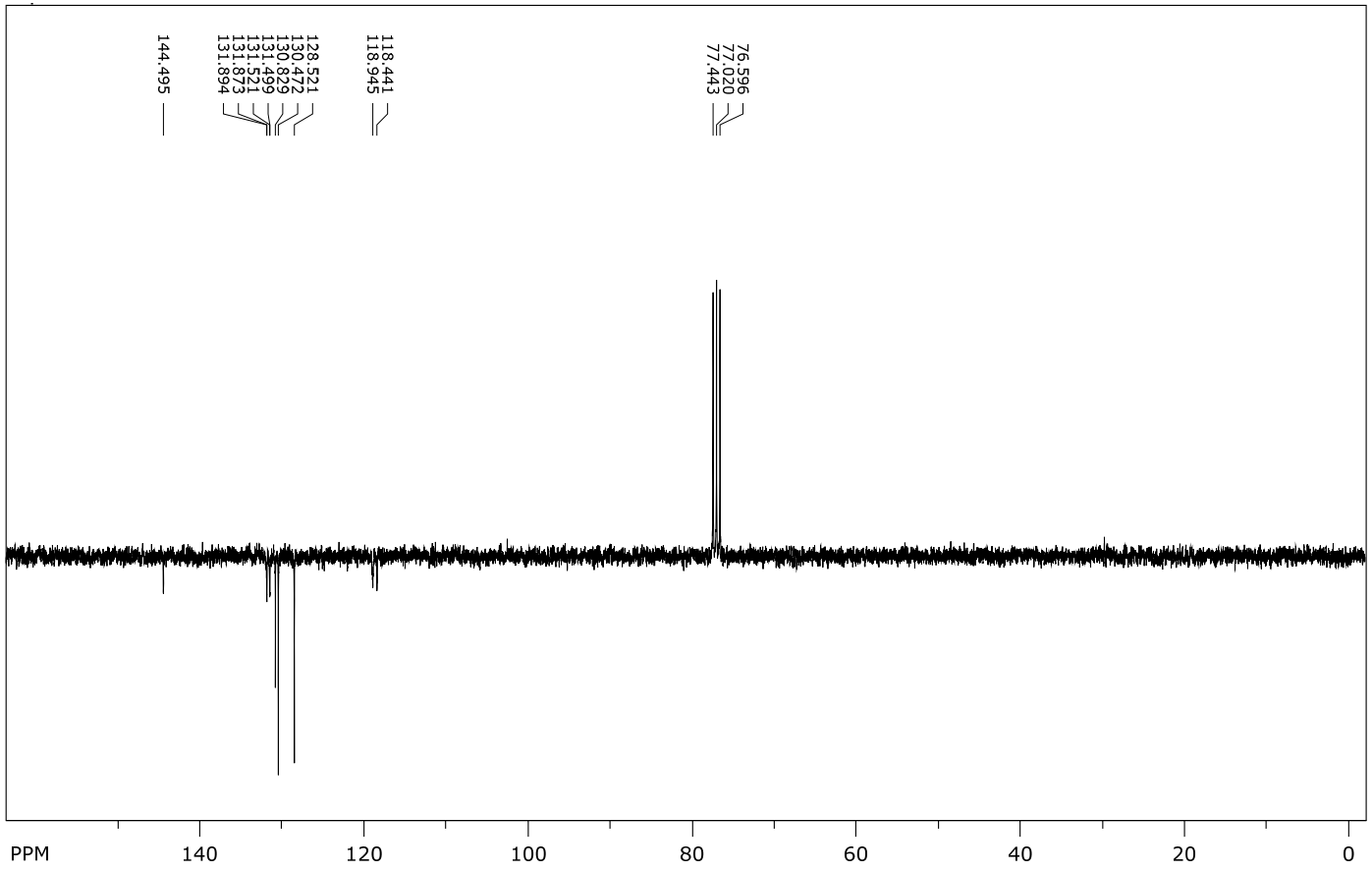

^{1}H NMR ($CDCl_3$, 300 MHz) of 9

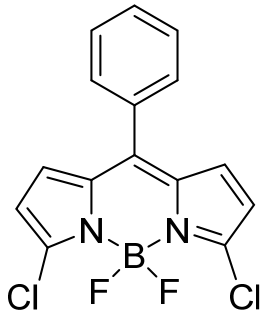

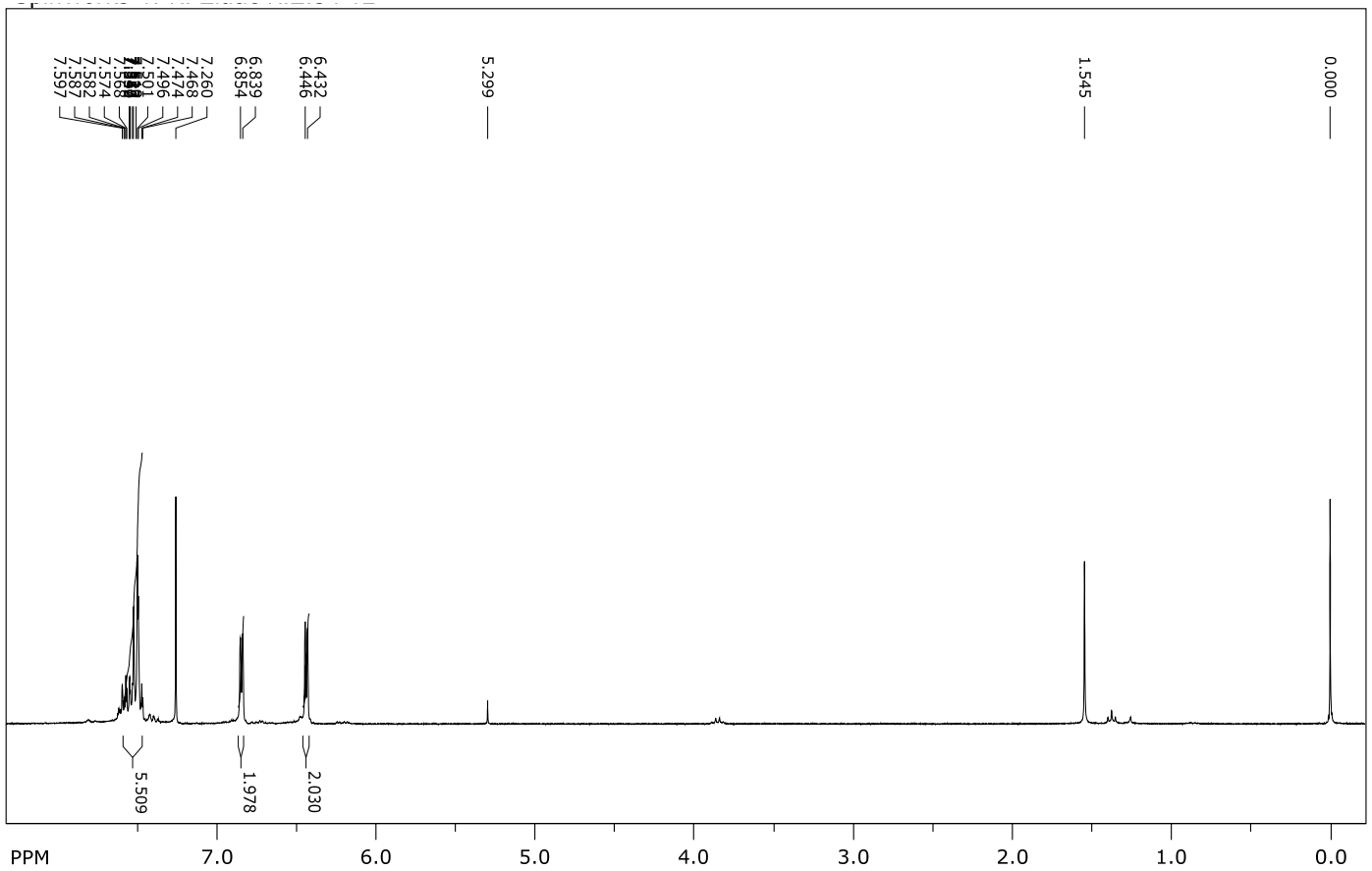

^{13}C NMR ($CDCl_3$, 75 MHz) of 9

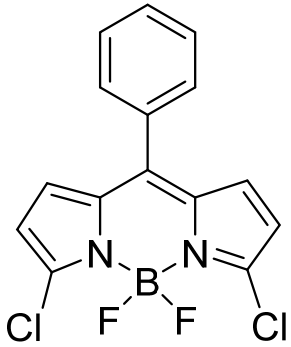

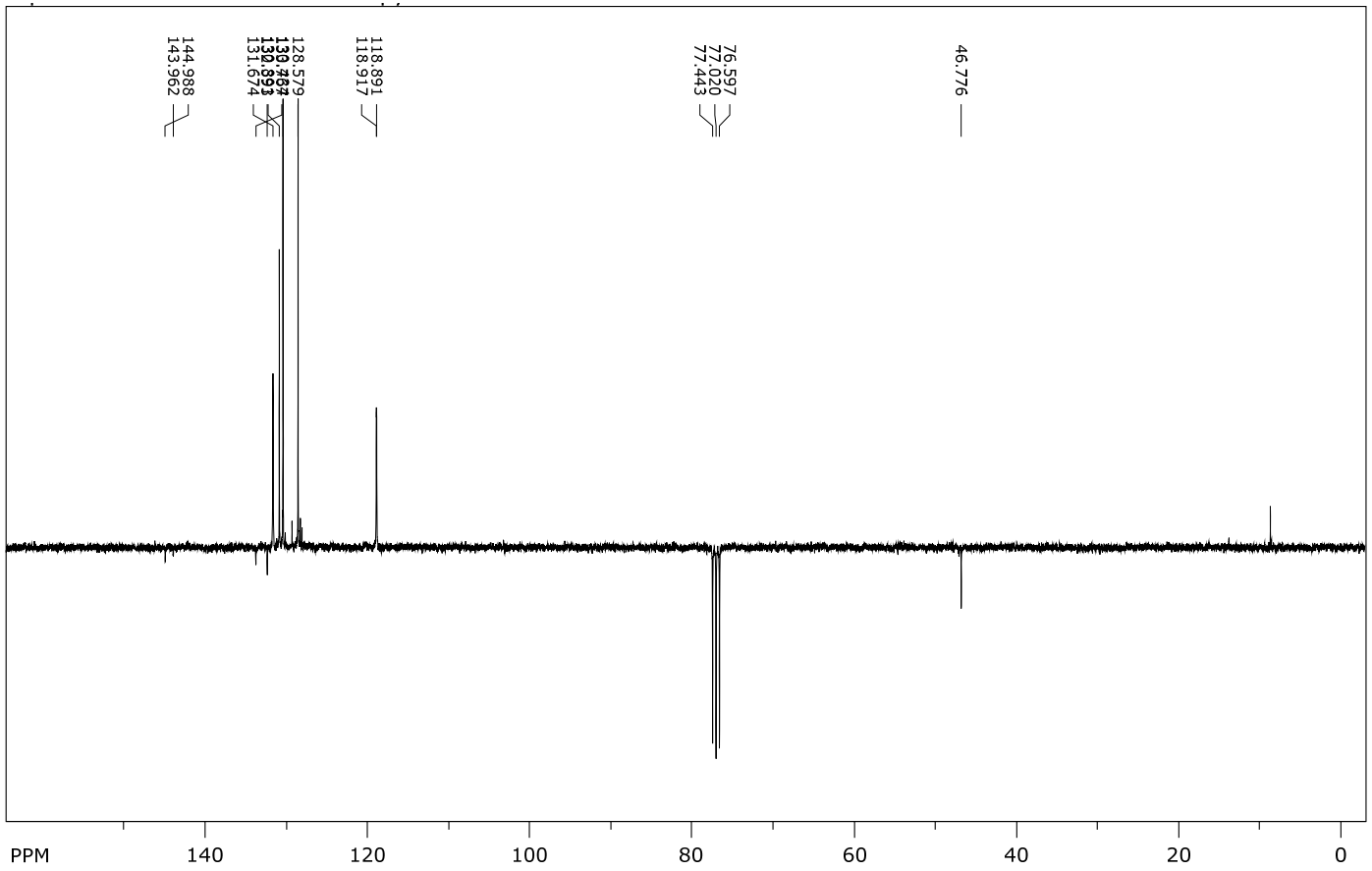

^{1}H NMR ($CDCl_3$, 600 MHz) of 7

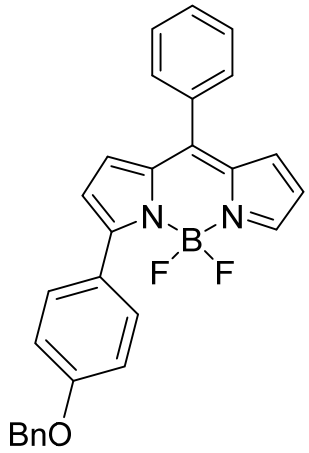

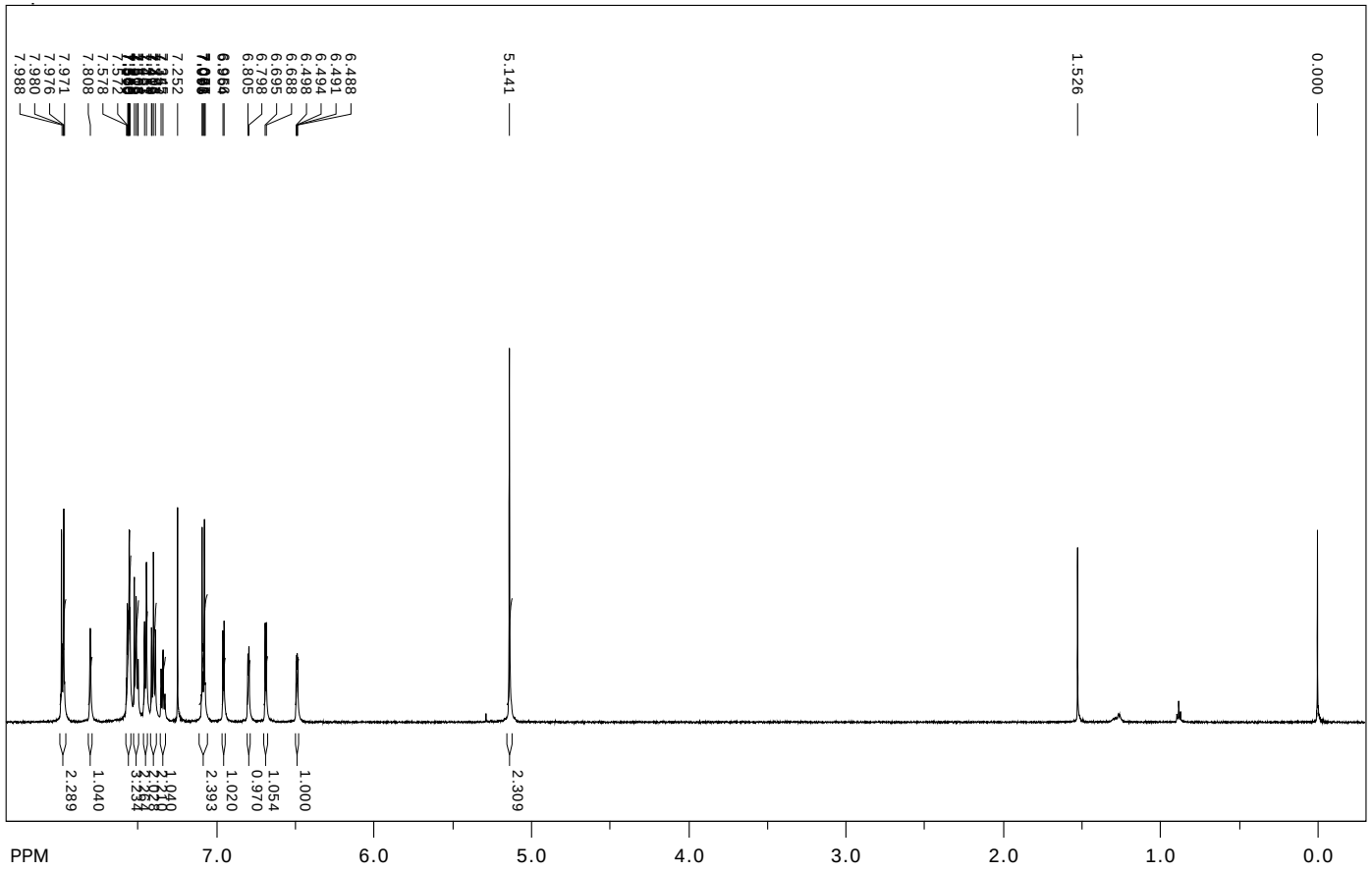

^{13}C NMR ($CDCl_3$, 150 MHz) of 7

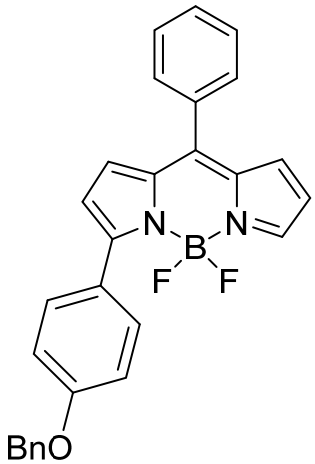

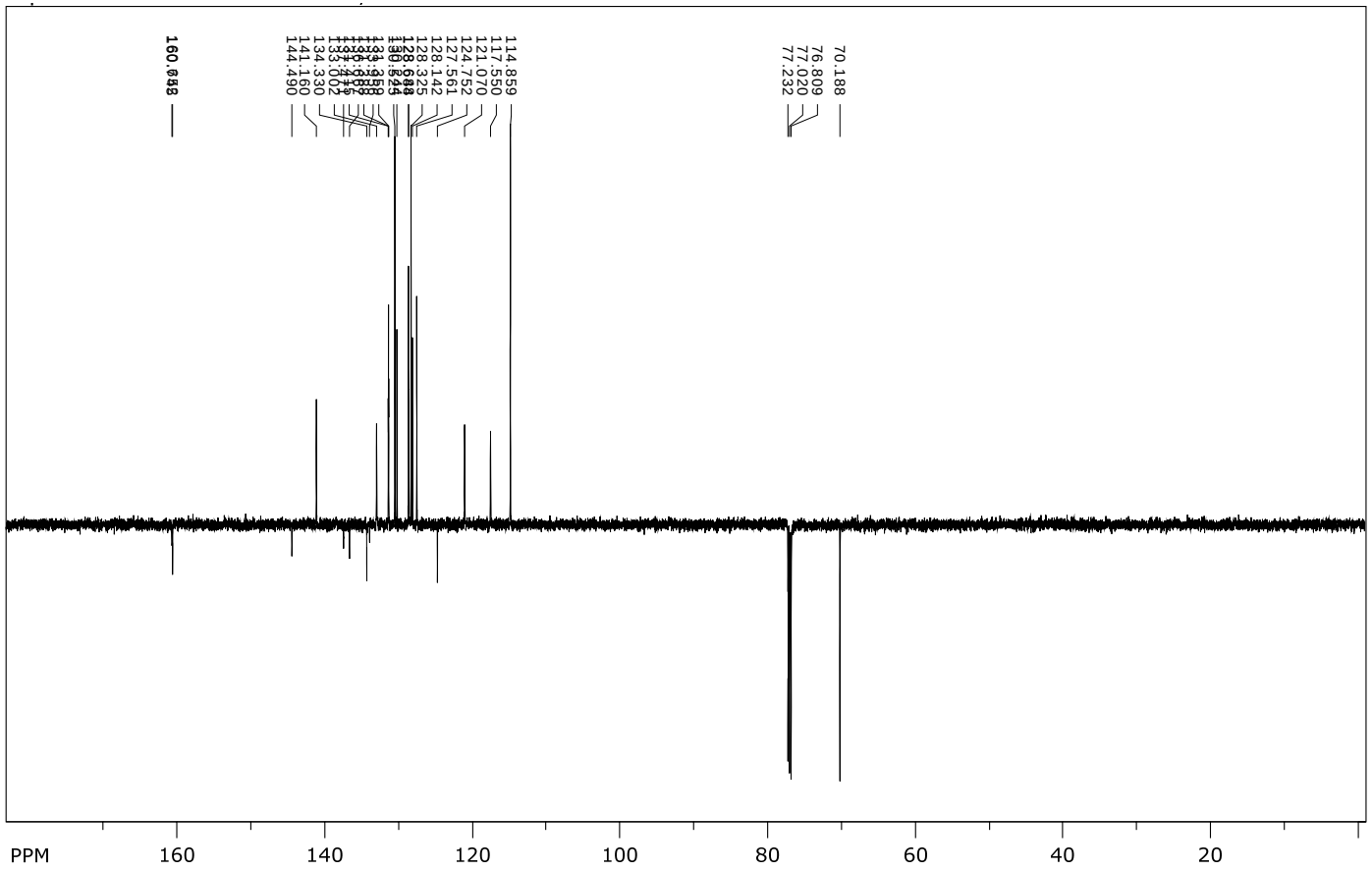

^{1}H NMR ($CDCl_3$, 600 MHz) of 11

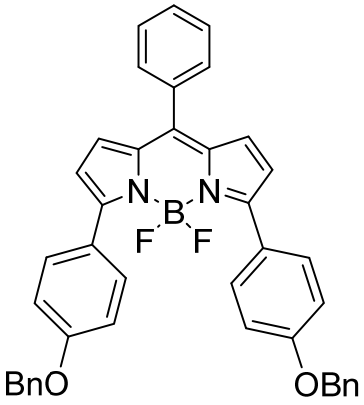

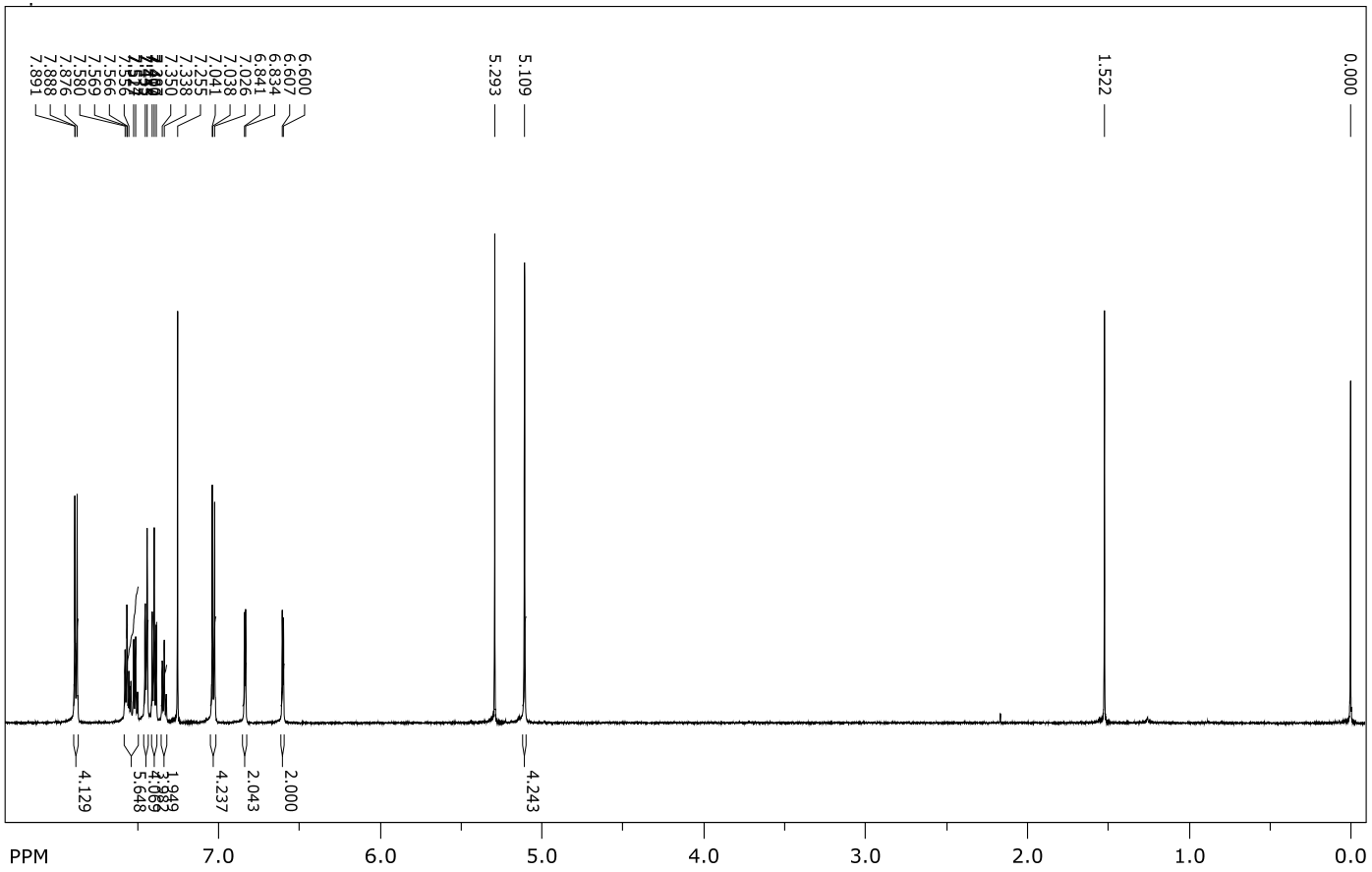

^{13}C NMR ($CDCl_3$, 150 MHz) of 11

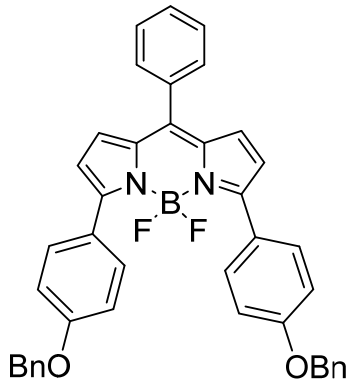

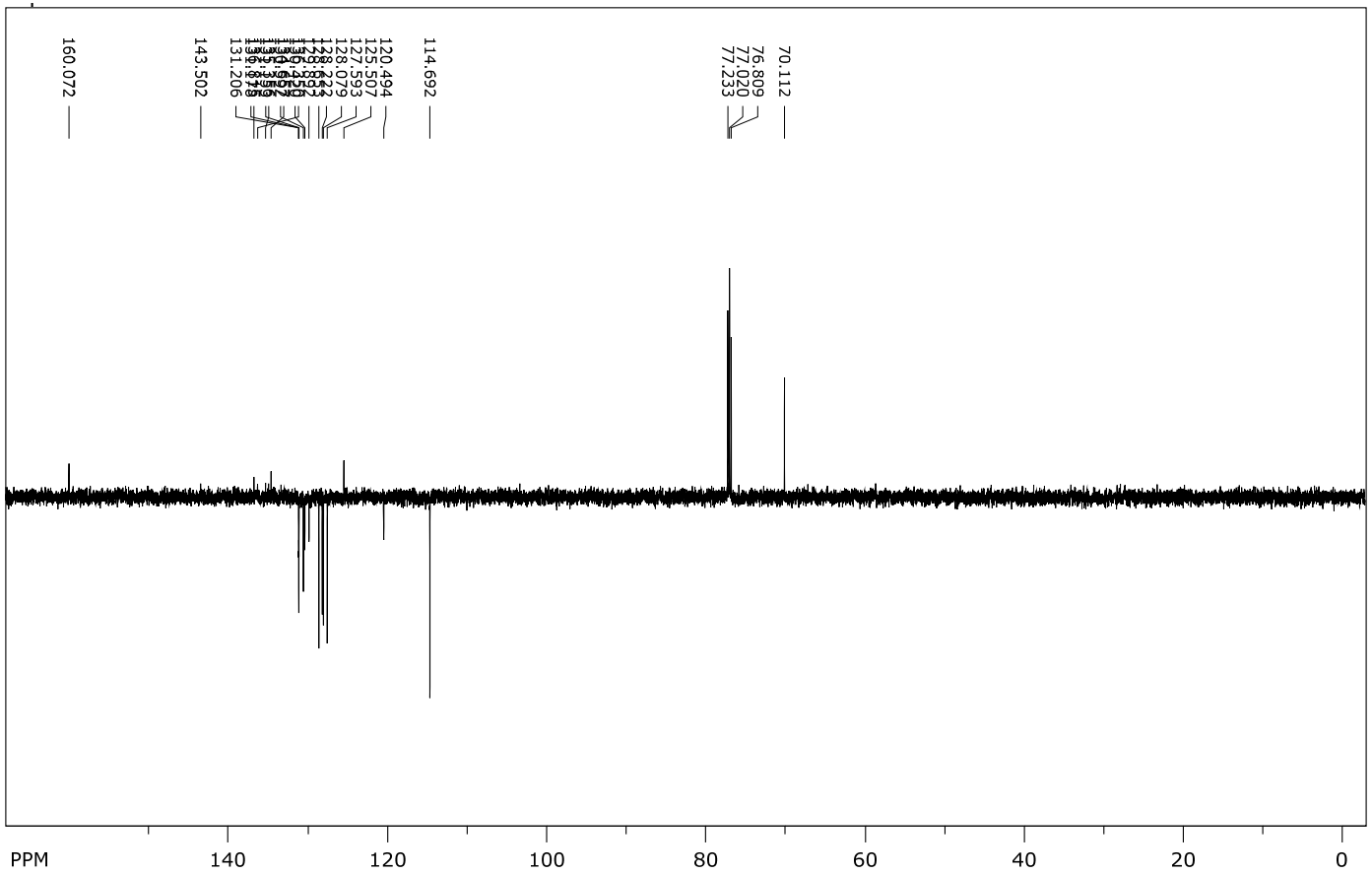

^{1}H NMR ($CDCl_3$, 600 MHz) of 10

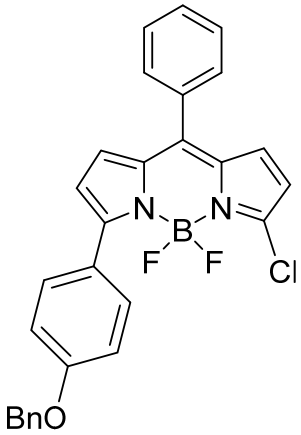

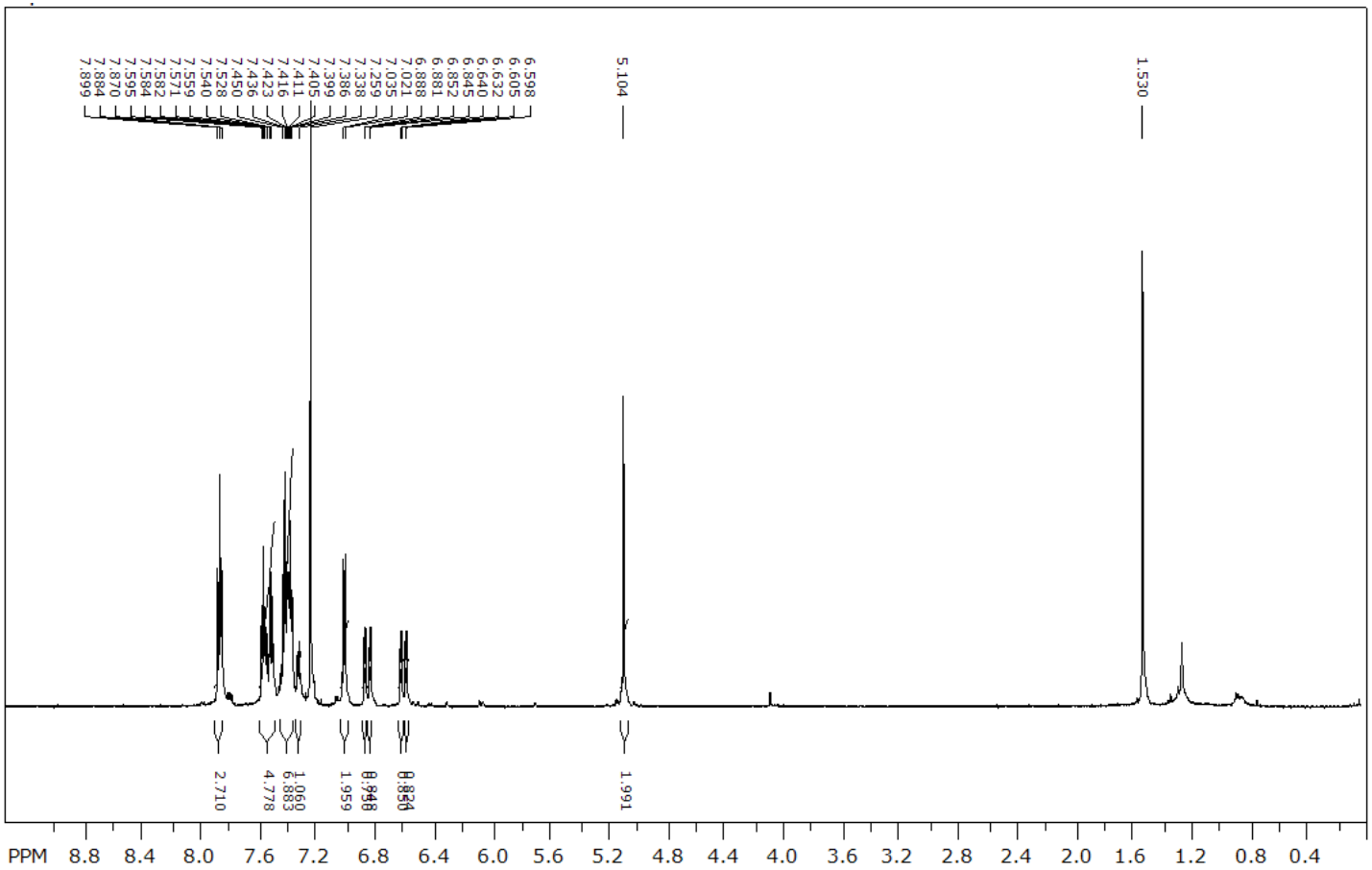

^{13}C NMR ($CDCl_3$, 150 MHz) of 10

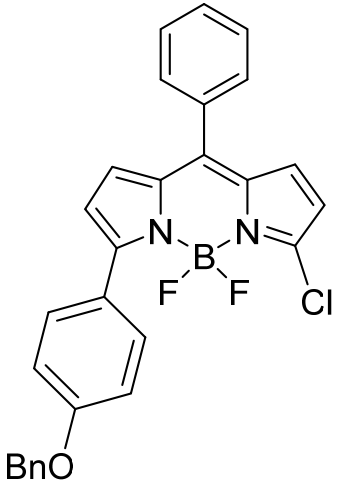

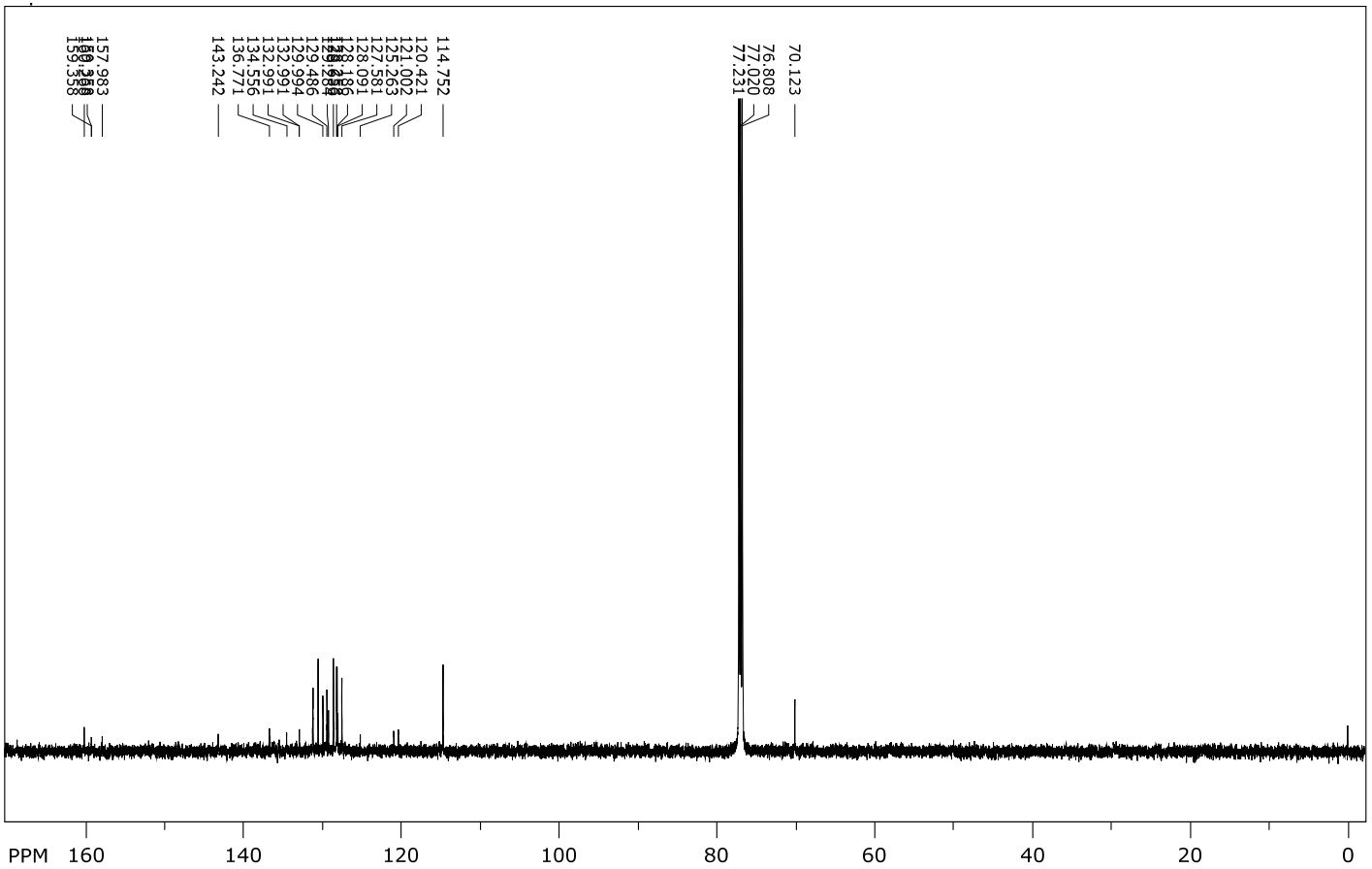

^{1}H NMR ($CDCl_3$, 600 MHz) of 8

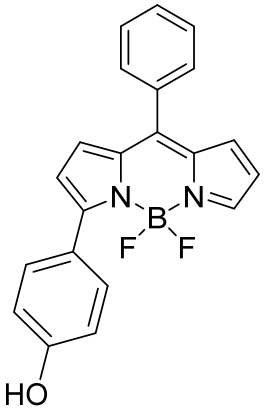

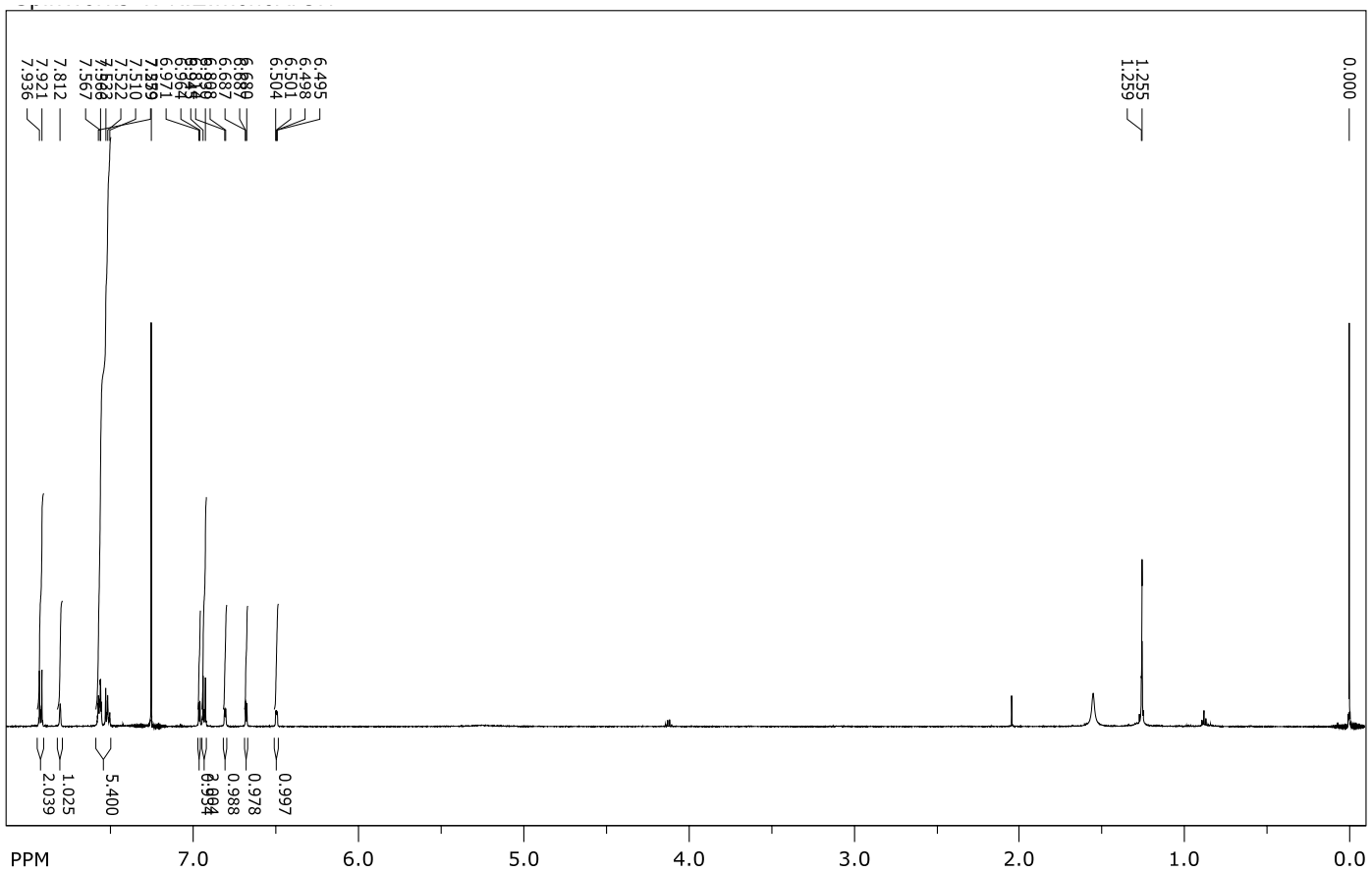

^{13}C NMR ($CDCl_3$, 150 MHz) of 8

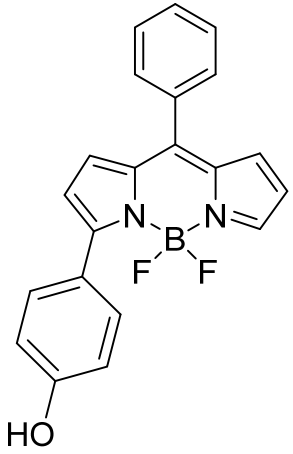

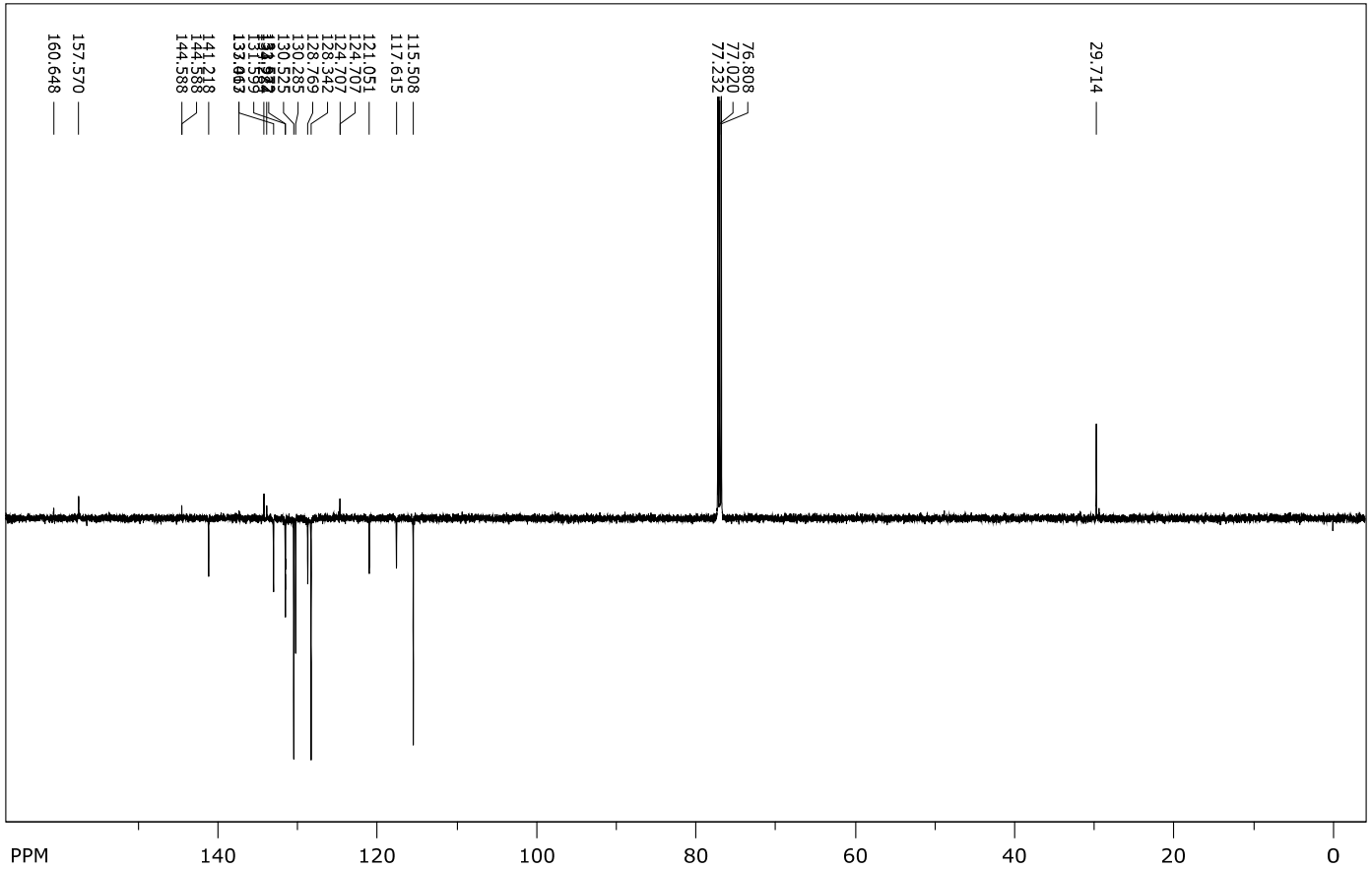

^{1}H NMR ($CDCl_3$, 300 MHz) of 12

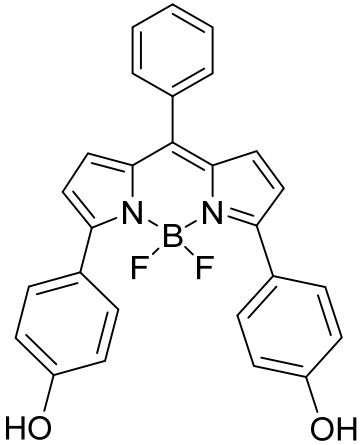

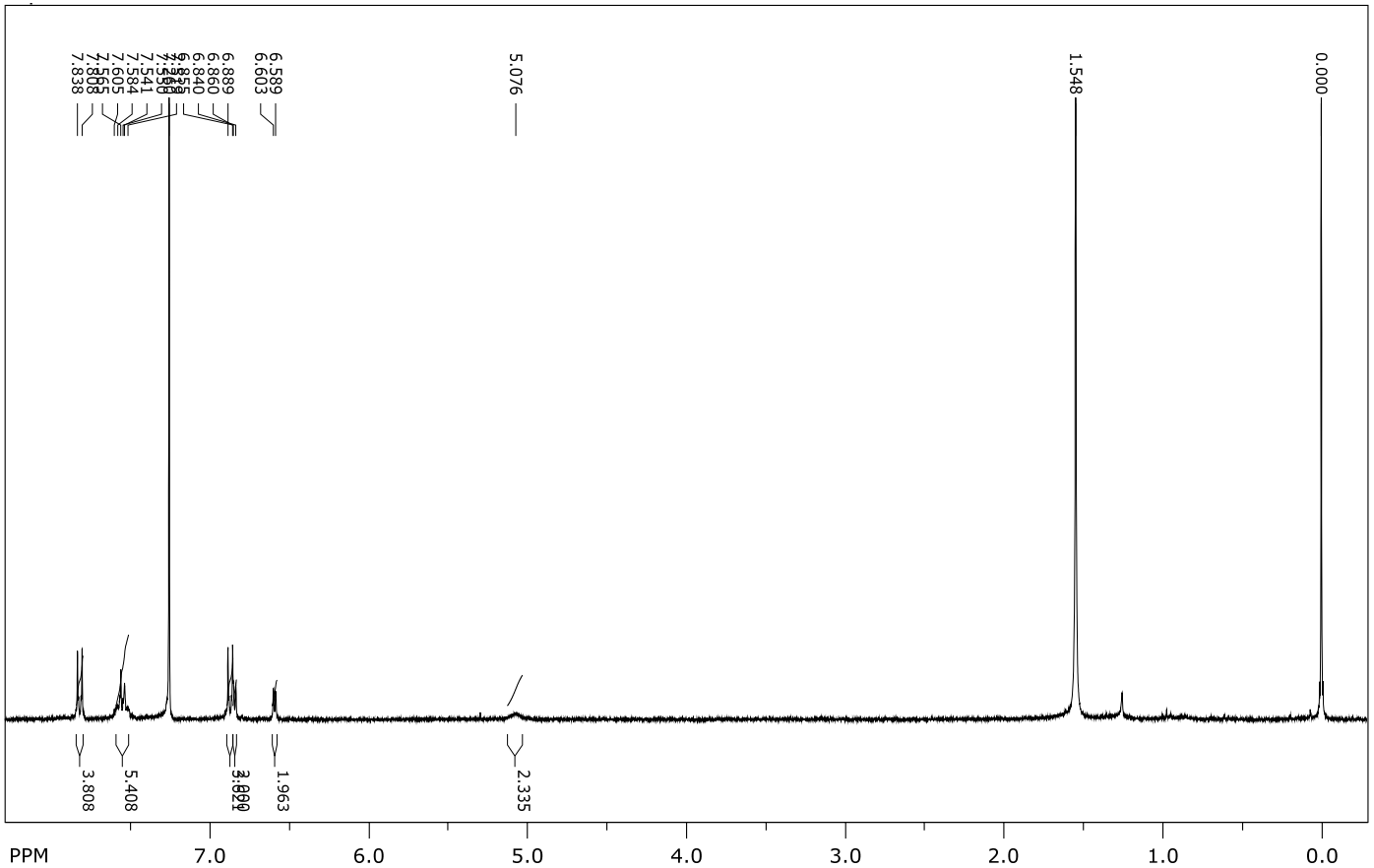

^{13}C NMR ($CDCl_3$, 75MHz) of 12

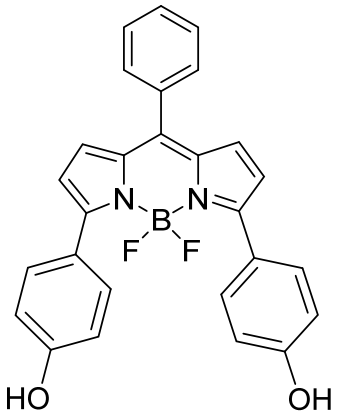

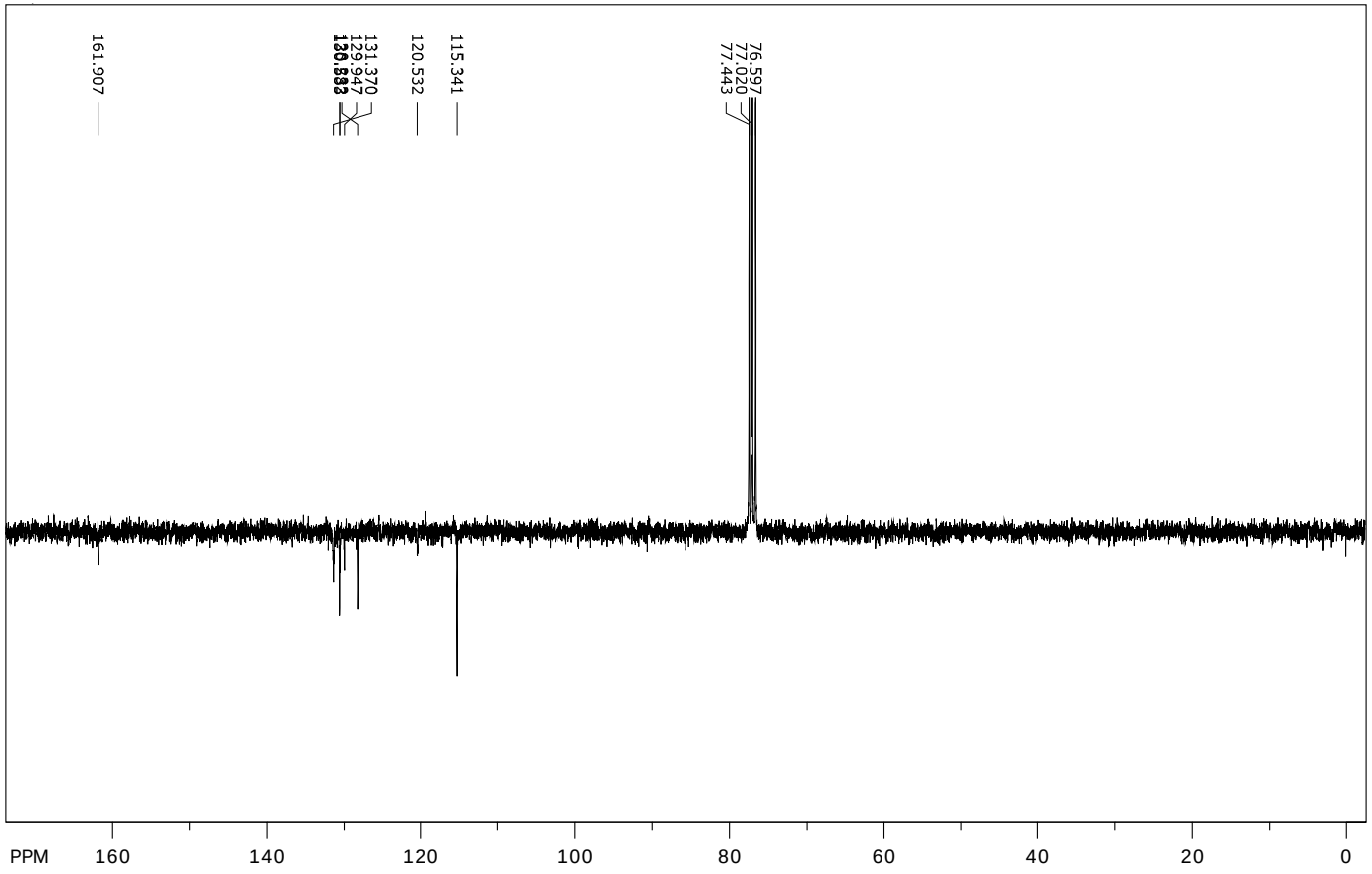

^{1}H NMR ($CDCl_3$, 300 MHz) of 13

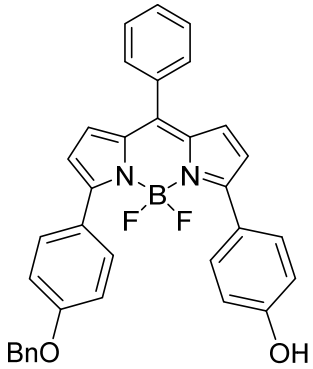

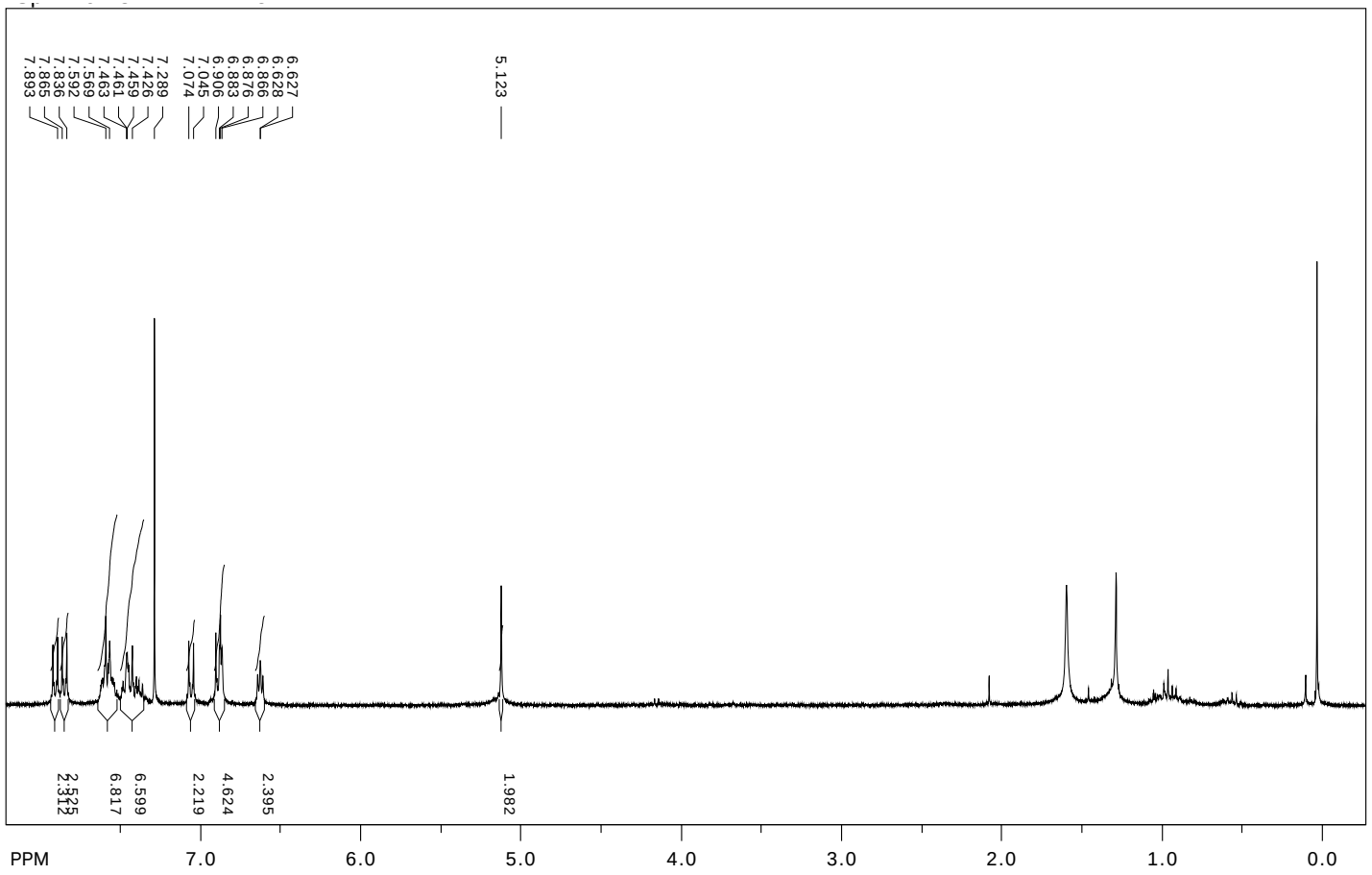

^{13}C NMR ($CDCl_3$, 75MHz, APT) of 13

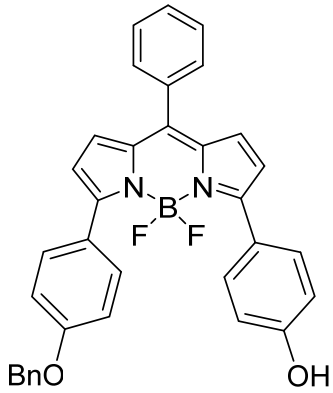

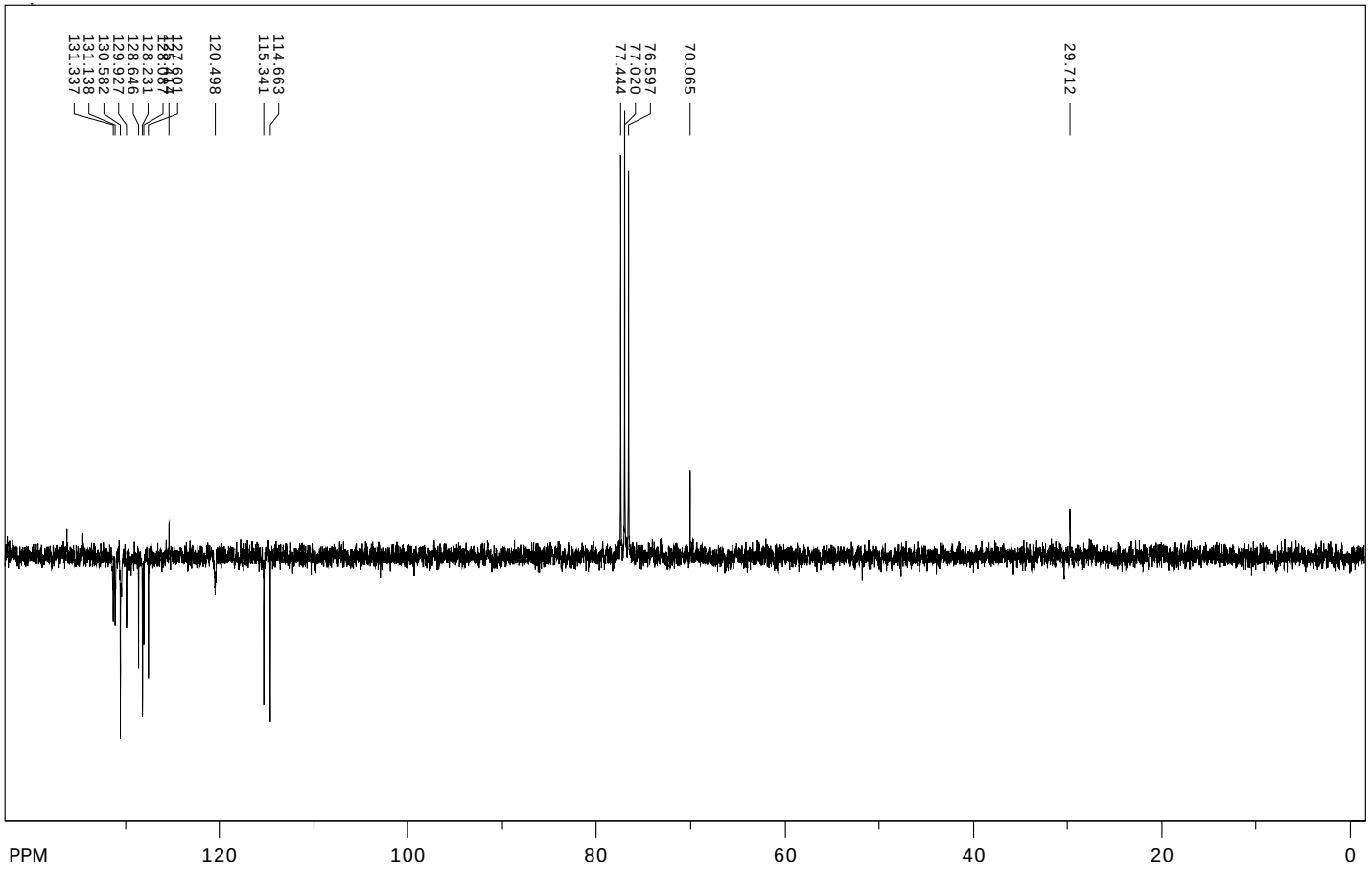

^{13}C NMR ($CDCl_3$, 75MHz) of 13

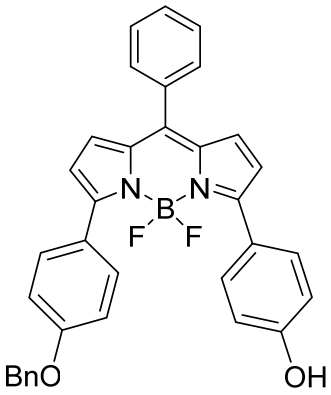

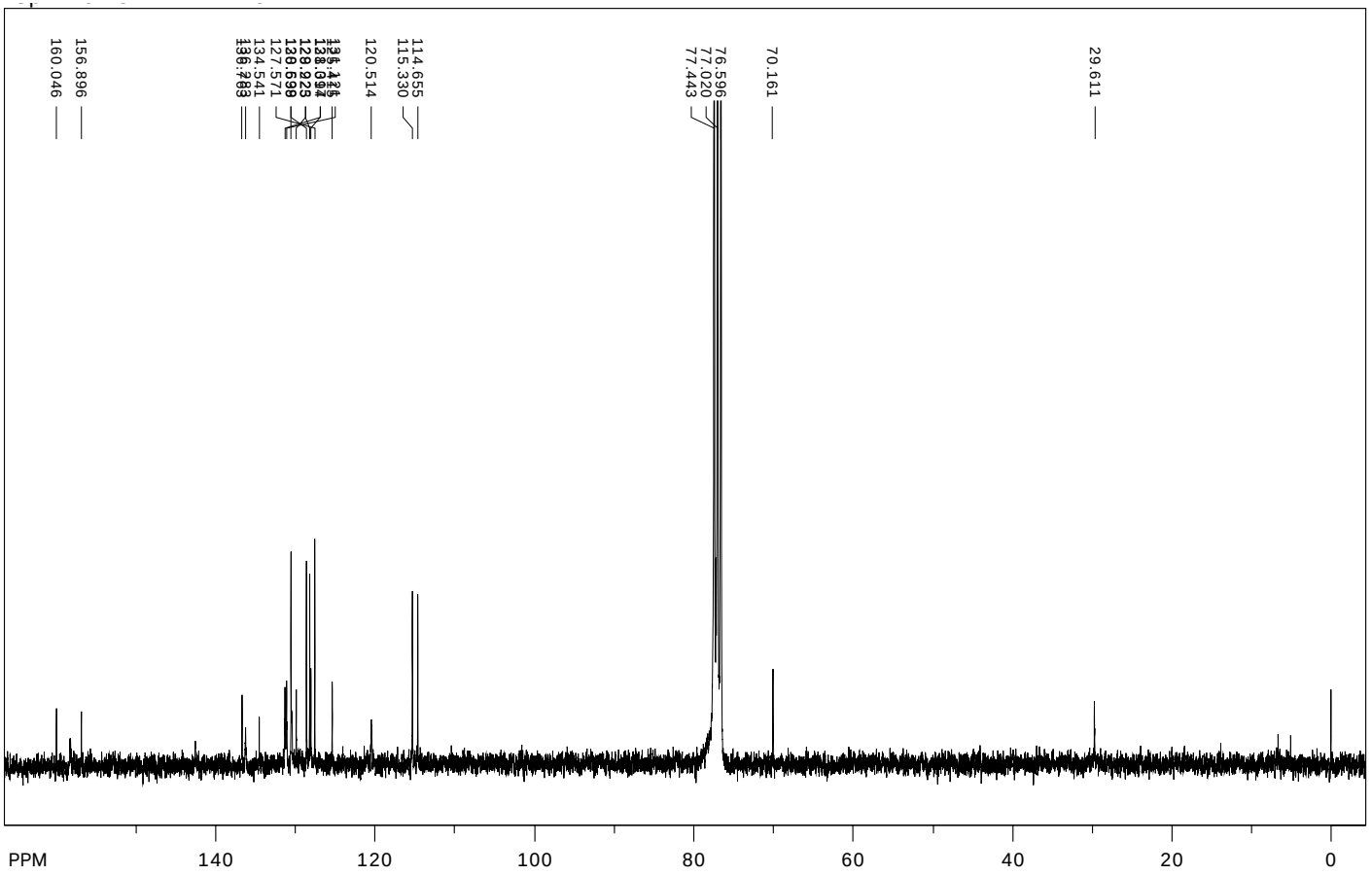

^{1}H NMR ($CDCl_3$, 300 MHz) of 1

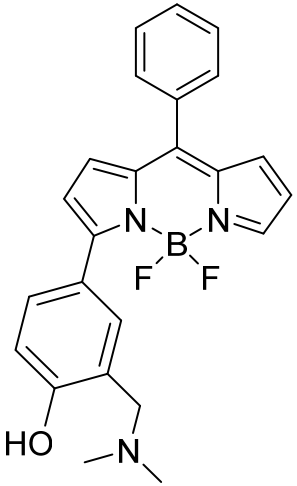

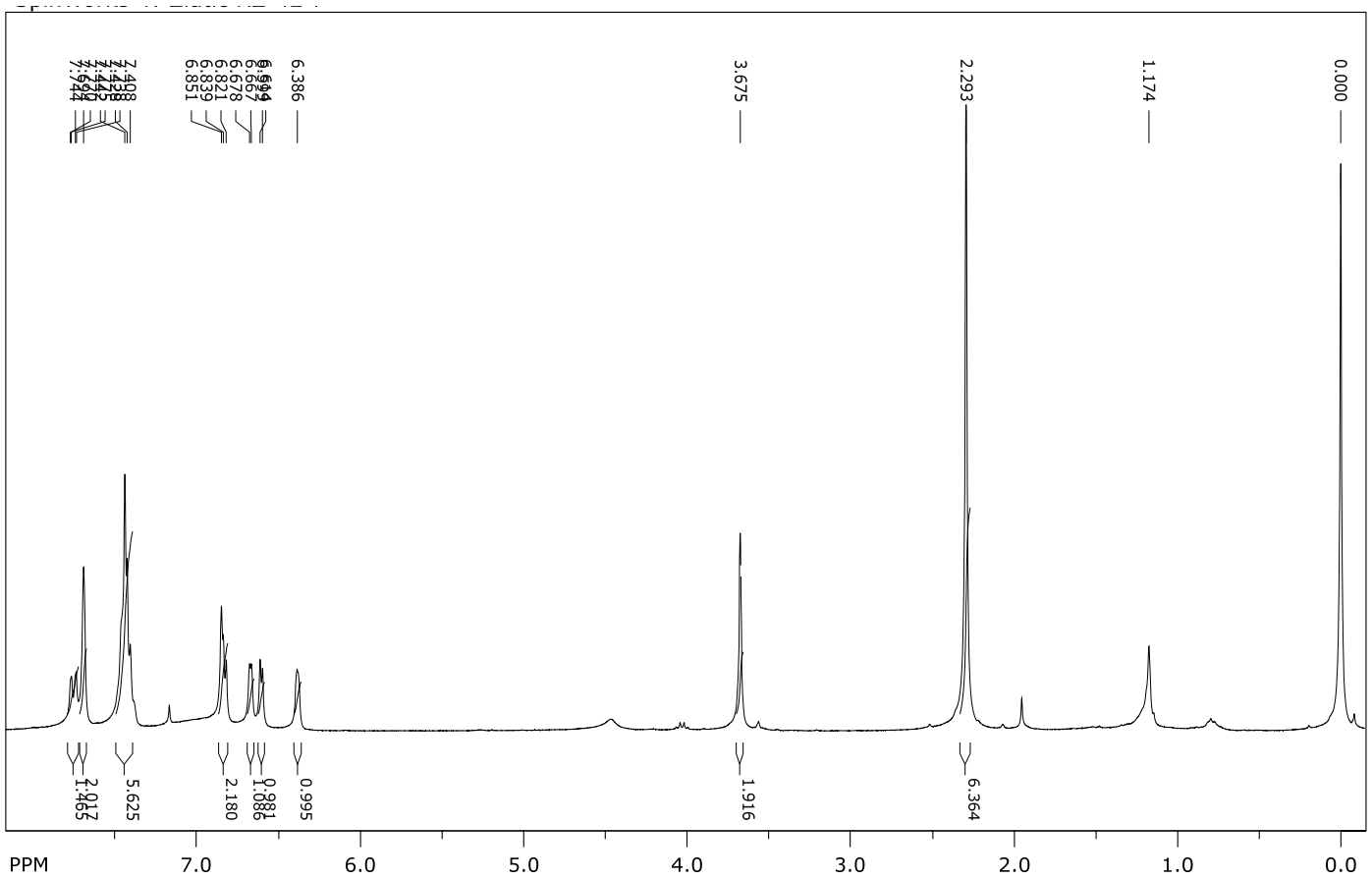

^{1}H NMR (CD_3OD, 300 MHz) of 1

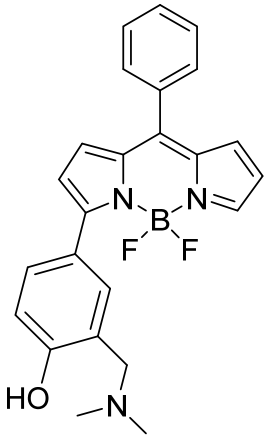

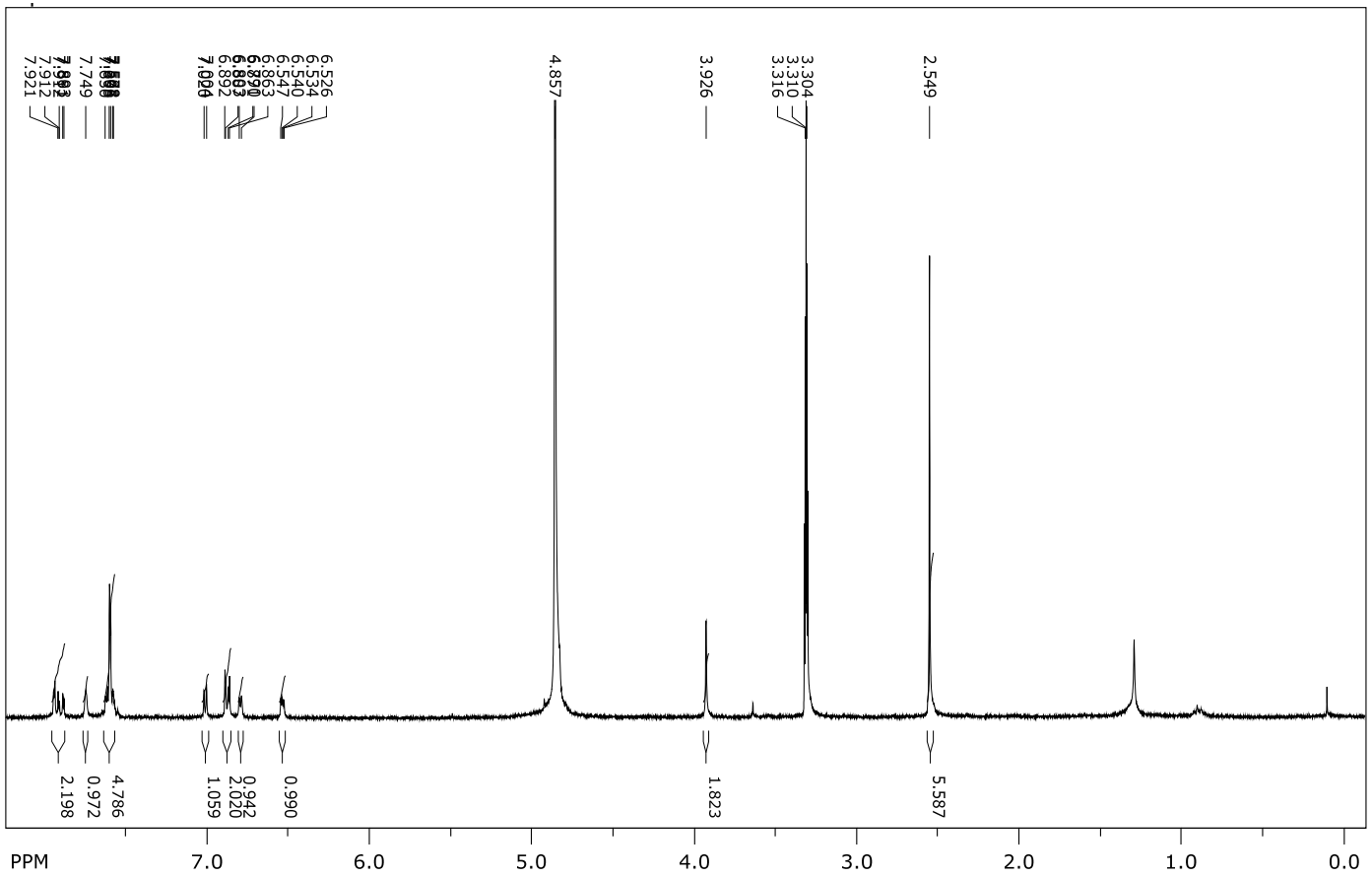

^{13}C NMR ($CDCl_3$, 75MHz) of 1

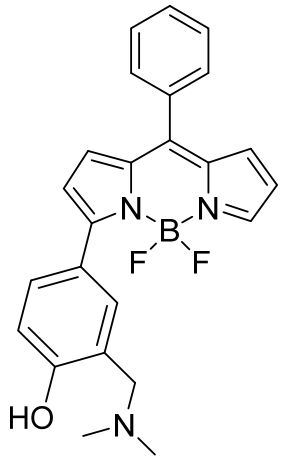

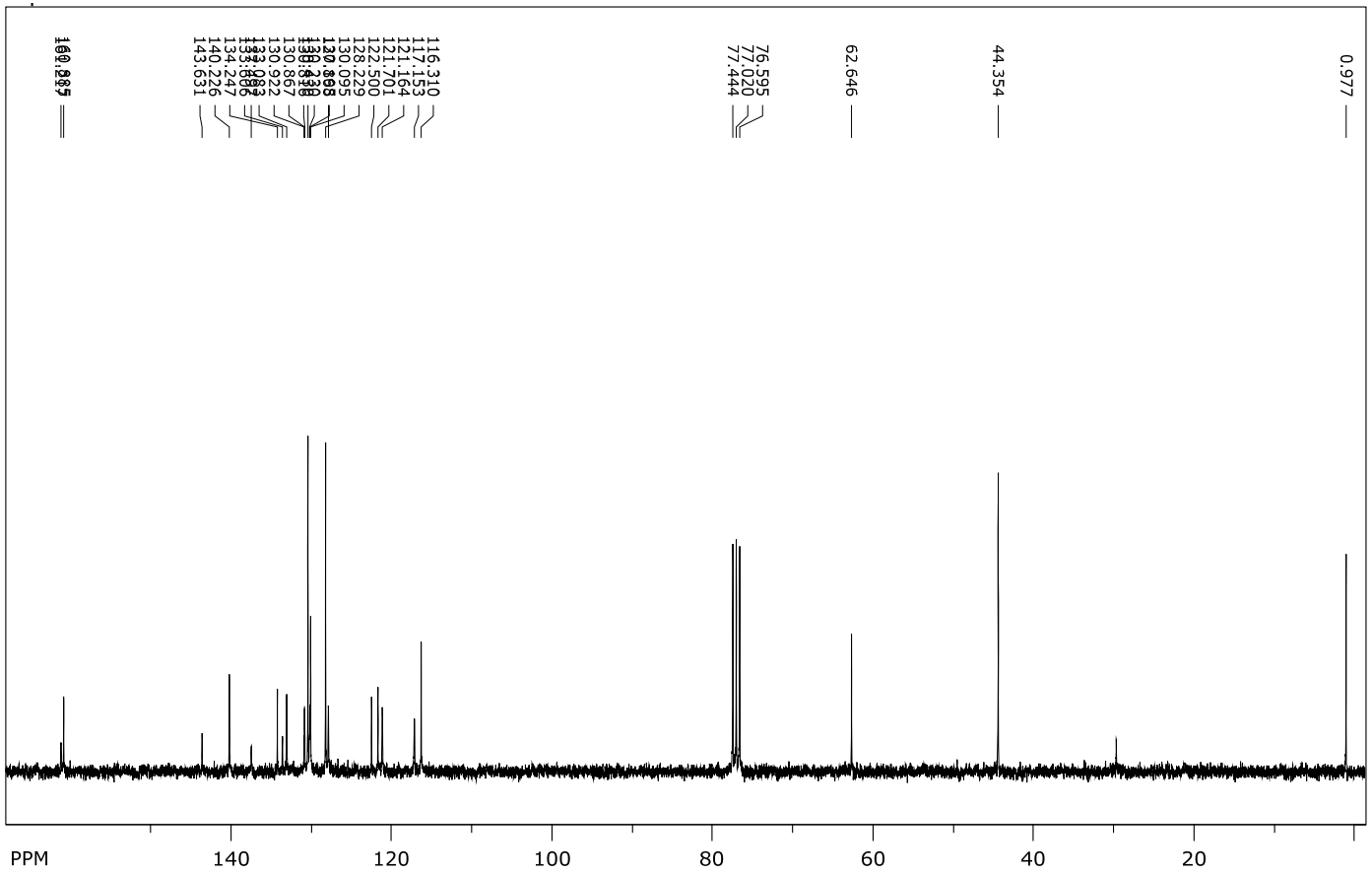

^{13}C NMR (CD_3OD, 75 MHz) of 1

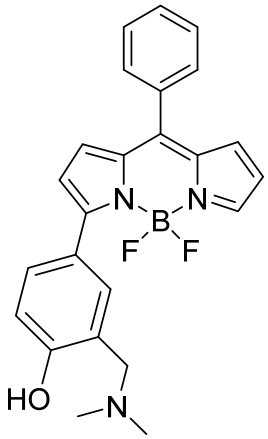

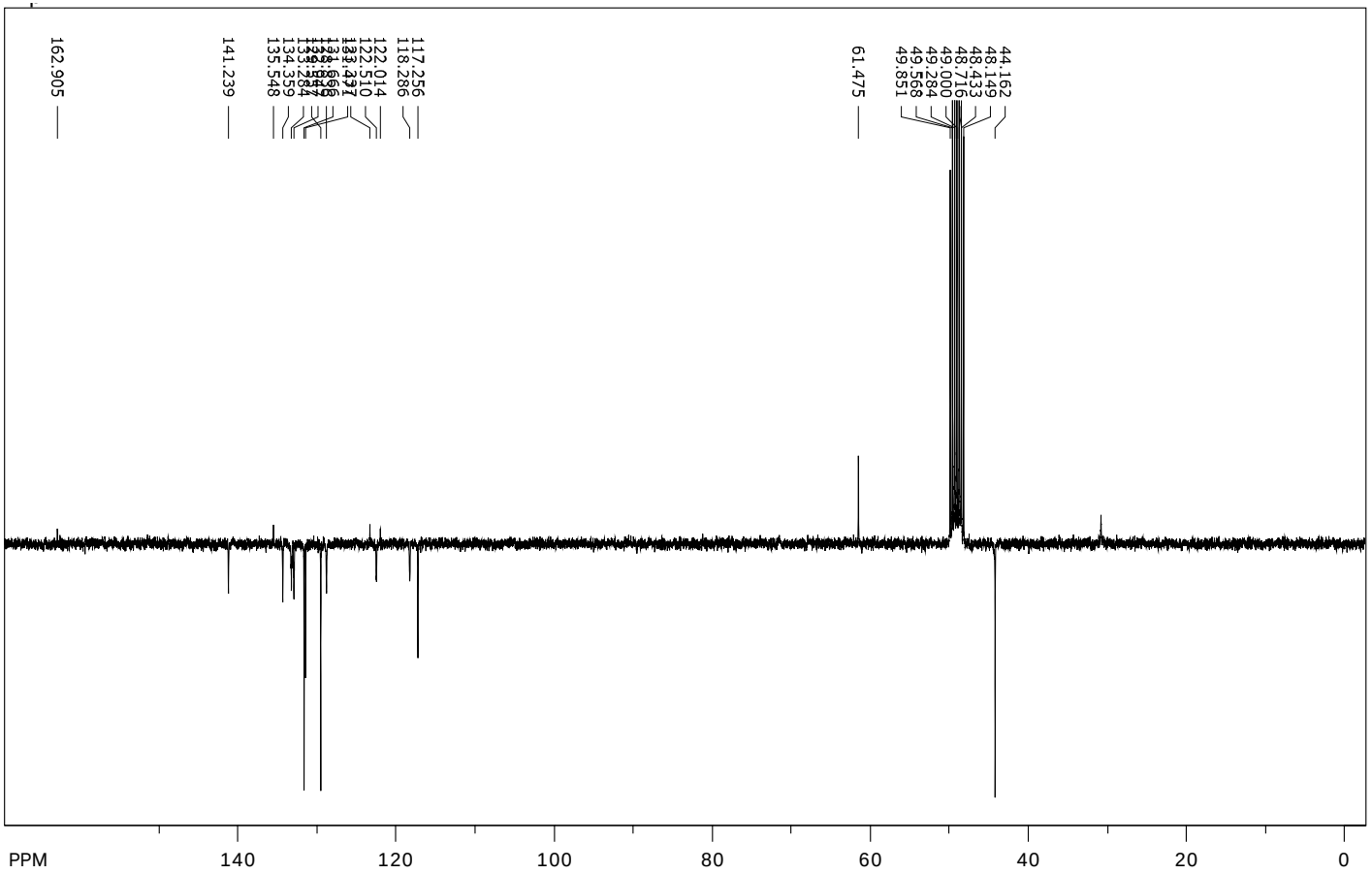

^{1}H NMR (CD_3OD, 600 MHz) of 1·TFA

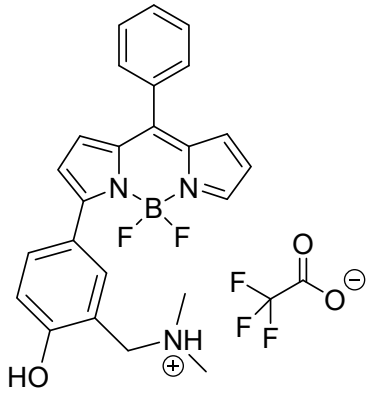

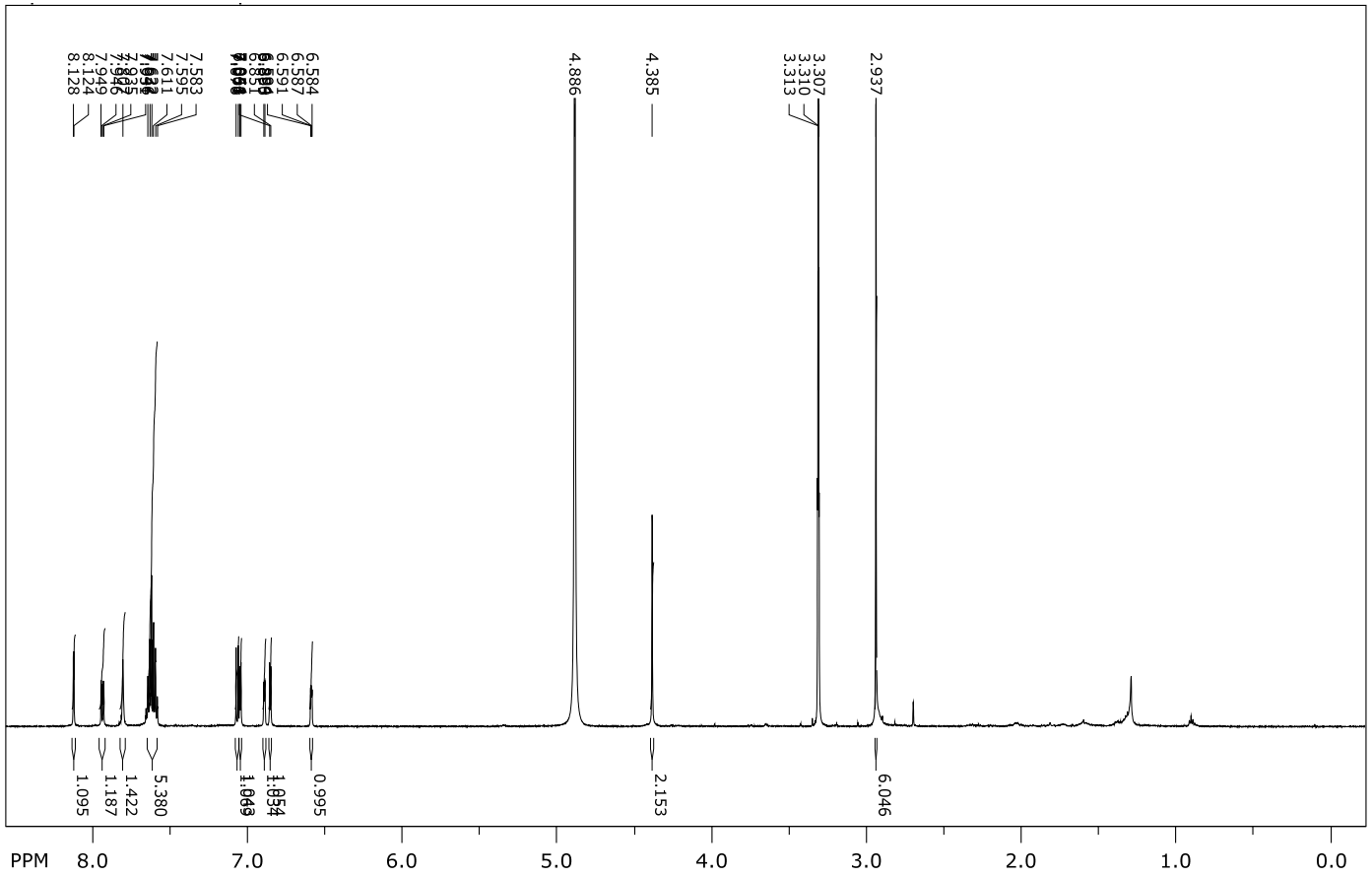

^{13}C NMR (CD_3OD, 150 MHz) of 1·TFA

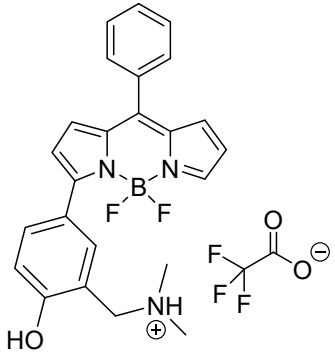

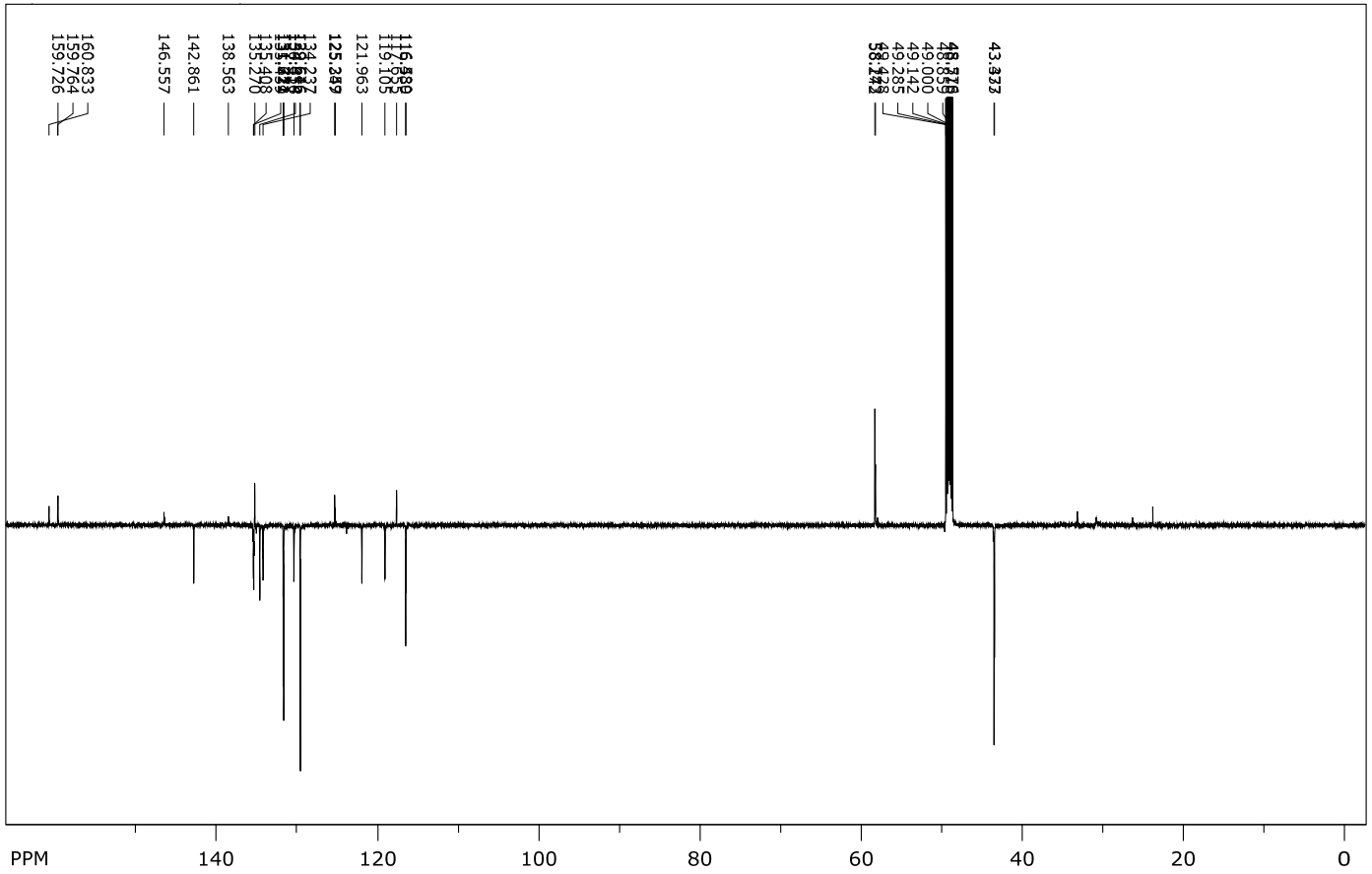

^{1}H NMR (CD_3OD, 600 MHz) of 2·TFA

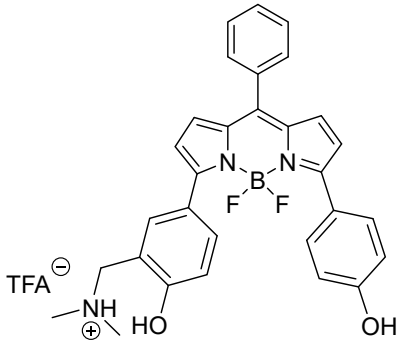

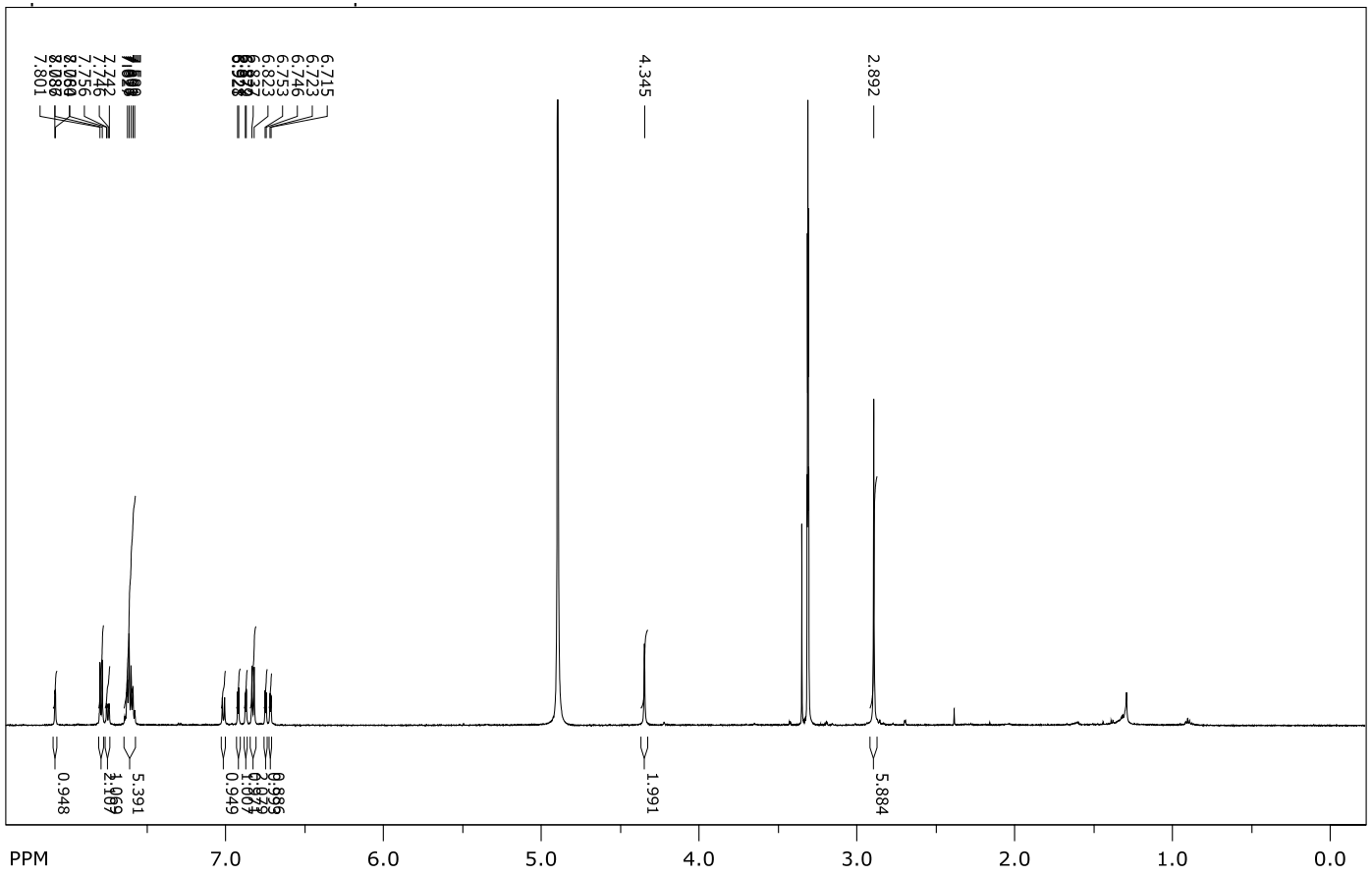

^{13}C NMR (CD_3OD, 75 MHz) 2·TFA

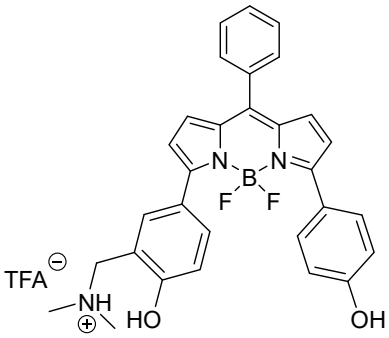

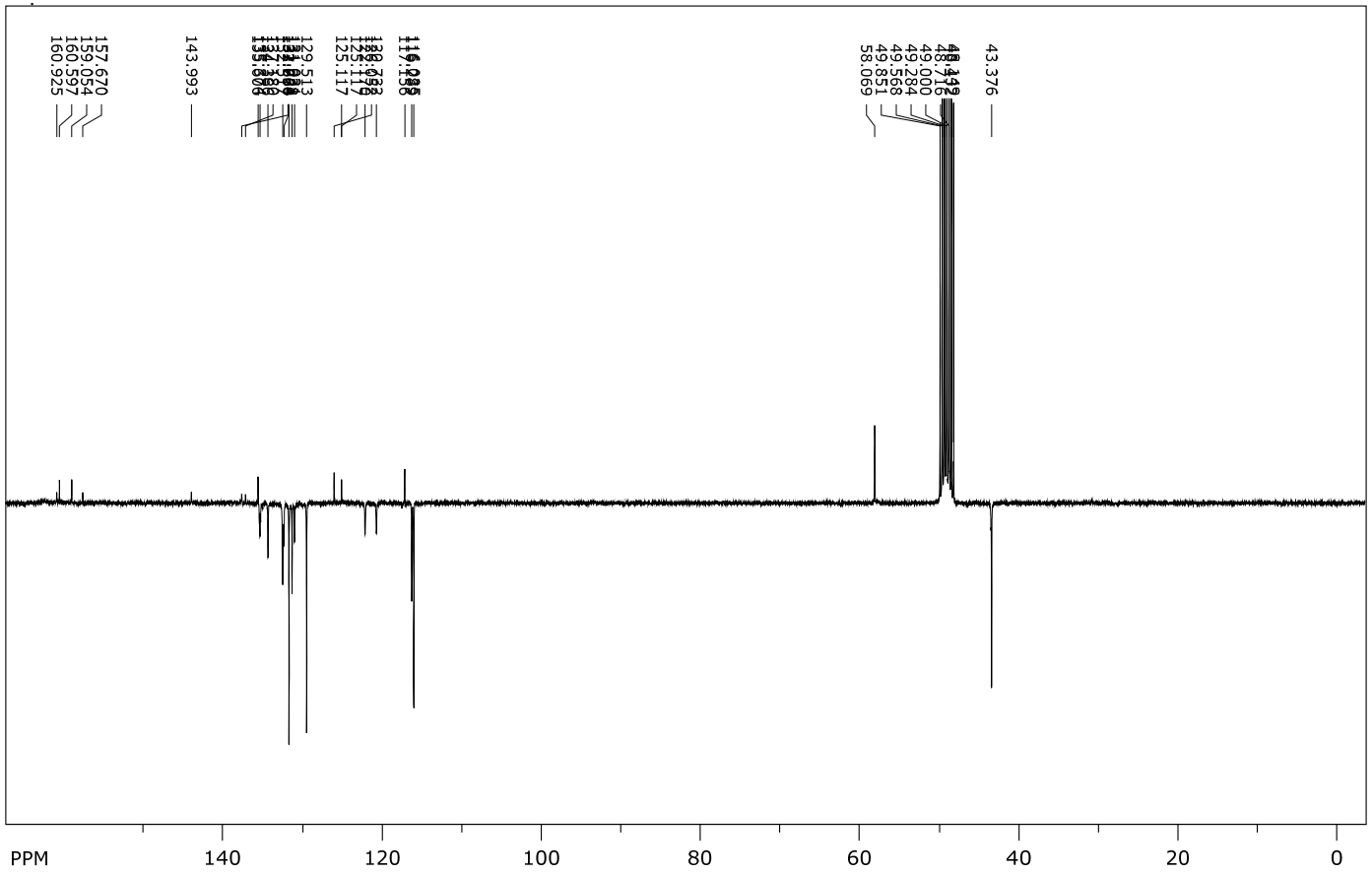

^{1}H NMR ($CDCl_3$, 300 MHz) of 3·TFA

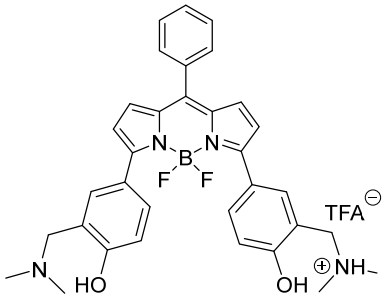

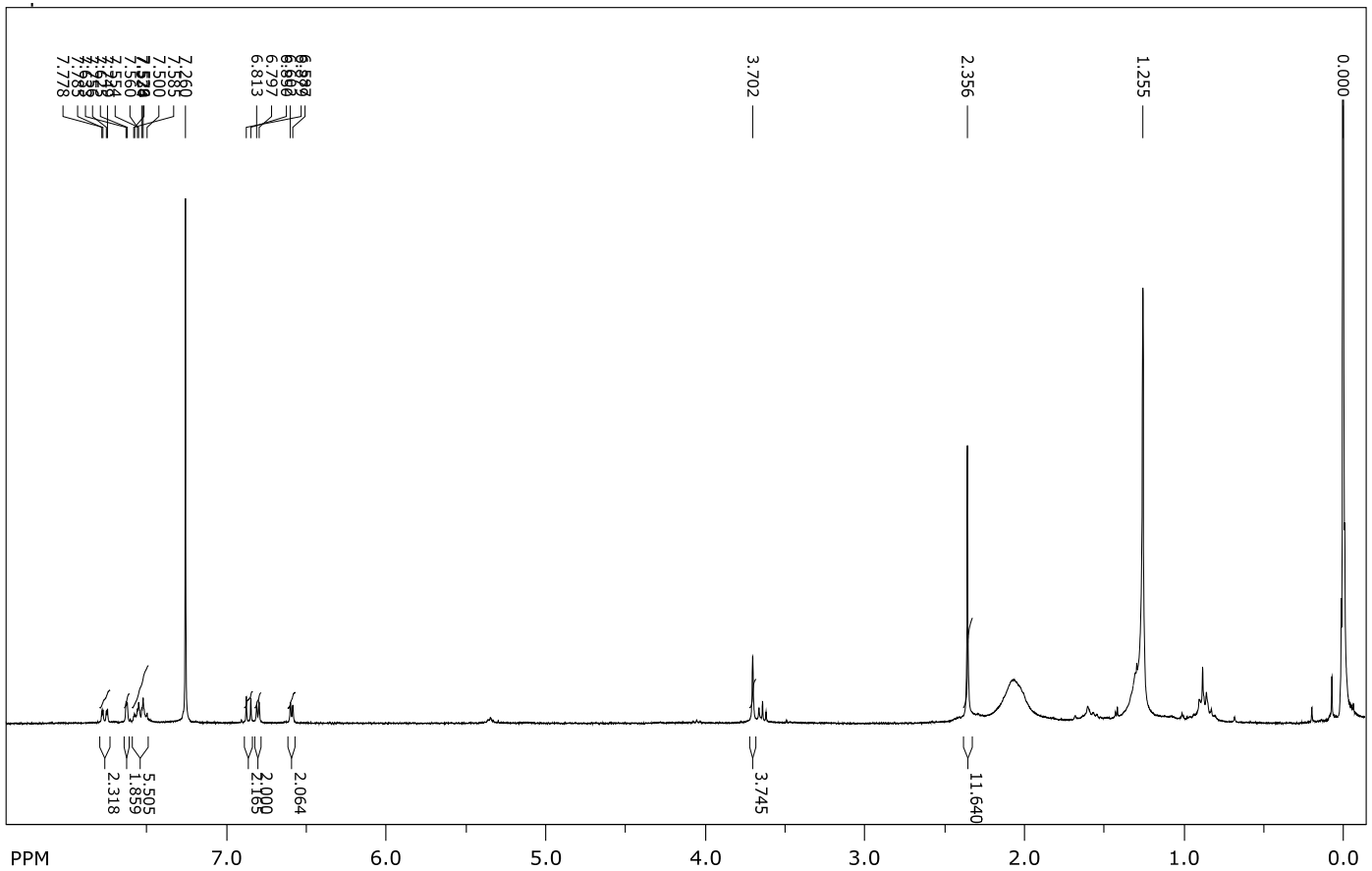

^{13}C NMR (CD_3OD, 150 MHz) of 3·TFA

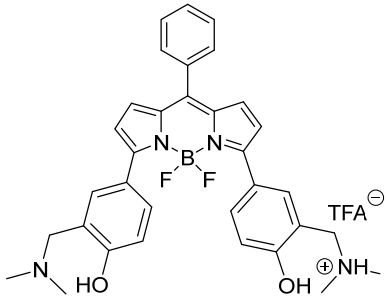

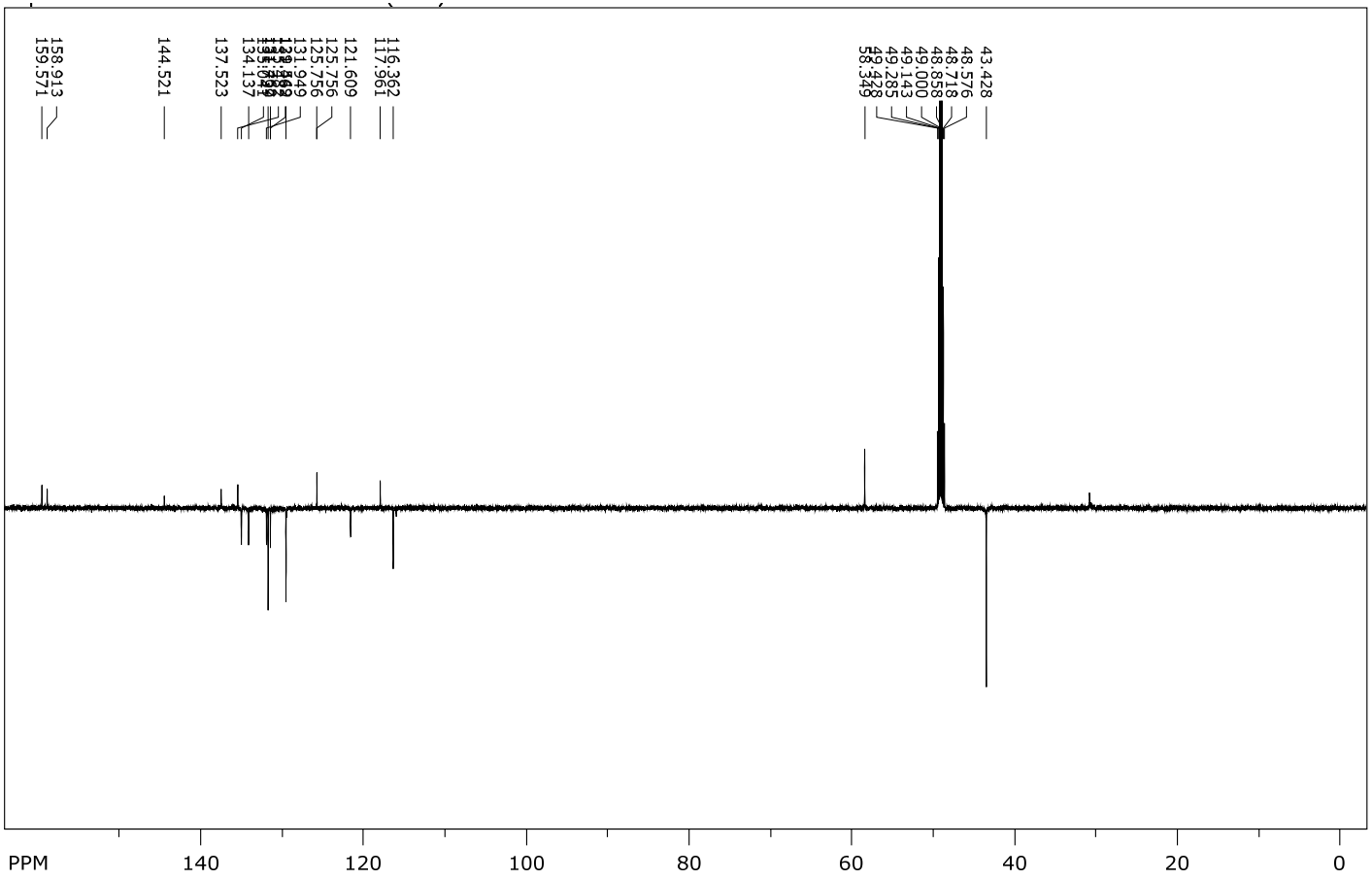

HSQC (^{1}H 600 MHz, ^{13}C 150 MHz, CD_3OD) of 3·TFA

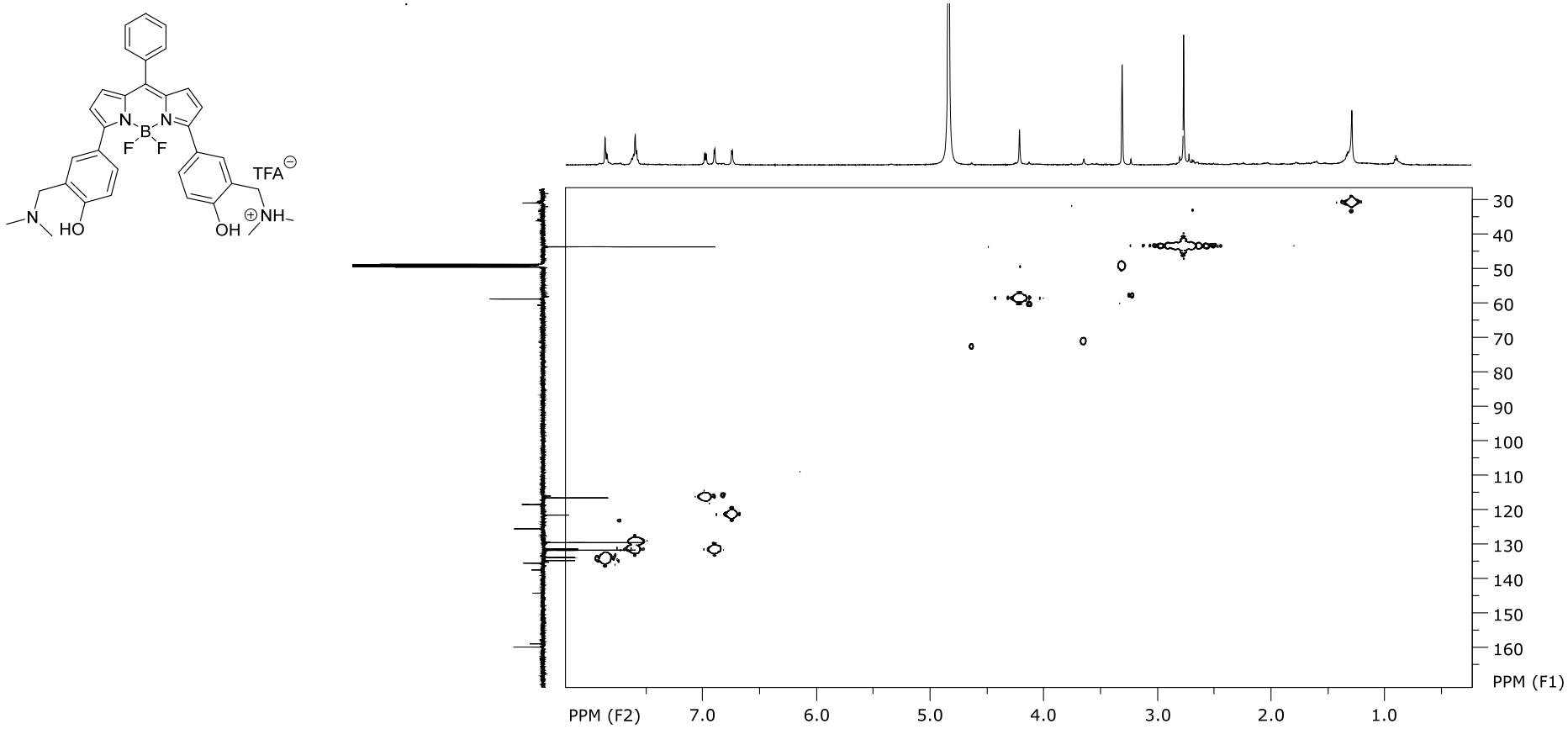

^{1}H NMR ($CDCl_3$, 300 MHz) of 4·TFA

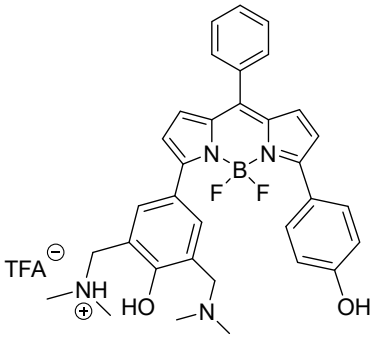

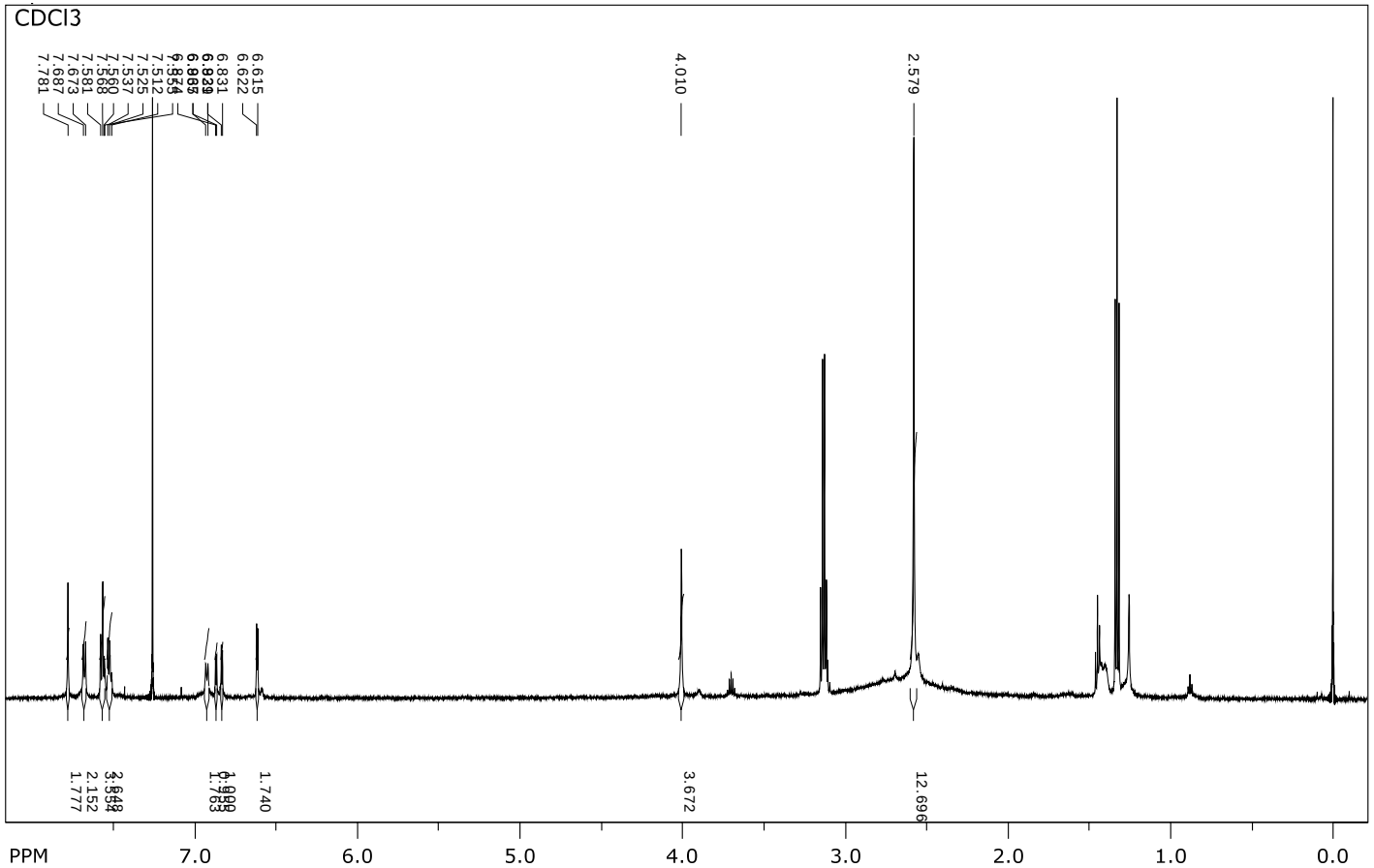

^{13}C NMR ($CDCl_3$, 150 Hz) of 4·TFA

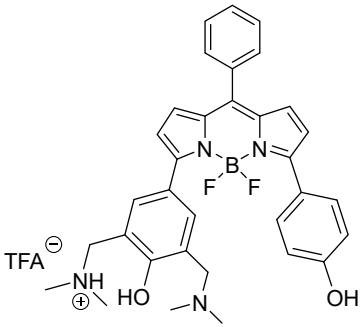

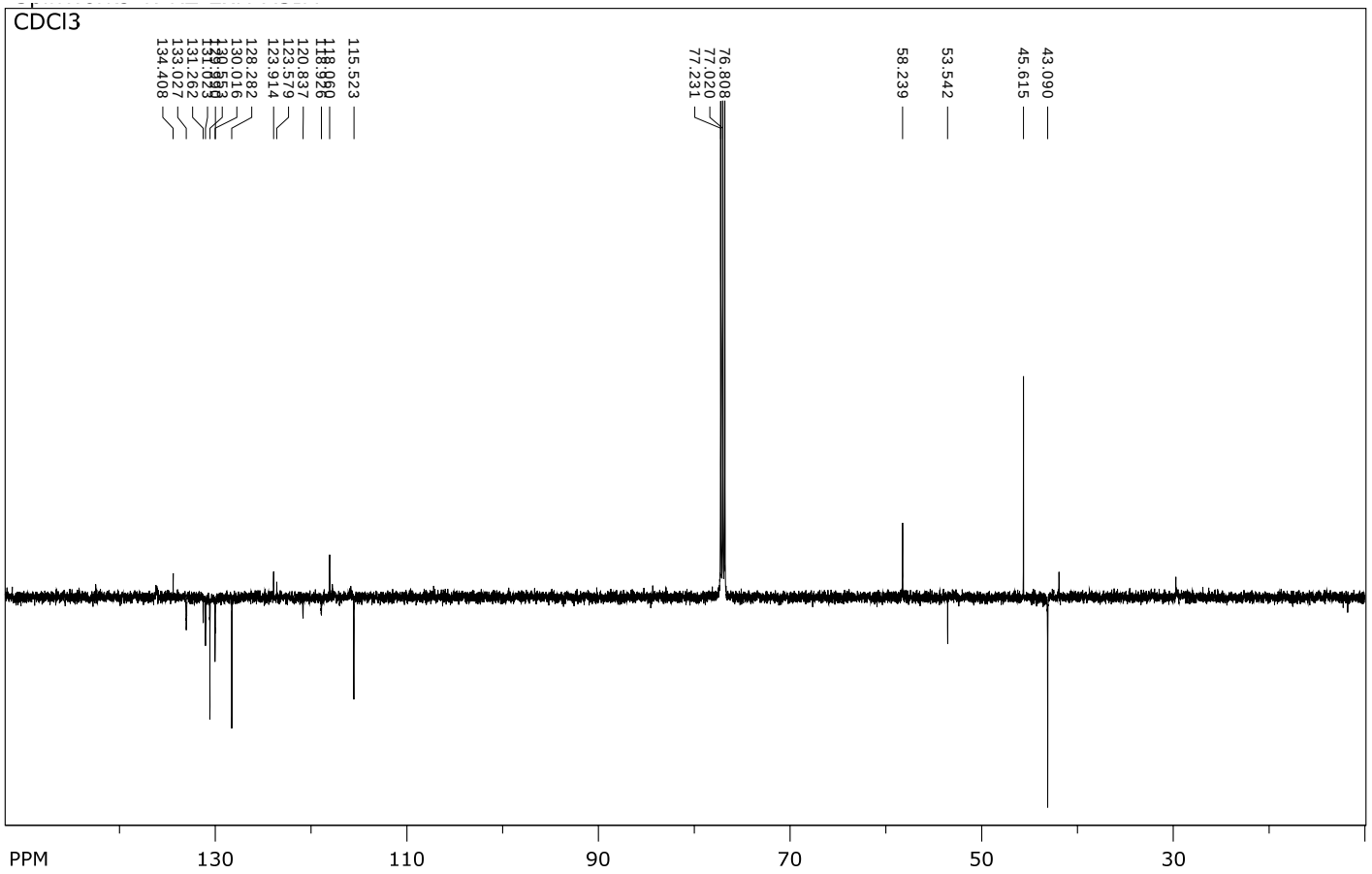

^{1}H NMR (CD_3OD, 300 MHz) of 4·TFA

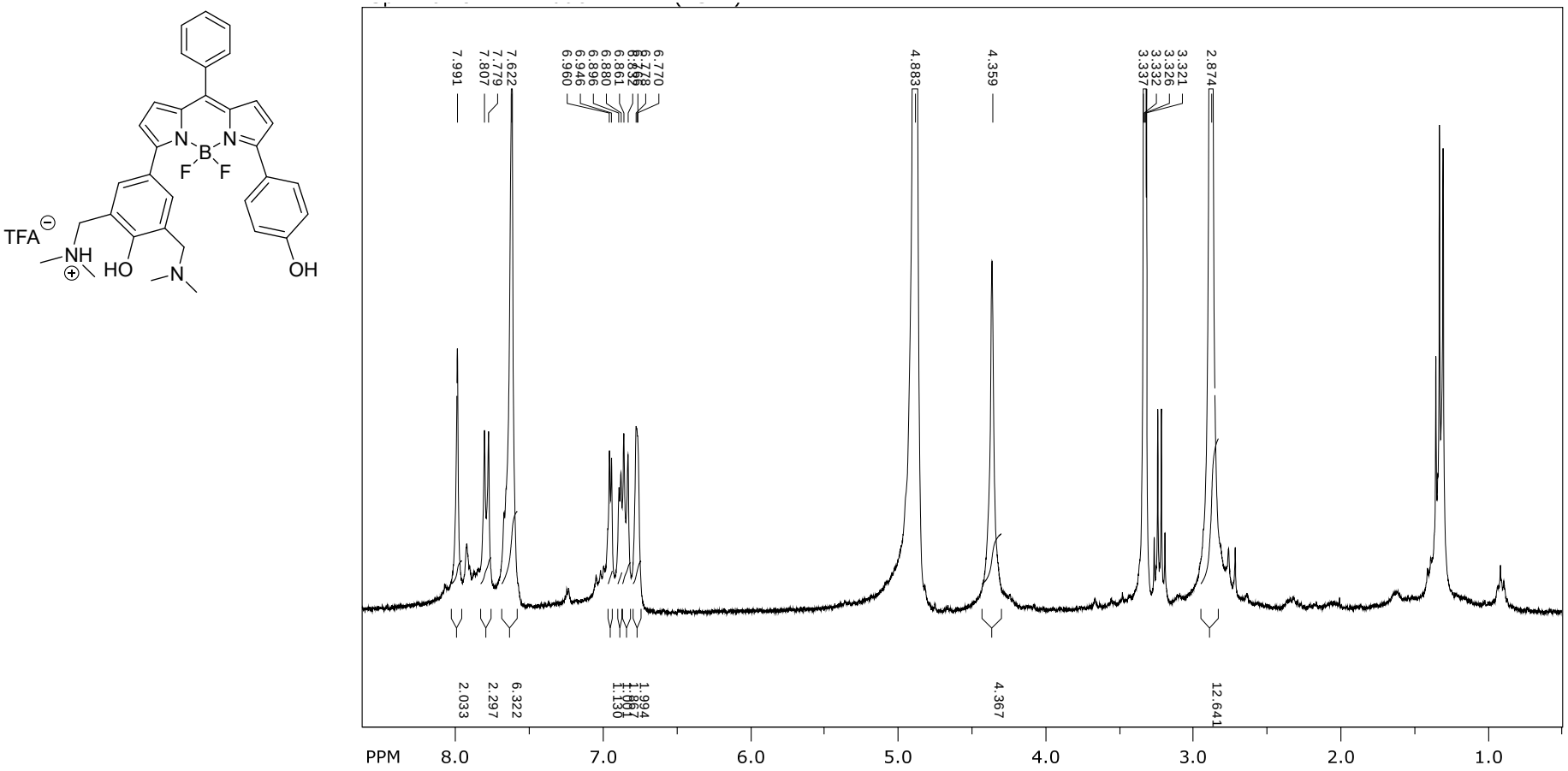

^{13}C NMR (CD_3OD, 150 Hz) of 4·TFA

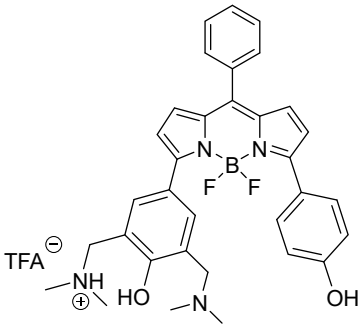

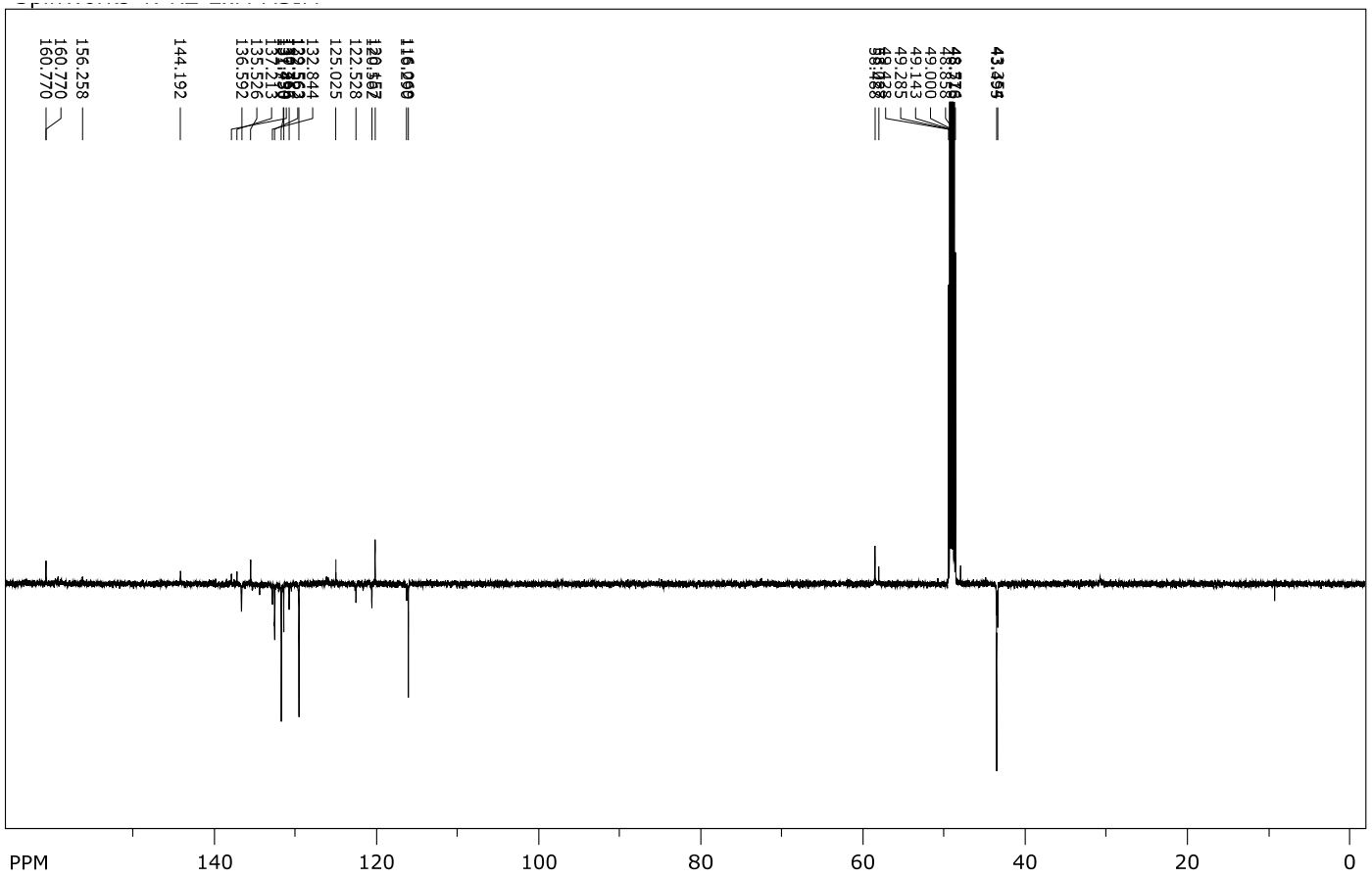

HSQC (^{1}H 600 Hz, ^{13}C 150 Hz, CD_3OD) of 4·TFA

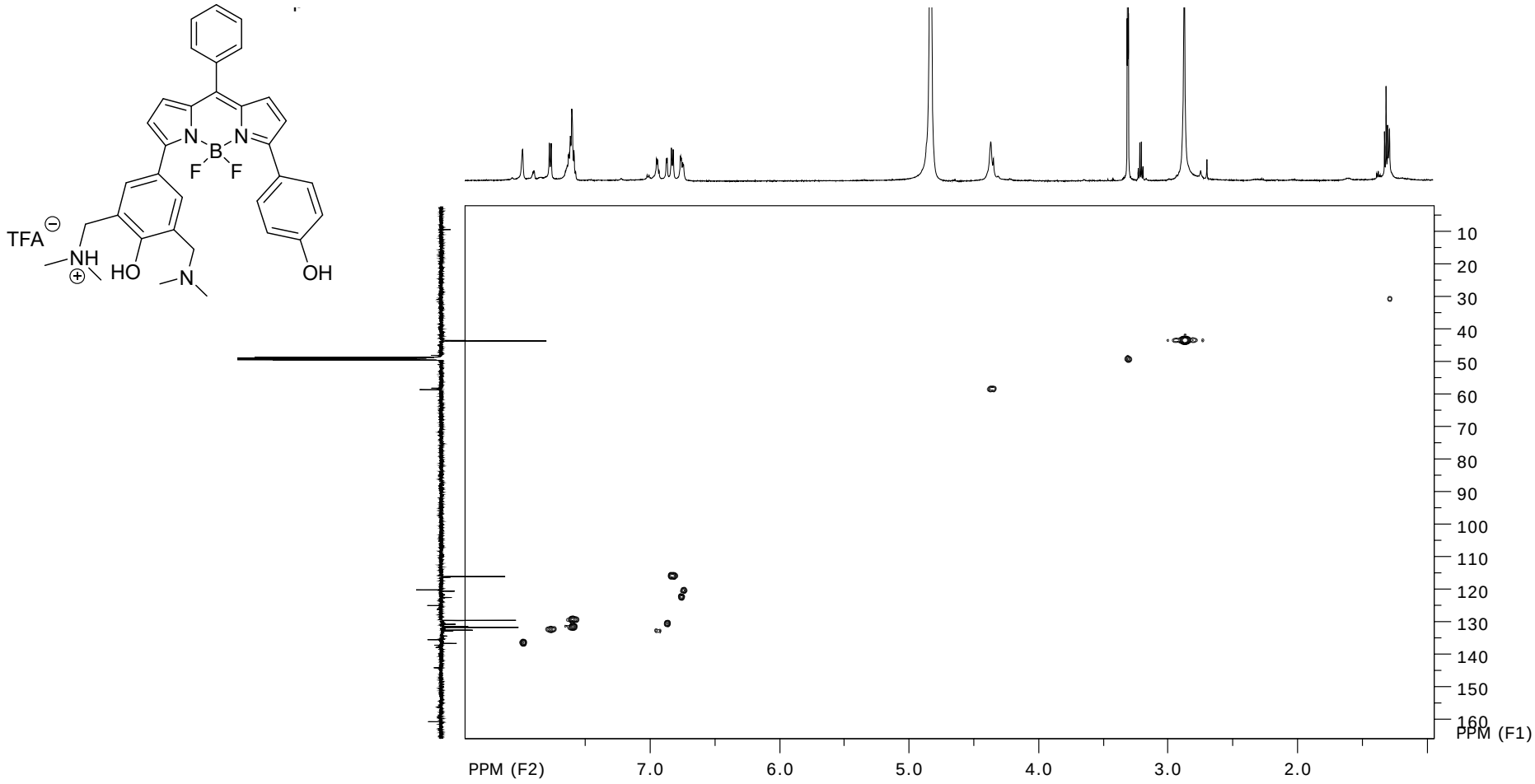

^{1}H NMR (CD_3OD, 300 MHz) of 5·TFA

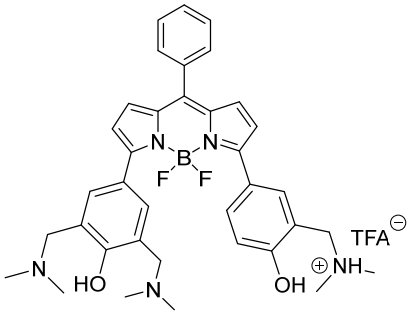

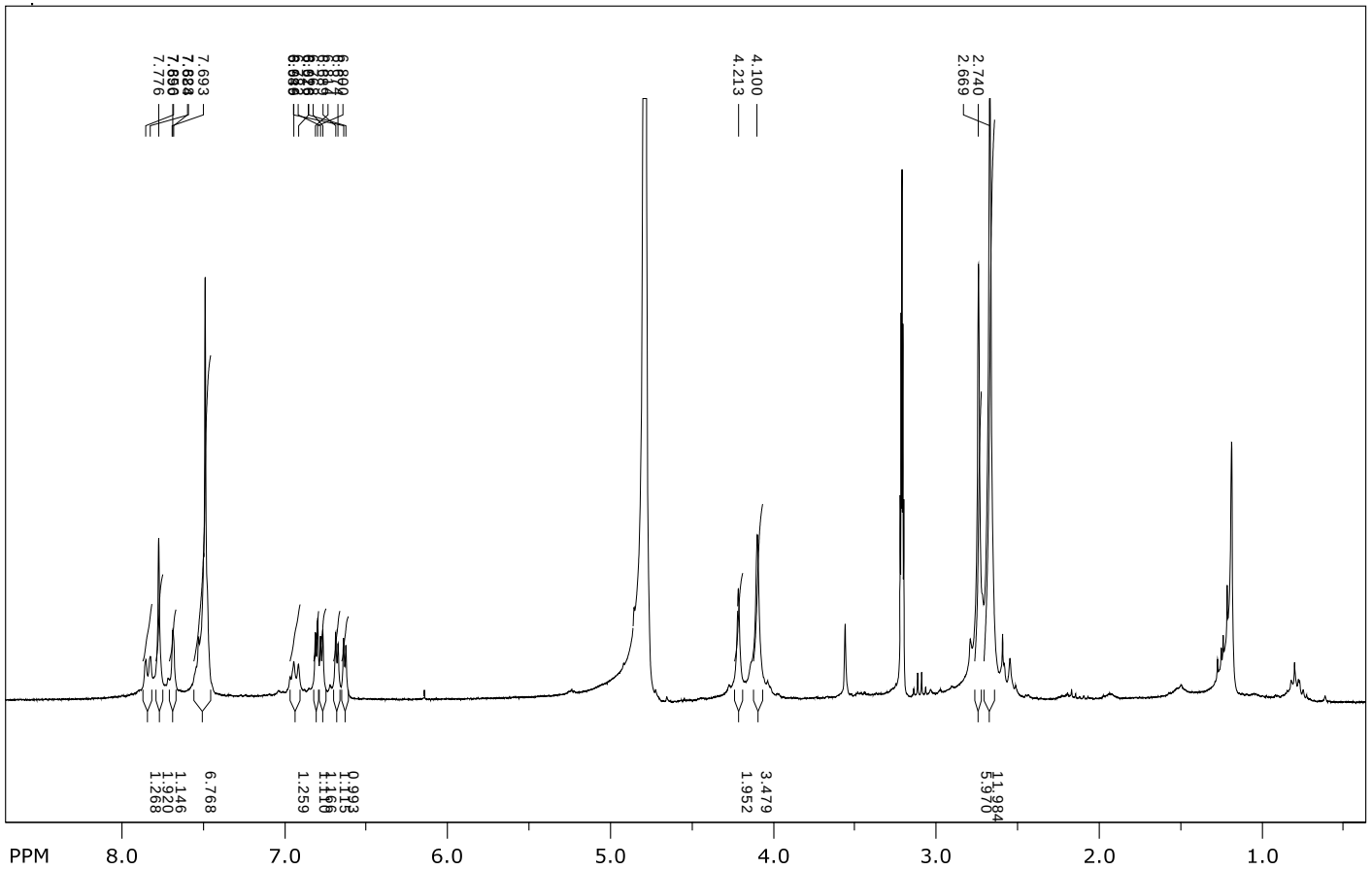

^{13}C NMR (CD_3OD, 150 MHz) of 5·TFA

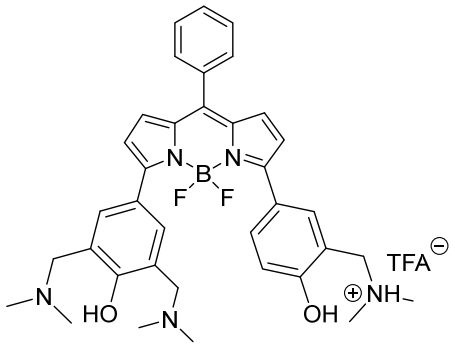

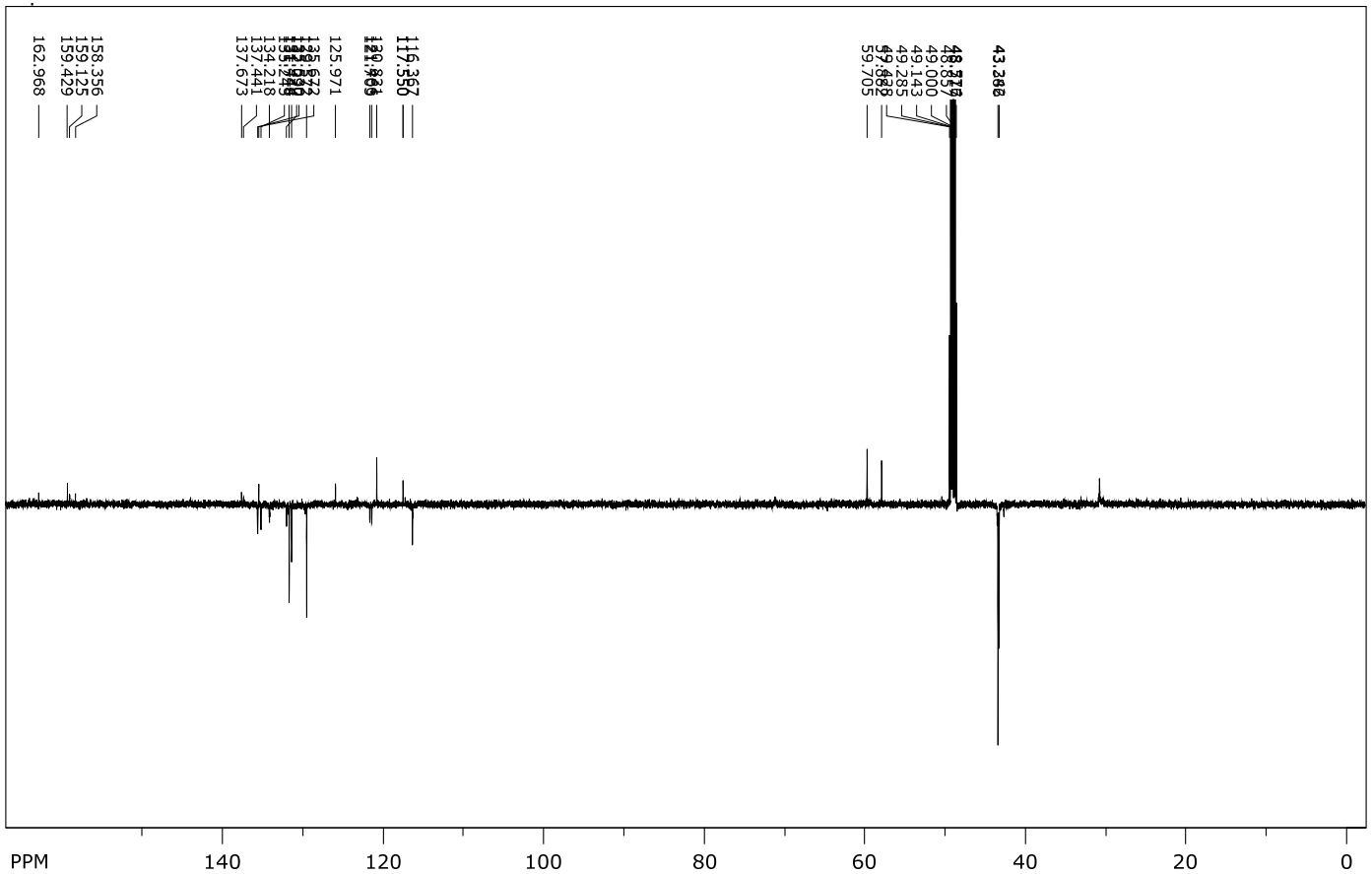

HSQC (^{1}H 600 Hz, ^{13}C 150 Hz, CD_3OD) of 5·TFA

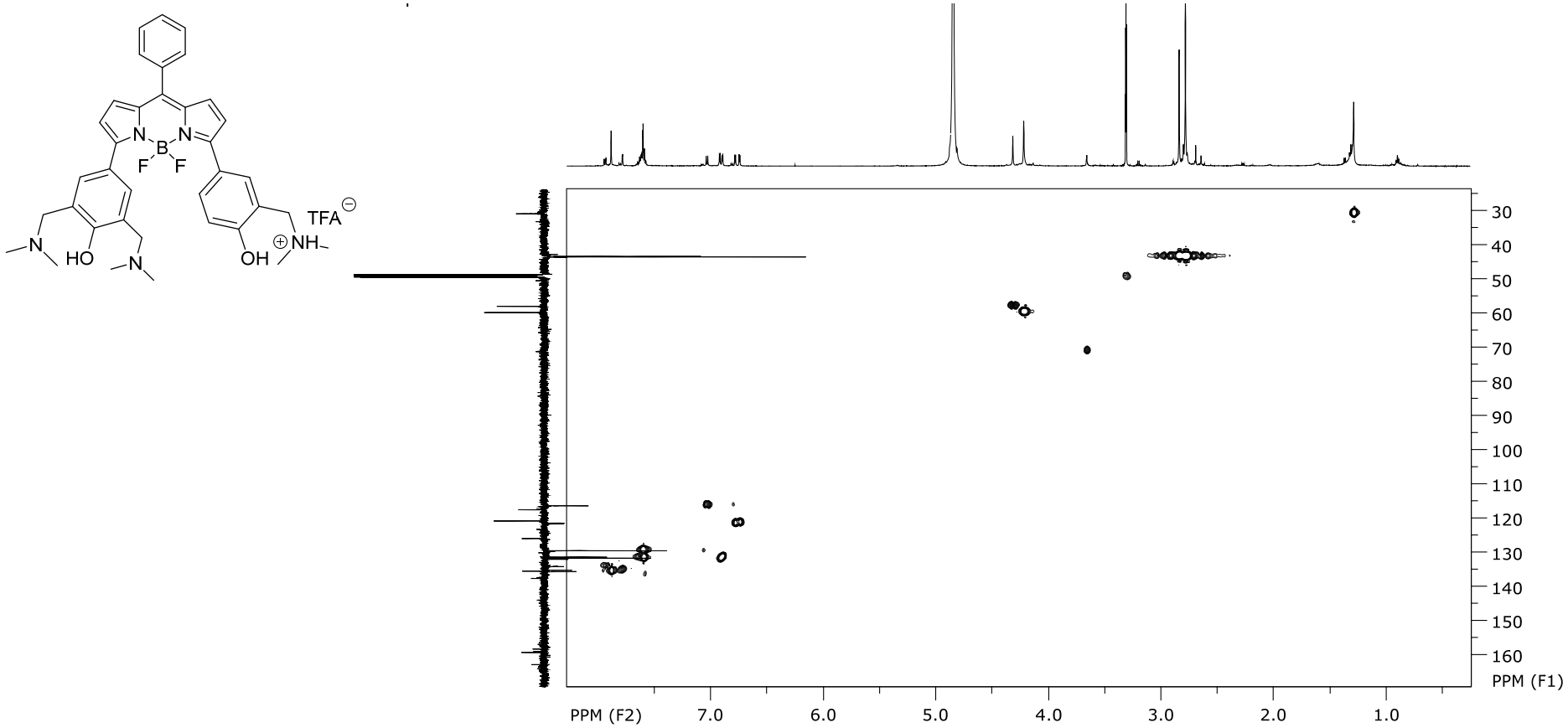

^{1}H NMR (CD_3OD, 600 MHz) of 1-OCH_3

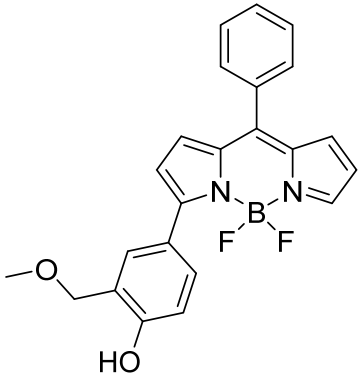

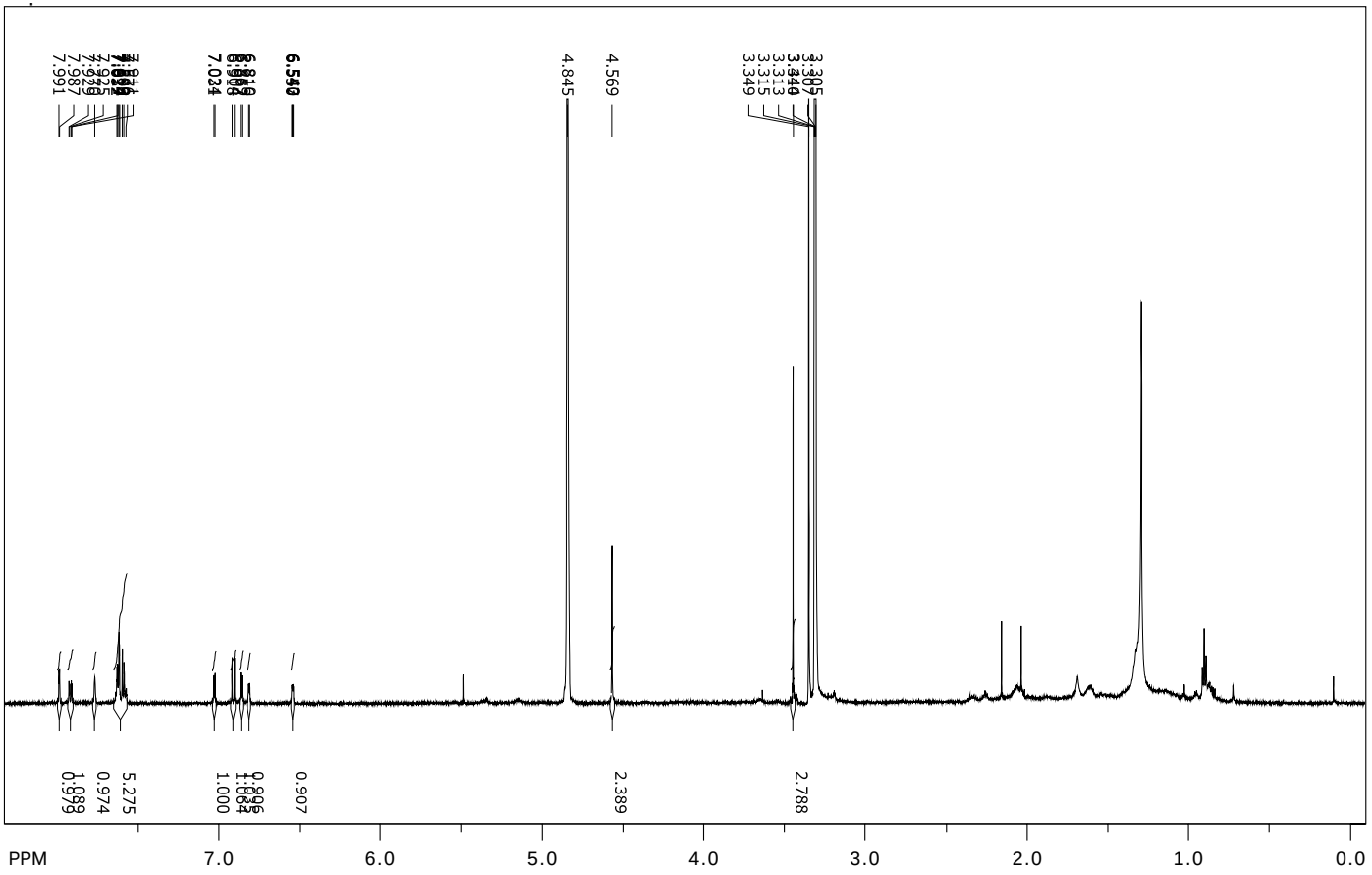

^{1}H NMR (CD_3OD, 600 MHz) of 2-OCH_3

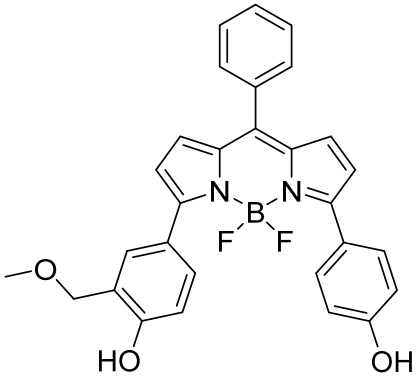

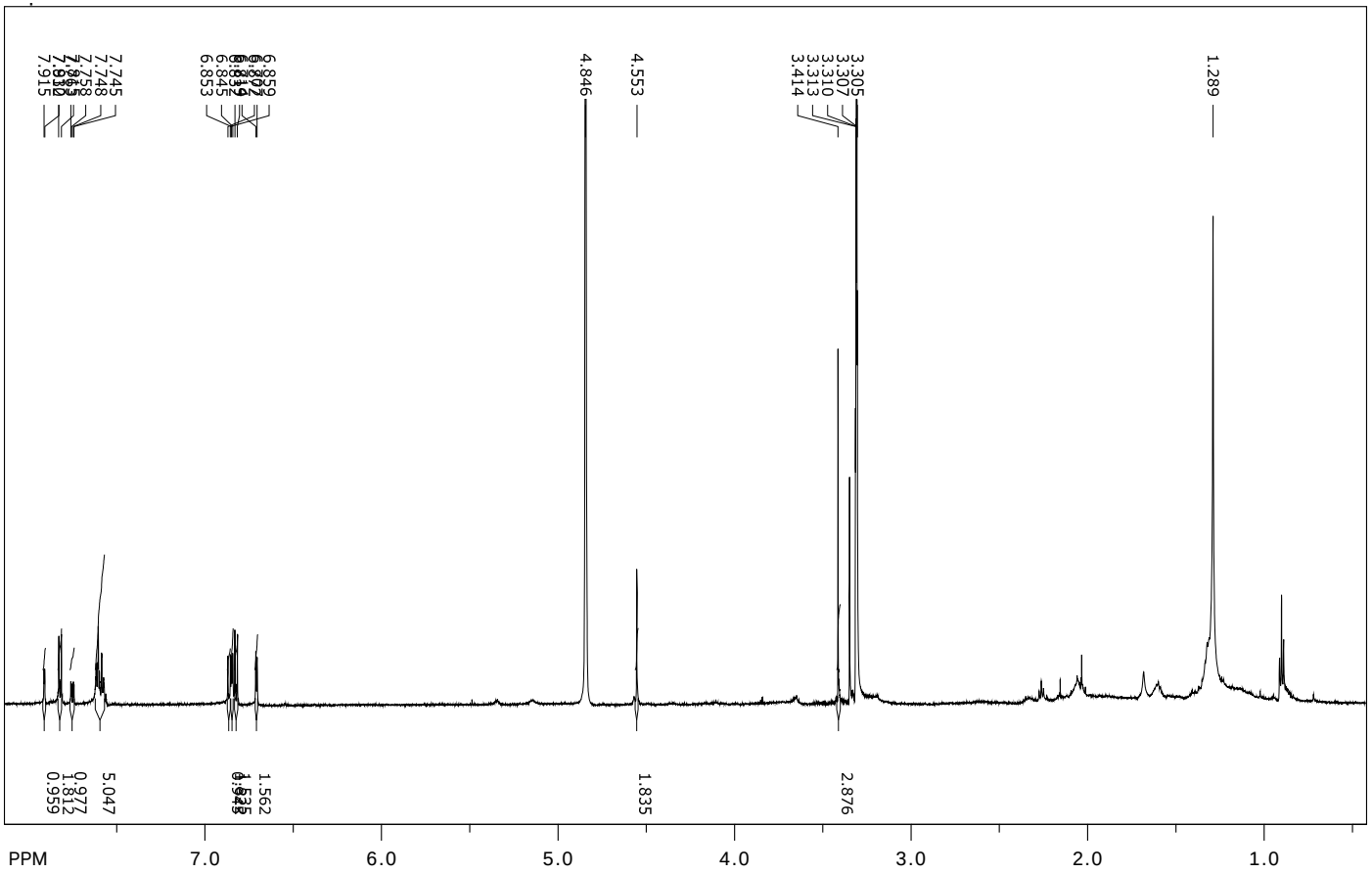

8. References

1 H. Shinohara, K. Honda, S. Misaki, E.Imoto, *Nippon Kagaku Zasshi* **1960**, *81*, 1740-1746.

[2] N. Basarić, M. Kralj, A.-M. Mikecin, M. Cindrić, Matej, Quinone-methide precursors with BODIPY chromophore, method of preparation, biological activity and application in fluorescent labeling, WO2017199056 A1 2017-11-23.

[3] Y.M. Chang, J. H. Park, S. W. Jun, J.-S. Kang, S. Lee, Dye comprising pyrromethene-boron complex compound with particular wavelength for display filter, PCT Int. Appl. (2015), WO 2015174663 A1 20151119.

[4] X. Zhou, C. Yu, Z. Feng, Y. Yu, J. Wang, E. Hao, Y. Wei, X. Mu, L. Jiao, Highly Regioselective α-Chlorination of the BODIPY Chromophore with Copper(II) Chloride, *Org. Lett.* **2015**, *17*, 4632-4635.

[5] M. Baruah, W. Qin, R. A. L. Vallee, D. Beljonne, T. Rohand, W. Dehaen, N. Boens, A Highly Potassium-Selective Ratiometric Fluorescent Indicator Based on BODIPY Azacrown Ether Excitable with Visible Light, *Org. Lett.* **2005**, *7*, 4377-4380.

[6] N. Boens, W. Qin, N. Basarić, J. Hofkens, M. Ameloot, J. Pouget, J.-P. Lefèvre, B. Valeur, E. Gratton, M. vandeVen, N. D. Silva, Jr., Y. Engelborghs, K. Willaert, A. Sillen, G. Rumbles, D. Phillips, A. J. W. G. Visser, A. van Hoek, J. R. Lakowicz, H. Malak, I. Gryczynski, A. G. Szabo, D. T. Krajcarski, N. Tamai, A. Miura, Fluorescence Lifetime Standards for Time and Frequency Domain Fluorescence Spectroscopy, *Anal. Chem*. 2007, **79**, 2137-2149.

[7] L. Uzelac, Đ. Škalamera, K. Mlinarić-Majerski, N. Basarić, M. Kralj, Selective Photocytotoxicity of Anthrols on Cancer Stem-like Cells: The Effect of Quinone Methides or Reactive Oxygen Species, *Eur. J. Med. Chem*., 2017, **137**, 558-574.

[8] A. Kamkaew, S. Hui Lim, H. Boon Lee, L. Voon Kiew, L. Yong Chung, K. Burgess, BODIPY Dyes in Photodynamic Therapy, *Chem. Soc. Rev.*, 2013, **42**, 77-88.